OBSERVATIONS IN A SEDIMENT-LADEN FLOW BY USE OF LASER-DOPPLER VELOCIMETRY

by

Catharine van Ingen

Project Supervisor:

Norman H. Brooks
James Irvine Professor of
Environmental and Civil Engineering

Supported by

National Science Foundation
Grant Numbers ENG75-15786, ENG77-10182, CME79-20311

Report No. KH-R-42

October 1981

ACKNOWLEDGEMENTS

This study is hardly the work of a single individual, but rather results from a collaboration of a number of people. To thank all of the contributors adequately is not possible; I am sincerely grateful for all of the time, tolerance, assistance and friendship from the many people named and unnamed upon whom I have relied.

First, and foremost, I would like to express gratitude and appreciation to Professor Norman Herrick Brooks for guidance, encouragement, and funding during this investigation. Dr. Brooks suggested the topic and was my principal advisor. His never failing optimism was always an inspiration and he was always able to transform my Sanskrit into intelligible English.

I am also indebted to Professor E. John List for numerous discussions on the analysis and physical interpretation of the data. His many suggestions and insights over the years were invaluable to this study.

The instrumentation could not have been built without the unique assistance of Elton F. Daly and Joe Fontana. From the smallest precision mirror mount to the major alterations of the flume support truss, Elton always had a better way.

The simple approach to laser velocimetry used in this study depends on the analog electronics contributed by Professor Ricardo Gomez. I have learned electronics by example; the formative lessons were most generously given by Professor Gomez. The Gomez magic boxes will never cease to amaze me.

Others also contributed to the development of the processing electronics. E. J. Siskind taught me about the brute force approach to grounding and the controlled approach to interfacing an external device to a computer. Discussions with Alan Barnes, John Gord, and Robert Landau yielded many, many helpful suggestions and comments. The electronics were constructed with the help of Sven Sondergaard, James Campbell, Jean Armistead, and Leonard Montenegro.

I would also like to thank the following people who, asking nothing in exchange, gave me access to their computer time, their computer facilities, and their computer expertise: Mark Bartelt, J. Blinn, K. Crandall, K. Clardy, DELCO-PEP, R. Feenstra, R. Flagan, W. Kropac, F. Nagy, C. L. Senior, and B. A. Zimmerman.

The continuing friendship and help of Joan Mathews, Pat Rankin, Pat Houseworth, Debbie Brownlie, Adelaide Massengale, Rayma Harrison, Gunilla Hastrup, and Melinda Hendrix-Werts is greatly appreciated. This thesis and other previous manuscripts could not have be prepared without them. Dave Byrum, Teresa Fall, and Phil Dubé provided help with the drawings and illustrations.

Discussions with fellow students have provided much needed support and camaraderie. I would especially like to thank Greg Gartrell, William Brownlie, Steve Wright, Derek Goring, Lisa Anderson, Jim Young, and Phil Roberts.

I have received much encouragement throughout the years from the Hydraulics faculty of the University of California, Berkeley. Initially instructors, now colleagues, Professors H. B. Fischer,

R. L. Wiegel, J. A. Hammack, and J. A. Harder remain valuable mentors.

The completion of this study required the special support given only by close friends. For assistance above and beyond that which can be considered normal, I would especially like to thank the Bunch, the Proprietors of Rent-A-Room, South, the staff of New York Consulting Buffoons, Inc., the Barracuda-in-Penguin-Clothing, and my favorite Sheep.

Financial support for this research was provided by the California Institute of Technology, which provided the laboratory facilities and a Graduate Teaching Assistantship during 1976 amd 1977, and the National Science Foundation under Grants ENG 75-15786, ENG 77-10182, and CME 79-20311.

This report was submitted to the California Institute of Technology on October 29, 1981, as a thesis in partial fulfillment of the requirements for the degree of Doctor of Philosophy.

ABSTRACT

The laser-Doppler velocimetry technique was adapted for use in sediment-laden flows. The developed instrumentation was used to make one-dimensional, instantaneous measurements of both fluid and sediment grain velocities throughout the water column in such a flow. The velocimetry results were obtained in a steady, uniform flow over a natural sediment bed in the high-transport, flat bed regime.

Laser-Doppler velocimetry is particularly attractive for use in sediment-laden flows as no calibration is required and no probe is introduced into the flow field. Measurements of the fluid velocity and the occurrence and velocity of individual sediment grains are possible with the instrumentation developed in this study. The major difficulties encountered are the possible conditional sampling, hence possible biasing, of the fluid velocity data and the failure of the instrumentation to record or resolve individual sediment grains at higher sediment transport rates. The instrumentation employed in this study is still in the developmental stages and suggestions for its improvement are given.

Despite the difficulties encountered, the data obtained in this study give some insights into the mechanics of suspension and entrainment of sediment during transport by water. The longitudinal turbulence intensity does not seem to be significantly affected by the presence of suspended sediment; the turbulence intensities observed in the sediment-laden flow of this study do not differ greatly from the values reported by previous investigators for clear fluid flows. The mean and standard deviation of the sediment

grain velocity were observed to be less than those for the fluid velocity in the lower portion of the flow, but respectively greater near the water surface.

The data demonstrate the shortcomings of the continuum approach to the mechanics of the suspension of sediment. The length (or time) scales of the fluid turbulence are smaller than the length (or time) scale of a set of sediment grains required to define suspended sediment concentration. Near the water surface, where the velocimeter acts as a grain counter, the probability density functions of the sediment grain inter-arrival times, the time between the detection of successive sediment grains, were observed to be negative exponentials. The transport of individual sediment grains might be modeled as a Poisson process.

This work is the foundation of an ongoing experimental program of direct measurements of the fine-scale, time-fluctuating characteristics of sediment-laden flows. This study developed and implemented instrumentation capable of making such measurements and established a conceptual framework for the subsequent interpretation of the data obtained. Two-dimensional measurements, with improved instrumentation, will give additional insights into the mechanics of sediment transport.

TABLE OF CONTENTS

LIST OF FIGURES

LIST OF TABLES

NOMENCLATURE

a	reference distance above the sediment bed
c	time-averaged sediment concentration at a point
$\bar{c}$	depth-averaged sediment concentration
$C(M)$	simple lag correlation coefficient
d	flow depth
dA	cross-sectional measurement area
d_g	geometric mean sediment grain size
f	Doppler frequency shift
f_b	friction factor of the sediment bed
f_j	fraction of the j^{th} sediment grain which passes through the laser beam intersection volume
f_m	measured value of f
$\frac{\Delta f}{f}$	relative error in Doppler frequency
$F(\nu)$	true Fourier transform
$F_N(\nu)$	discrete Fourier transform
F_R	Froude number = $\frac{u}{\sqrt{gd}}$
k	von Karman constant
M	lag index
m	mass of a sediment grain
m_j	mass of the j^{th} sediment grain
N_I	number of fluid velocity observations
N_J	number of sediment grain velocity measurements
$P(\nu)$	true power spectral estimate
$P_N(\nu)$	discrete power spectral estimate

P_s	stream power
P_{sw}	power to suspend sediment
Q	flow discharge
q	fluid flux per unit area
Q_s	total sediment transport rate
q_s	sediment discharge per unit area
R	hydraulic radius
$R(\tau)$	true auto-correlation coefficient
R_e	Reynolds number = $\frac{4Ru}{\nu}$
S	slope of the flow energy grade line
T	measurement period
t_i	time of measurement of the i^{th} fluid velocity event
t_j	time of measurement of the j^{th} sediment grain velocity event
u	longitudinal velocity component
u_i	i^{th} fluid velocity measurement
$\tilde{u}$	longitudinal sediment slip velocity
$\bar{u}$	mean fluid velocity
$\sqrt{\overline{u'^2}}$	longitudinal fluid turbulence intensity
u_{g_j}	j^{th} sediment grain velocity measurement
$\bar{u}_g$	mean sediment grain velocity
$\sqrt{\overline{u_g'^2}}$	sediment grain velocity standard deviation
u_*	fluid shear velocity
u_{*_b}	bed shear velocity
v	vertical velocity component
$\tilde{v}$	vertical sediment slip velocity
v_s	settling velocity of sediment grains

y	distance in the vertical direction
y_o	reference position of the sediment bed
z	Rouse exponent = $v_s/k\beta u_*$
α	constant
β	constant of proportionality $\beta = \varepsilon_s/\varepsilon_m$
$\gamma_N(\nu)$	power spectral window function
δ	Kroneker delta function
ε_m	turbulent diffusion coefficient for momentum
ε_s	turbulent diffusion coefficient for sediment
Δt	determined observation time
$\overline{\delta t_g}$	mean sediment grain inter-arrival time
$\sqrt{\overline{\delta t_g'^2}}$	sediment grain inter-arrival time standard deviation
$\delta_N(\nu)$	Fourier transform spectral window function
σ_g	geometric standard deviation of sediment grain size
λ	wavelength of laser light
$\psi_M(\tau)$	probability density function of lag time τ at lag interval M
ρ	fluid density
ρ_s	sediment density
η	frequency
ν	frequency
ν_s	sampling frequency
ϕ	half angle of laser beam intersection
τ	lag time
τ_o	boundary shear stress

overbar ($\overline{\quad}$)	mean value of a quantity
prime (')	fluctuating part of a quantity

Subscripts

g	denotes sediment grain value
i	fluid measurement index
j	sediment grain measurement index
k	integer index

CHAPTER 1

INTRODUCTION

After decades of laboratory and field research, the fundamental fluid mechanics of sediment transport is still only partially understood. As a result, predictions of gross flow parameters, friction factor and sediment discharge are difficult for uniform, steady flows and nearly impossible for non-uniform or non-steady flows. Until the small-scale time-fluctuating nature of sediment-laden flows is understood, the river engineer will be limited to the empirical methods now used to make such predictions.

Previous investigations have, for the most part, been limited to time-averaged measurements of flow variables due to lack of instrumentation. The effect of suspended sediment on the turbulent structure of the fluid has been theorized from measurements of sediment concentration and fluid velocity which were averaged over long sampling times and large sampling volumes. Also, most measurements have been made with some type of probe. The introduction of a probe into a sediment-laden flow deforms the flow field by deflecting the individual sand grains which collide with the probe and inducing local scour of the movable sediment bed.

In this study, a laser-Doppler velocimeter was developed and used to make instantaneous measurements of both fluid and sediment grain velocity throughout the water column. No probe was introduced into the flow field. The flow was not artificially distorted. Furthermore, the instrument needs no calibration for velocity measurements. The motions of individual sediment grains in the transporting fluid were observed.

The laser-Doppler technique has become well established for velocimetry of homogeneous fluid flows. Applications of the technique to two-phase flows are still relatively new. There are unique difficulties and limitations of the technique when applied to sediment-laden fluid flows. The instrumentation described in this study is clearly still in its developmental phase.

This new ability to make such fine scale measurements forced an examination of the traditional thinking about sediment transport. The motion of individual sediment grains, as well as collections of such grains, must be considered; sediment transport mechanics may be viewed as sediment grain kinetics. The traditional continuum approach, based on sediment concentration and its fluctuations, cannot adequately describe the experimental data. In fact, discussing sediment entrainment and suspension in terms of concentration may well obscure some of the fundamental mechanics of sediment-laden flows.

A review of previous theoretical and experimental investigations of the basic mechanics of sediment transport is given in Chapter 2. The traditional thought about suspension and entrainment of sediment by water is traced. Relevant experimental results are summarized.

A discussion of the meaning of fluid turbulence and an approach to sediment transport mechanics from the kinetics of individual sediment grains is given in Chapter 3. The form of the raw laser velocimetry data is presented. How such data can be processed to give insight into the basic mechanics of sediment transport is discussed. The meaning of sediment concentration and its relationship to individual grain motions is explored.

The application of the laser-Doppler velocimetry to sediment-laden flows is detailed in Chapter 4. The particular difficulties encountered in this study are discussed.

Chapter 5 enumerates and explains the velocimetry data analysis procedures. The errors inherent in the technique and the details of the data processing are discussed.

The experimental apparatus is briefly described in Chapter 6. A general description of the experimental flow conditions and the procedures followed is given in Chapter 7. The processed data are presented in Chapter 8 and discussed in Chapter 9. Suggestions for further work are also given in Chapter 9. The summary and conclusions of this study are presented in Chapter 10.

This work is the first portion of on ongoing experimental program to investigate the fine-scale time-varying characteristics of sediment-laden flows. The goal of this portion was two-fold. First was the development and implementation of instrumentation capable of observing these characteristics. Second was the development of a conceptual framework for the interpretation of the data obtained and to relate this new data to the results of previous investigations. This thesis reports on the development of the one-dimensional velocimetry system and the results obtained. The conceptual framework for the anticipated two-dimensional observations is established here. The necessary modifications to existing instrumentation are being made to implement the two-dimensional velocimetry system for continued research following this thesis.

CHAPTER 2

LITERATURE REVIEW

Previous investigations on the basic mechanics of turbulent sediment suspensions, including the effects of sediment grains on turbulent flow characteristics, have been primarily experimental. The relevant literature includes studies of flows transporting neutrally buoyant particles as well as studies of sediment-laden flows. This chapter reviews the various types of investigations relevant to the understanding of the entrainment and suspension of sediment in a turbulent fluid and relates that previous work to the present inquiry.

2.1 Theoretical studies of sediment suspension

A theoretical expression for the vertical sediment concentration distribution in a two-dimensional open channel flow was developed by O'Brien (1933) and expanded by Rouse (1937). By equating the upward diffusion of suspended sediment due to turbulence to the rate of settling due to gravitational force, they obtained the suspended load differential equation

$$v_s c + \epsilon_s \frac{\partial c}{\partial y} = 0 \qquad (2.1.1)$$

Here, y is measured vertically upward from the sediment bed, ϵ_s is the turbulent diffusion coefficient for sediment, c is the time-averaged suspended sediment concentration, and v_s is the settling velocity of the sediment grains in clear, stagnant fluid. In this form, the equation can only be solved if ϵ_s and v_s are known. If, following von Karman (1934), the diffusion coefficient for sediment is assumed proportional to the diffusion coefficient for fluid momentum, a

solution can be obtained. In a two-dimensional open channel flow, the momentum diffusion coefficient may be derived for the logarithmic velocity profile, giving

$$\epsilon_m = ku_*y(1 - \frac{y}{d}) \qquad (2.1.2)$$

where k is the von Karman constant, u_* is the fluid shear velocity ($u_*= \sqrt{\tau_o/\rho}$), d is the fluid depth, τ_o is the boundary shear stress, and ρ is the fluid density. Assuming that

$$\epsilon_s = \beta\epsilon_m \qquad (2.1.3)$$

where β is presumed to be a constant and substituting into equation 2.1.1 above, the solution is

$$\frac{c}{c_a} = (\frac{d-y}{y}\frac{a}{d-a})^z \qquad (2.1.4)$$

where c_a is the concentration at depth a and z is the "Rouse" exponent ($z=v_s/\beta ku_*$). The above equation was not expected to be reliable very near the bed (y=0) or very near the surface (y=d) as the velocity profile deviates from the logarithmic law in those regions.

Einstein and Li (1958) proposed an intermittent model of the laminar sublayer. The sublayer was supposed to behave cyclically, growing in thickness, then rapidly disintegrating. In this manner, velocity fluctuations could diffuse and extend throughout the flow. The entrainment of individual sediment grains from the bed would take place during the disintegration phase.

The intermittent behavior of the laminar sublayer was explicitly studied by Sutherland (1966). He made simultaneous observations of a dye streak near a flat sediment bed and the movement of individual

sediment grains. When the local dye line was disrupted, grains moved. He hypothesized that turbulence from the main flow impinges on the bed, disrupting the laminar sublayer and entraining sediment.

Large scale, coherent structures or bursts as the mechanism for sediment suspension were suggested by Jackson (1976). Observers of rivers have long noticed that the water surface is periodically disturbed by boils containing large amounts of suspended sediment. Recent developments in the study of turbulent shear flows (for example Offen and Kline (1975)) indicate that these boils may well be the result of large upward-tilted streamwise vortices. Thus, sediment grains may be periodically entrained at the bed and rapidly transported upward through the entire water column. Grains return to the bed relatively slowly, due to the action of gravitational forces. This argument was supported qualitatively by river data. Clouds of suspended sediment are also easily observed in flumes.

A theoretical treatment of particles suspended in turbulent flows was published by Hino (1963). A decrease in the von Karman constant with increased particle concentration was predicted. For neutrally buoyant particles, a predicted increase in root mean square turbulence intensity, $\sqrt{u'^2}$, agrees with the experimental data described below. The predicted slight decrease in $\sqrt{u'^2}$ for settling (negatively buoyant) particles is not in agreement with the prior experimental observations discussed in Section 2.3.

2.2 Experimental studies of mean properties in sediment-laden flows

The first experimental investigation of the effects of suspended sediment on the transporting flow was by Gilbert (1914). Contrary to his expectations, he noted that fluid discharge, sediment discharge and channel slope were not simply related.

The suspended load equation was experimentally verified by Vanoni (1946). Moreover, the experiments demonstrated that suspended sediment at alluvial concentrations affects the turbulent characteristics of the flow. Vanoni observed an increase in the slope of the velocity profile, or decrease in the von Karman constant, with increasing sediment load. Near the bed, the velocity profile departed from the logarithmic profile. Vanoni speculated that the presence of sediment suppressed or damped out turbulence, causing the mixing of momentum to be reduced, thus reducing the von Karman constant.

Vanoni's results were confirmed and expanded by his students, Ismail (1952), Brooks (1954) and Nomicos (1956). Ismail noted that the flow resistance in a sediment-laden flow was increased over that in a clear fluid flow only when bed forms occurred. He found that β was a function of sediment size (β=1.5 for d_g=0.10 mm, β=1.3 for d_g=0.16 mm).

In a more careful analysis, Brooks noted a variation in β of only 0.93 to 1.10 with sediment size. This analysis includes a decrease of the mean sediment size with elevation in the suspension due to selective sorting and reduction of the fall velocity due to particle interference. He concluded that β is very close to 1.0. This analysis demonstrated the need to consider sediment size variations with height

above the bed when applying the suspended load equation. For each sediment size fraction, a mean fall velocity is computed. The suspended sediment samples were sieved into separate size fractions and vertical sediment concentration profiles and z values were obtained for each size fraction.

Brooks also considered the meaning of the "sediment bed". To compute the total sediment discharge, the integral

$$\int_{y_o}^{d} u\, c\, dy \qquad (2.2.1)$$

where u is the fluid velocity is performed. Here, y_o is chosen to be small distance above y=0, as otherwise the integral diverges for $z \geq 1$. Four reasonable possibilities were proposed

$$y_o/d = \begin{cases} = 2d_{50}/d & 2d_{50} \text{ above the bed as lower limit of suspension} \\ = 11.6\nu/u_* d & \text{estimated laminar sublayer} \\ = e^{-ku/u_*} - 1 & u(y_o/d) = 0 \text{ by the logarithmic velocity law} \\ \left[\dfrac{c(y=\frac{d}{2})}{c_b}\right]^{1/z} & c(y_o/d) = \text{bed concentration} \end{cases} \qquad (2.2.2)$$

Brooks advocated the use of the maximum y_o. He also reported a deviation from the predicted suspended sediment profiles in the upper half of the flow. He concluded that in this region, where the shear stress and concentration gradients are small, the assumption that mixing of sediment is proportional to the mixing of fluid momentum is no longer valid.

Nomicos observed the effects of increasing sediment concentration on the flow. He formed a stable artificial flat bed of sediment in a

recirculating flume. Flows at the same discharge and depth with increasing, but small, amounts of sediment in the flume system were observed. His experiments showed that, with the flow Reynolds number and boundary roughness held constant, an increased sediment load decreased the friction factor. The velocity profile was observed to differ greatly from the logarithmic law near the bed.

Einstein and Chien (1952,1955) proposed modifications to the suspended load theory based on a mixing length concept. Their expression contained an unevaluated constant. Flume experiments did not help to evaluate the constant, and as such the expression is of little practical use. They also correlated the value of the von Karman constant to the ratio of the power to suspend sediment, P_{sw}, and the stream power, P_s. This ratio is given by

$$\frac{P_{sw}}{P_s} = \frac{(\frac{\rho_s}{\rho} - 1)\, v_s \bar{c}}{uS} \qquad (2.2.3)$$

where ρ is the fluid density, ρ_s is the sediment density, g is the gravitational constant, S is the slope of the flow energy grade line, and $\bar{c}$ is the depth-averaged concentration. The ratio can be used to predict k.

Bagnold (1954) suggested that collisions between individual sediment grains provide the shear to suspend sediment. He performed experiments using neutrally buoyant particles in the annular space between two concentric cylinders to confirm this. The intergranular stress was found to be very small when the concentration of sediment was below 0.25 per cent by volume. Thus, grain collisions may only be important near the sediment-bed where the sediment concentration

approaches this value.

2.3 Experimental studies of fluctuating properties in sediment-laden and related fluid flows

In order to appreciate the effects of suspended sediment on turbulence characteristics, a knowledge of those characteristics in clear fluid flows is necessary. The first measurements of turbulent velocity fluctuations in a two-dimensional flow field were made by Laufer (1950). Data were obtained with a hot-wire anemometer in a wide rectangular air duct with smooth walls. He found that longitudinal turbulence intensity, $\sqrt{\overline{u'^2}}$, has a minimum at the centerline y=d/2 (analogous to the free surface in an open channel) and a maximum, approximately twice the wall shear velocity, at a small distance from the wall. As Reynolds number decreased, the relative turbulence intensity was observed to increase.

Turbulence measurements in a water flow in a flume were obtained by Raichlen (1967) using a hot-film anemometer. The relative longitudinal turbulence intensity, $\sqrt{\overline{u'^2}}/u$, was observed to be a maximum near the flume bottom and decreased toward the free surface. Neither a clear maximum in turbulence intensity nor a change in turbulence intensity with Reynolds number were noted. Turbulent length scales were found to be proportional to the flow depth.

Blinco and Partheniades (1971) used a hot-film anemometer to measure turbulence characteristics over smooth and rough boundaries (d_g=2.54 mm for the latter). They found that $\sqrt{\overline{u'^2}}$ was affected by the boundary roughness. A maximum in $\sqrt{\overline{u'^2}}$ was noted at some distance from the wall. The position of the maximum $\sqrt{\overline{u'^2}}$ was strongly related to

the boundary roughness; as the boundary roughness increased, the maximum was observed further away from the boundary.

Measurements in flows transporting neutrally buoyant particles were reported by Elata and Ippen (1961). An impact tube pressure transducer was used to measure longitudinal velocity fluctuations in flows with up to 0.25 per cent by volume polystyrene spheres. An increase in turbulence intensity and a decrease in von Karman constant were noted with increased particle concentration. A small increase in friction factor with increased particle concentration was reported. Elata and Ippen concluded that suspended particles do not damp turbulence, but rather change its structure. They speculate that the particles cause increased production of small scale eddies, on the order of the particle size. The major effect of suspended particles occurs near the flow boundary. Particle size is judged to be more important than particle buoyancy in altering the fluid turbulence. These results were confirmed by Daily and his co-workers (1961,1964,1966).

Bohlen (1969) made hot-wire anemometer measurements in flows transporting particles which were only slightly negatively buoyant. The experiments were made in an open channel, 3 cm deep, using silicon oil as the transporting fluid. Particle concentrations from 0.8 to 3.5 per cent by volume were observed. The mean particle fall velocity (d_g=0.595 mm) was 0.37 cm/sec. Bohlen reported a decrease in the von Karman constant and an increase in turbulence intensity. He noted that a maximum in $\sqrt{\overline{u'^2}}$ near the bed as in clear fluid flows did not exist in particle-laden flows. Turbulence intensity increases with particle

concentration throughout the depth, but particularly so near the boundary. Eulerian velocity fluctuation auto-correlations did not show any obvious effects of particle presence. Bohlen notes that particles colliding with the probe may introduce error in velocity fluctuation measurements due to vibration of the wire. At the low concentrations used, he judged the error to be negligible.

Hot-film anemometer measurements in sediment-laden flows were taken by Mc Quivey (1973). He reported higher turbulence intensity in flows transporting sediment than in clear water flows with the same flow depth, shear velocity and boundary roughness. His raw anemometer data contained large voltage spikes which he attributed to sand grains colliding with the probe tip. Peaks in the velocity auto-correlation due to collision-induced vibrations of the probe were also reported. Mc Quivey stated that these effects need not invalidate the data taken. He recommended a procedure of removing the spikes, and the application of a correction developed for fluid contaminated by dust or bubbles. Knowledge of the vibrational charateristics of the probe was said to allow better interpretation of the auto-correlation and power spectrum.

Investigators have applied the laser-Doppler technique to sediment-laden flows; however, such applications have been primarily for preliminary instrument development purposes rather than investigations of the physics of the fluid-sediment interaction. Müller (1973) compared measurements of mean velocity and longitudinal turbulence intensity in a movable bed sediment-laden flow ($u=68.8$ cm/sec, $d=2.57$ cm) with measurements in a clear fluid flow over a fixed sediment bed. A commercially available velocimeter with

conventional transmitting optics and a frequency tracker processor was used. An increase in turbulence intensity was reported. As explained in Chapter 4, the increase may be primarily due to the spectral broadening inherent in frequency tracker processor.

Müller and Glover (1977) proposed a method for avoiding saturation of the photodetector due to the larger light scattering by the sediment grains. A vertical sediment-laden flow of unreported concentration was used to test the method. Durst (1978) detailed a method used successfully in turbulent gas flows with glass spheres (d_g=100, 200, 400, and 800 μm). The concentration of the spheres was not reported. Complex receiving optics and electronics were used to separate the light scattered by the spheres from that by the gas flow tracer particles. The method is said to be applicable to sediment-laden water flows.

Luque and van Beek (1976) reported measurements of turbulent bed shear stress obtained by laser-Doppler velocimetry in flows near the threshold of motion. A slight decrease in root mean square bed shear stress, on the order of 10 per cent, was noted with the initiation of sediment motion. No direct velocity measurements were reported.

2.4 Summary

The interactions between suspended sediment and fluid turbulence have, for the most part, been surmised from measurements which are averaged over large spatial and temporal samples.

The relevance of measurements in flows with suspensions of neutrally buoyant particles to sediment-laden flows is limited. First, no fixed bed of the transported particles is formed. The bottom channel roughness is unaffected. Moreover, neutrally buoyant particles do not create a density gradient in the flow. Density, turbulence generation and turbulence dissipation are quite interrelated. The density is most affected in a sediment-laden flow near the boundary, the site of turbulence generation.

Measurements of turbulent flow characteristics in two-phase flows with hot wire and hot film anemometers are limited by calibration difficulties. The abrasion of the probe tip and the vibration of the probe due to particle impact creates long term drift in the velocity measurement. Also, any probe distorts the local fluid flow field especially near the sediment bed, which is scoured locally in the vicinity of the probe.

As the laser-Doppler velocimetry technique is still relatively new to the field of experimental fluid mechanics, few applications of the technique to particle-laden fluids have been reported. Most publications demonstrate the success of the application of an experimental apparatus to a flow situation, rather than exploring the fluid mechanics of that flow in detail.

To understand the fundamental mechanics of sediment-laden flows, measurements of the fine-scale, time-fluctuating flow characteristics are required. Laser-Doppler velocimetry is the most promising technique because it allows direct non-intrusive measurements of the flow velocity.

CHAPTER 3

FLUID TURBULENCE AND SEDIMENT GRAIN KINETICS

By use of laser velocimetry it is possible to observe directly the motion of individual sediment grains and the turbulent fluid which is transporting such grains. To make use of such data, the mechanics of sediment entrainment and suspension must be examined on a granular scale. Furthermore, this approach must be reconciled with the traditional continuum approach, utilizing the concepts of mean sediment concentration and turbulent diffusion in deriving the suspended load equation. The mean motion of a collection of sediment grains must be related to the motion of the individual grains.

This chapter discusses the general case of data available from a two-dimensional laser-Doppler velocimeter. The instrument developed during and employed in this study is a one-dimensional velocimeter, measuring only the streamwise velocity component. The one-dimensional results obtained are a subset of the two-dimensional results discussed.

The basic data received from a two-dimensional velocimeter consist of a set of four scalar time series

$$\begin{matrix} u\,(t_i) \\ v\,(t_i) \end{matrix} \qquad i=1,2,3,\ldots,N_I$$

$$\begin{matrix} u_g(t_j) \\ v_g(t_j) \end{matrix} \qquad j=1,2,3,\ldots,N_J$$

where u and v are streamwise velocity and vertical velocity and the subscript g denotes sediment grain values. Note that the times of measurement t_i and t_j are not coincident. The raw data from a single experiment consists of a set of such velocity observations at each of

several vertical positions within the flow field, all on the flume axis.

3.1 A grain-by-grain approach to the mechanics of sediment-laden flows

Consider the sediment grain measurements at a single vertical position. The intersecting laser beams form a measurement volume with an effective frontal area, dA. Note that the effective frontal area is a function of the actual, optically determinable, laser beam intersection cross-sectional area, the geometry of the receiving optics, and size of the scattering particles. The effective area is small, on the order of a few times the cross-sectional area of a single sediment grain. If every grain which passed through this area generated a single good velocimetry signal, the velocimeter would be, effectively, a particle counter. The sediment mass flux through the effective frontal area would be given by

$$q_s(dA,\Delta t) = \frac{1}{\Delta t\, dA} \sum_{j=1}^{N_J} m_j f_j \qquad (3.1.1)$$

where f_j is the mean fraction of the volume of the jth grain which passed through the area dA, m_j is the mass of the jth sediment grain, N_J is the number of sediment grains observed in time Δt, $q_s(dA,\Delta t)$ is the sediment transport rate (mass/time/area), and Δt is the sampling time. To determine f_j, the exact trajectory through the beam intersection volume of the sediment grain must be known. This is not feasible. A grain need never be wholly contained within the volume yet will generate a valid velocimetry signal. A sediment grain may graze the volume without generating a valid velocimetry signal. If each

grain is assumed to have $f_j=1$, the sediment flux may be overestimated during the time that a grain is observed and underestimated during the time that no grain is observed. Averaging over a large number of grains, however, the contribution to the sediment flux by the grains which graze the beam intersection volume should balance the excluded portions of the grains which generate valid velocimetry signals. That is, in the mean, the two effects will tend to cancel. Thus, for a uniform sand, the above simplifies to

$$q_s(dA,\Delta t) = \frac{mN_J}{\Delta t\, dA} \qquad (3.1.2)$$

The effective frontal area, dA, remains to be determined. There is a physical surface area to the laser beam volume, but due to the small size of the volume, on the order of a few grains, the physical area is not the effective area. Most grains which generate good velocimetry signals will never be more than half contained within the physical beam intersection volume. To determine the effective frontal area, calibration is necessary. Thus, the mean sediment transport rate may be determined by the velocimeter only after calibration with traditional suction sampling tube measurements. The resulting calibration is only valid for the long time-averaged mean transport rate.

Unfortunately, the actual situation is more complex. While the effective scattering volume is small, it is large enough to allow multiple grains to pass through simultaneously. The probability of the scattering by multiple grains is a function of the scattering volume size, the grain size, and the local grain concentration. If every grain velocimetry signal is assumed to be generated by a single

sediment grain, the sediment flux will be underestimated. As the sediment flux increases, the probability of scattering by multiple grains increases, and the error in the estimate of the flux increases. The sediment transport rate may be determined by the velocimeter after calibration with traditional suction sampling tube measurements, but the calibration will not be linear.

From the above raw data, it is possible to compute a time series of sediment grain inter-arrival times, δt_{g_j}, and their mean, $\overline{\delta t_g}$.

$$\delta t_{g_j} = \frac{1}{2} (t_{j+1} - t_{j-1})$$

$$\overline{\delta t_g} = \frac{1}{N_J - 1} (t_{j=N_J} - t_{j=1}) \qquad (3.1.3)$$

Thus, the mean sediment transport rate is inversely proportional to the mean sediment grain inter-arrival time. Similiarly, fluctuations in the transport rate are related to fluctuations in the reciprocal of grain inter-arrival time. Periods of high relative transport are associated with relatively short grain inter-arrival times; low transport with long grain inter-arrival times.

The mean and variance of the grain velocity may be calculated for an ensemble of grains passing through the measuring volume. The grain data may also be split into two groups: upward-moving grains and downward-moving grains. Note that the mean grain velocity and inter-arrival time of the upward-moving grains need not be equal to the means of the downward-moving grains on the average over time. For the transport in the vertical to be in equilibrium, all that is required is that the number flux of the upward-moving grains be equal to the number flux of the downward-moving grains through the measuring volume. If

large scale turbulent bursts are a primary entrainment mechanism, it may well be that the mean velocity of the upward-moving grains is larger than that of the downward-moving grains.

Now consider the full data set. It is possible to relate fluid velocity measurements with sediment grain velocity measurements. The grain slip velocities, computed in this way, are given by

$$\begin{aligned} \tilde{u} &= u_{g_j} - u_i \\ \tilde{v} &= v_{g_j} - v_i \end{aligned} \qquad (3.1.4)$$

The computation may be made for any t_i and t_j, but is only physically meaningful if the time lag between measurements, $/t_i-t_j/$, is small with respect to the turbulence time scale. The mean vertical slip velocity may be compared to the quiescent fall velocity (the average rate of fall of the grain in clear quiescent water) to determine the effects of turbulence and sediment transport on sediment grain settling. The grain record may be again split into upward-moving and downward-moving grains. Upward-moving grains should be associated with upward-moving fluid parcels, fluid parcels with positive vertical fluid velocity.

Correlations of grain inter-arrival times with fluid velocity may also be computed. The correlations of fluid velocity fluctuation with the inverse of sediment grain inter-arrival time have important physical interpretations. As noted above, the inverse of the sediment grain inter-arrival time is a measure of the sediment transport rate. Thus, the above are correlations of transport rate and fluid velocity. If these correlations are made with the divided grain record, with upward-moving and downward-moving grains, the correlations give insight into entrainment. If large scale turbulent bursts are a primary

entrainment mechanism, positive fluid velocity fluctuations should be associated with low sediment grain inter-arrival times. Settling, downward-moving grains should be diffuse, have longer inter-arrival times, and not be associated with strong positive fluid velocity fluctuations. A measure of the length scale over which the sediment grain is affected by the fluid turbulence may be made by computing the above at different lag times.

In summary, a sediment-laden flow is a mixture of flowing fluid and individual moving sediment grains. The motion of the grains is affected by and affects the fluid motion, but may be examined independently. The sediment transport rate may be considered independently of the fluid discharge or suspended sediment concentration. Direct measurements of grain motions give insight into certain details of the mechanisms of suspension and entrainment.

3.2 Sediment concentration and the continuum approach to the mechanics of sediment-laden flows

It remains to tie the laser velocimetry measurements and the grain-by-grain viewpoint to previous measurements and theory. Central to previous work is the concept of sediment concentration. Concentration is usually defined as the ratio of the sediment mass discharge through some sample area to the total volume flux through the same sample area. In alluvial flows, the total volume flux is effectively equal to the fluid volume flux. Thus, sediment concentration is given by

$$c(T) = \frac{q_s(T)}{q(T)} = \frac{1}{\bar{T}\bar{u}dA_s} \sum_{j=1}^{N_J} m_j \qquad (3.2.1)$$

where c(T) is the sediment concentration (mass/volume), dA is the inflow cross-sectional sampling area, m_j is the mass of the jth sediment grain, N_j is the number of grains collected, T is the sampling time, and $\bar{u}$ is the mean inflow velocity. For a uniform sand, this simplifies to

$$c(T) = \frac{mN_J}{T\bar{u}dA_s} \qquad (3.2.2)$$

Note that the concentration is not only a function of the sediment transport but also of the fluid volume flux.

Imbedded in the concentration approach is the assumption that a sediment-laden flow may be treated as a continuum. It is assumed that sediment grains may be treated as a tracer, similiar to dye, heat, or buoyancy. This approach is only valid if the length and time scales of the relevant fluid properties are on the same order of those of the tracer properties. For molecular tracers, such as dye, the validity is obvious. For sediment, the concept must be applied with care.

Mean sediment concentration must be defined over a large number of grains, a large sample volume and large sampling time. In the case of traditional sampling tube samples, which have a sample volume of one liter, the number of grains collected per sample typically ranges from one thousand to one million. The sampling time is on the order of three minutes. The sampling tube collects some large set of grains which is sampled and weighed. The sampling tube is, in effect, a grain counting device. Grains are not individually counted; however, the number of grains collected in a suction sample may be computed for sediments of known size distribution. The mass collected per unit time is the sediment flux through the sampling tube intake area. A sediment

concentration measurement is then derived from that measured sediment flux by dividing by the fluid volume flux. In analysis, that concentration "measurement" is then multiplied by the mean velocity measurement (at the same point) to compute the sediment transport rate. The sediment transport rate is the originally measured quantity. In other words, sediment concentration is not measured directly with a sampling tube; it is the sediment transport rate through the sampling tube tip which is observed.

Concentration fluctuations (c') must also be defined over some number of grains. Fluctuations in concentration are a function not only of the "instantaneous" sediment transport, but of the "instantaneous" volume flux. Usually, fluctuations in concentration are defined to derive an expression for fluctuations in transport. This is the case in the suspended load equation which expressed the vertical conservation of sediment flux as

$$\overline{(v_s + v')(c + c')} = v_s c + \overline{v'c'} = 0 \qquad (3.2.3)$$

The first term, $v_s c$, is the mean sediment transport due to gravity (negative for settling down). The second, $\overline{v'c'}$, is the net upward transport due to fluid turbulence. Both terms apply to averages over some volume of fluid which contains both upward-moving and downward-moving grains. It is not possible to assign individual grains to either term. The motion of an individual grain is determined by both effects.

The term $\overline{v'c'}$ is the correlation of the vertical fluid velocity fluctuations and the sediment concentraton fluctuations. If the length scales of the two processes are disparate, the expression losses its

physical significance. In alluvial flows, particularly in laboratory flumes, this is the case. Consider the case of fine sand, d_g=0.25 mm, in transport (u=50 cm/sec, d=7.5 cm). At common equilibrium concentrations, on the order of 0.3 grams per liter, the grains will be separated by about 20 grain diameters, approximately 5 mm. Measurements by Raichlen (1967) in a clear water flow may be used to estimate the turbulence length scales. Even if the "instantaneous" concentration is defined over a sample volume containing only ten grains, the volume required would be approximately three times that of a turbulent eddy with a diameter equal to the fluid turbulence micro scale (estimated as 0.1 times the depth).

The flow volume actually sampled is a long filament of the flow. In the case of a suction sampling tube, a one liter sample is typically a filament 90 meters in length. The cross-sectional area of the laser velocimeter is substantially smaller than that of a suction sampling tube. To sample a one liter volume of the flow, the velocimeter must observe a filament approximately 500 meters in length. To observe ten sediment grains, the velocimeter will sample a 5 cm filament. This length is on the order of the turbulence macroscale of the flow. The two processes, fluid velocity fluctuation and sediment concentration fluctuation, seem to have quite different length scales. This is an artifact of the relatively large length scale required to define sediment concentration fluctuations.

The suspended load equation is a statement of the competing effects, gravity and fluid turbulence, which suspend sediment. Computation of a $\overline{v'c'}$ term would not give insight into actual

entrainment mechanisms. Nor is there insight into the fine scale, time-varying structure of the fluid-sediment mixture. There are many complex small scale interactions in a sediment-laden flow which cannot be adequately described by time-averaged quantities and continuum concepts. However, grain motion measurements, together with fluid turbulence measurements, should yield valuable insight into the mechanisms of suspension and entrainment when examined on a grain by grain basis.

3.3 Fluid turbulence and Eulerian measurements of fluid velocity fluctuations

Consider first only the fluid velocity measurements. The data are similar to the majority of the existing experimental observations of turbulence. Comparision of the data obtained in a sediment-laden flow to similar data obtained in a clear fluid flow would seem to allow direct determination of the effect of transported sediment on the fluid turbulence. Unfortunately, such a determination is not simply possible.

Most experimental observations of turbulence in fluid flows are Eulerian. The fluid velocity is sampled at a single spatial location over some observation time which is long with respect to the time scales of any fluctuations in the flow. The data from several locations, obtained at non-coincident times, are used to infer the Lagrangian behavior of the flow field. The behavior of a fluid parcel as it moves through space is extrapolated from measurements of a number of fluid parcels which pass a set of known spatial locations.

The validity of inferring the Lagrangian nature of sediment-laden flows is questionable. A flow transporting sediment has, by necessity, a movable, deforming boundary. Even in the relatively simple case of transport in the flat bed regime, the flow boundary, the sediment bed, is continously in motion. In fact, the bed is defined primarily by convention, typically by the elevation observed in a quiescent flume. No rigorous determination of the location at which the fluid and sediment motion ceases has been made.

The motions of the flow boundary have two important consequences. First, the time required to observe all possible fluctuations of the flow is determined not only by the time scales of the fluid turbulence, but also by the time scales of the bed deformations. Observations over a few minutes are typically sufficient to characterize the fluid velocity fluctuations in fixed-boundary flows. In a sediment-laden flow, to characterize the bed motion adequately may require hours of observation. Second, a measurement location may be fixed at a point in space, but not fixed with respect to the boundaries of the flow field. This is most obvious if dunes are present.

The importance of the bed deformation on various flow properties is related to the magnitude of the deformation and the sensitivity of the selected flow property. Long term, spatially averaged properties, such as fluid discharge, are relatively insensitive to even large fluctations in bed elevation. Average fluid velocity at a point may be sensitive only to large changes in bed elevation. Fluid velocity fluctuations and local values of boundary shear may be sensitive to relatively small fluctuations in the bed elevation.

The order of magnitude of the change in fluid velocity due to small fluctuations in bed elevation may be estimated by a simple calculation. Assume the fluid velocity follows the logarithmic law and that the variation in the bed elevation is sinusoidal. The velocity at a fixed point in space will vary over the period of the bed oscillation. The observed standard deviation in the fluid velocity is shown in Figure 3.3.1 for various amplitudes of bed distortion. The fluctuations induced, even for the relatively small amplitudes considered, are of the order of the velocity fluctuations experimentally observed in turbulent flows.

Thus, it is not meaningful simply to compare velocimetry observations in movable boundary flows with observations in fixed boundary flows. In a fixed-bed flow, the velocity fluctuations are due solely to fluid turbulence. In a movable bed flow, the observed velocity fluctuations may also be due to deformations of the flow field. The turbulent kinetic energy of the fluid may be reduced with respect to that in a clear fluid flow due to the work done to suspend sediment, yet the fluid velocity fluctuations observed at a fixed point in space may be increased.

There exists an additional mechanism for the generation of fluid velocity fluctuations. Clear fluid flows with density stratification support internal waves. A fluid flow with suspended sediment is a density-stratified flow. The density gradient is a function of the sediment concentration gradient.

$$\frac{\partial \rho}{\partial y} = \left(\frac{s-1}{s}\right) \frac{\partial c}{\partial y} = -\left(\frac{s-1}{s}\right) cz \left(\frac{d}{d-y}\right) \frac{1}{y} \qquad (3.3.1)$$

where ρ is the flow density, s is the specific gravity of the sediment

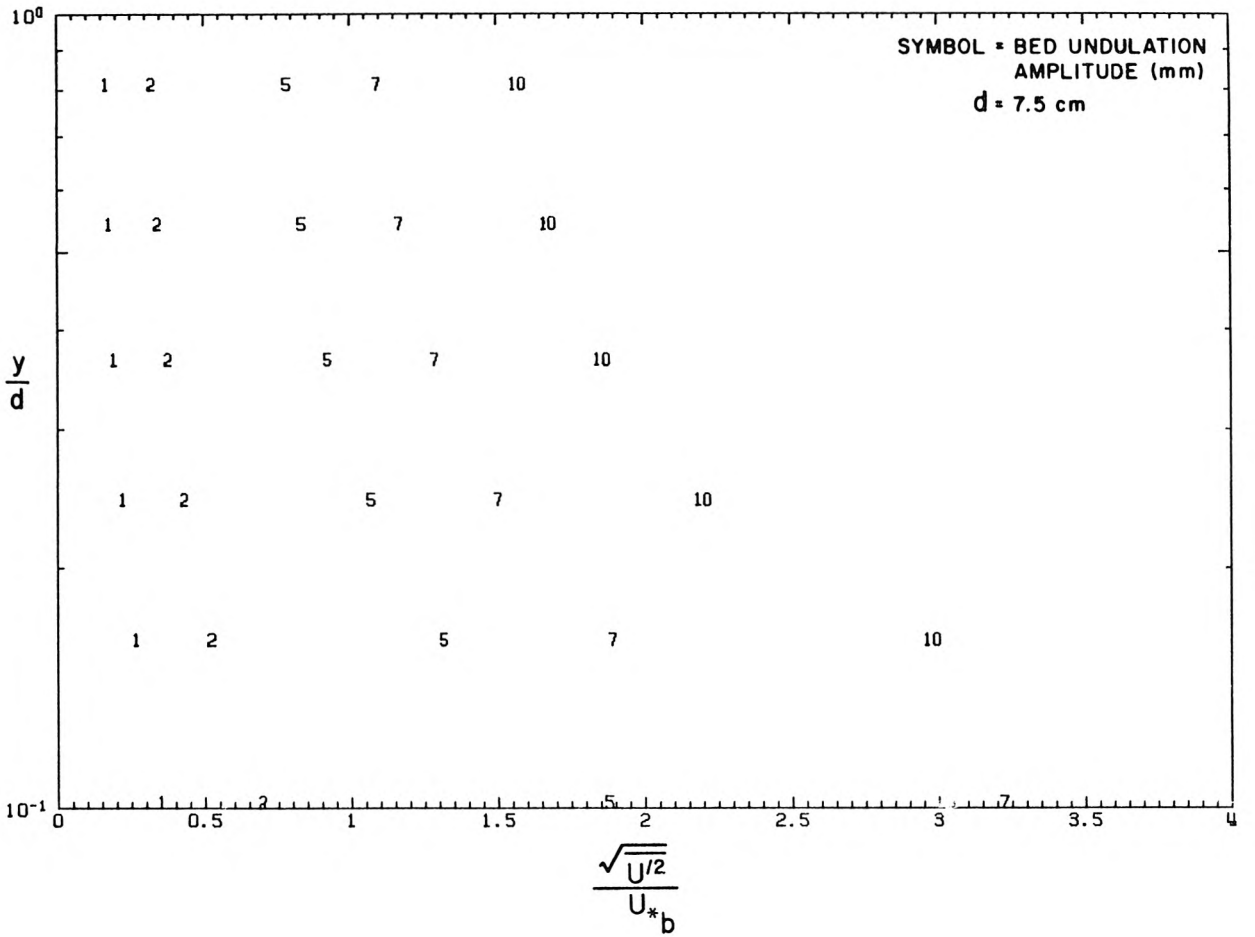

Figure 3.1.1 Computed velocity standard deviation due to oscillations of the sediment bed

and c is the sediment concentration (mass/volume). The time scale of such wave motion is determined by the Brünt-Väisälä frequency, given by

$$N^2 = -\frac{g}{\rho}\frac{\partial \rho}{\partial y} \qquad (3.3.2)$$

where N is the Brünt-Väisälä frequency and g is the acceleration of gravity. The frequency therefore will vary from 0 at the free surface to approximately 3 Hertz near the bed surface. Thus, velocity fluctuations with time scales on the order of the turbulence macroscale may occur due to internal wave motions.

In summary, the velocity fluctuations observed in a sediment-laden flow may be caused by migrating bed forms and internal waves in addition to fluid turbulence. Thus, it is not possible simply to determine the effects of sediment entrainment and suspension on the fluid turbulence. In fact, due to the long times required to characterize some bed forms, the quantity of data required to observe all existing fluctuations in the velocity may well be prohibitively large.

CHAPTER 4

LASER-DOPPLER VELOCIMETRY APPLIED TO SEDIMENT-LADEN FLOWS

The laser-Doppler technique has been used quite successfully in homogeneous fluid of two-phase gaseous flows. The technique does not distort the flow field and no calibration is required. Thus, it is particularly attractive for use in sediment-laden flows. There are, however, unique difficulties with the technique when applied to such flows. This chapter discusses the application of the technique to a sediment-laden flow. It is not intended to describe in detail the basic technique, but rather to give an overview of the specific system developed for use in sediment-laden flows in this study. For a general discussion of laser-Doppler velocimetry, see Durst, Melling and Whitelaw (1976). For a detailed description of the system developed in this study see van Ingen (1980) and van Ingen (1981).

Due to lack of instrumentation, most previous investigations of sediment-laden flows have been limited to time-averaged measurements of flow variables. Also, most measurements have averaged over a large spatial volume. The interactions between fluid turbulent structure and suspended sediment have been theorized from the mean sediment concentration and mean velocity profiles. Hot-film anemometry has been done in sediment-laden flows, but the technique has real disadvantages. Sediment grains collide with the probe tip, seemingly causing short voltage spikes in the signal. Rapid abrasion of the probe tip gives long term calibration difficulties due to the changing thermal conductivity of the probe surface. Moreover, the local flow field is deformed by grain-probe collisions in two ways: vibrations of the

probe at its natural frequency are induced and the sediment grains are deflected from their natural trajectory. The gross flow field is also distorted, as the introduction of any probe in the vicinity of the movable sediment bed induces scour.

In homogeneous fluid flows, the laser-Doppler technique depends on the presence of small scattering particles. The flow is either seeded (particles are added to the fluid) or filtered to obtain a diffuse distribution of scattering particles. Ideally, at any instant only one particle is present in the measuring volume. The particles are chosen to be small enough ($\sim$10 μm) to follow the small scale fluid flow. In a sediment-laden flow, there are sediment grains also in suspension. These grains are quite large with respect to the small fluid tracer particles and need not follow the flow as the smaller particles do. The sediment grain concentration is determined by the flow mechanics; near the bed, the concentration becomes large and the grains are not diffuse.

For the laser-Doppler technique to be useful in a sediment-laden flow, the light scattered by the fluid tracer particles must be detectable and distinguishable from that scattered by the sediment grains. The measuring volume must be such that the sediment grains appear diffuse, that is, there are times in which only a fluid tracer particle is in the measuring volume.

Figure 4.1.1 shows the basic dual-scattering optical arrangement used in one-dimensional laser-Doppler velocimetry. The laser light beam is split into two beams of equal intensity, which are then made to intersect at a point within the flow field. When a particle passes

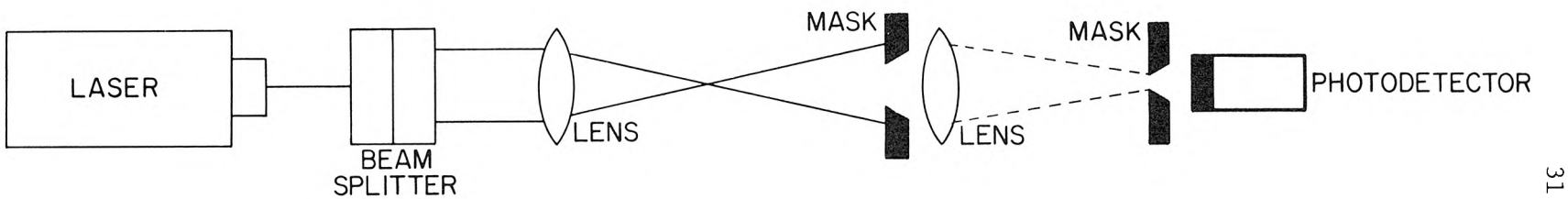

Figure 4.1.1 Basic one-dimensional dual-scatter optical arrangement for laser-Doppler velocimetry

through the laser beam, it scatters light which is frequency shifted according to the Doppler principle. The frequency shift, f, is given by

$$f = \frac{2u\sin\phi}{\lambda} \qquad (4.1.1)$$

where u is the particle velocity, 2ϕ is the beam intersection angle and λ is the wavelength of the incident light. The frequency shift is small with respect to the frequency of the incident light. The beam intersection volume is imaged on the surface of a photodetector by a collecting lens. When a particle passes through the beam intersection, it scatters light from both beams simultaneously. The collected light focused at the photodetector is a combination of light scattered from both beams. The response of a photodetector is slow with respect to the frequency of light, but not slow with respect to the difference frequency of the combined light.

The photodetector output current is proportional to the square of the intensity of the incident light. A typical photodetector output signal generated by a fluid tracer particle in a clear fluid flow appears in Figure 4.1.2.a. The signal consists of two parts: the pedestal or offset current and the Doppler modulated burst current. The offset current is caused by the Gaussian light intensity of the laser light beams. The total amplitude of the photodetector current is a function of the scattering particle size, the particle trajectory through the measurement volume and the geometry of the transmitting optics. The ratio of the pedestal amplitude to the Doppler burst amplitude is also a function of these factors.

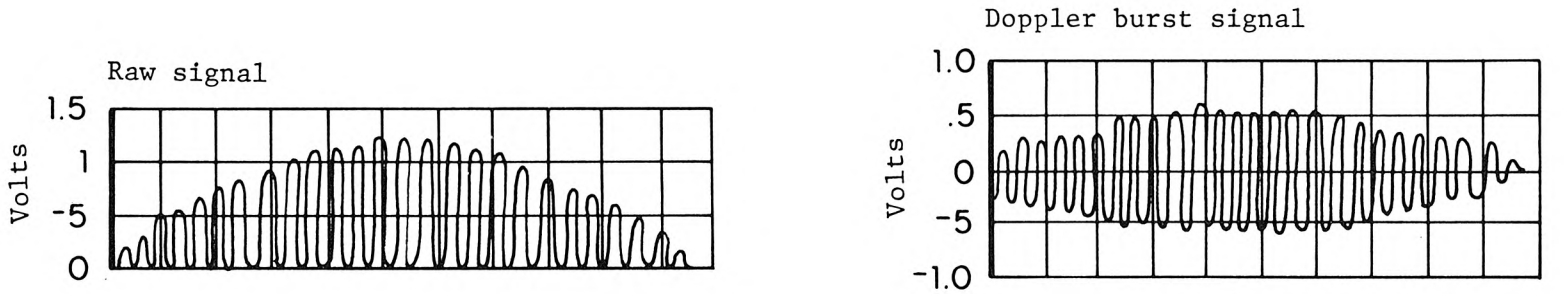

Figure 4.2.1.a Fluid tracer particle

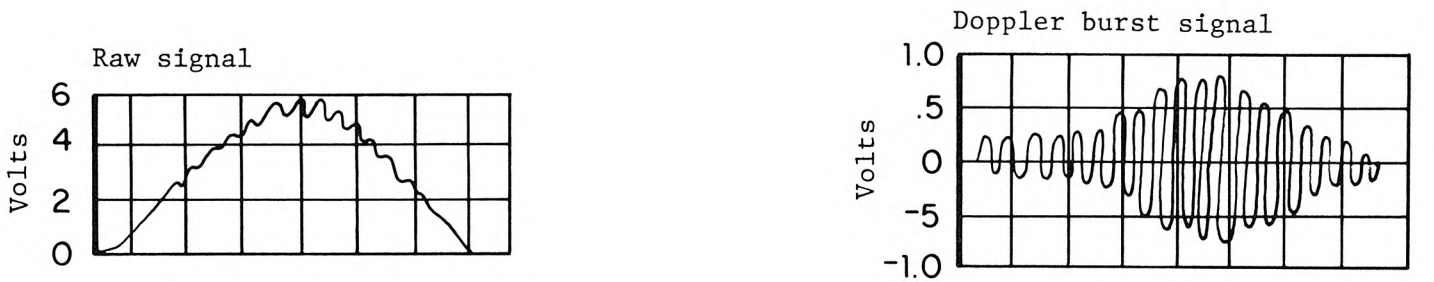

Figure 4.2.1.b Sediment grain

Figure 4.2.1 Typical photodetector output signals

A typical signal generated by a sediment grain using conventional dual-scatter optics is shown in Figure 4.1.2.b. That the light scattered by large particles is also Doppler scattered was demonstrated by Durst (1973) in experiments with steel balls. The signal shown in the figure was generated by a sediment grain cemented to a lucite disc. The disc was rotated at a known speed causing the cemented grains to pass through the measuring volume at a known velocity. Despite the non-sphericity of the grain surface, sediment grains do generate reliable Doppler modulated burst signals. It is therefore possible to measure directly the velocity of a sediment grain in situ.

In sediment-laden flows, the sorting of signals generated by sediment grains and fluid tracer particles can be accomplished by measuring the pedestal amplitude. Larger particles scatter more light. Since sediment grains are commonly on the order of 300 μm, they scatter much more light than the 10 μm fluid tracer particles. To distinguish various sediment sizes, however, is not simple. The exact particle trajectory through the measurement volume must be known. The preliminary experiments with the cemented grains on the rotating disc confirmed this. It is, however, quite simple to distinguish signals generated by sediment grains from signals generated by dust, polystyrene latex spheres, milk, latex paint particles, or other commonly used fluid tracer particles.

Sediment grains scatter so much more light than the smaller fluid tracer particles that detecting both types becomes a problem. The photodetector and processing electronics must be sufficiently sensitive to low amplitude scattering to detect the small particles, yet

sufficiently insensitive such that the large grains do not saturate the system. Also, a sediment grain which passes through a beam just outside the measuring volume scatters enough light to mask the scattering by a fluid tracer particle passing simultaneously through the beam intersection. This occurrence generates a burst of noise which must be distinguished from the Doppler burst generated by the particles and grains passing through the beam intersection. Thus, the transmitting optics must be such that there exist instants when not only are there no sediment grains within the measuring volume, but there are no grains in the beams near the volume.

In ordinary laser-Doppler applications, the angle of laser beam intersection is quite small ($\sim$2 degrees). This results in an elliptical measuring volume whose major diameter is on the order of fifty times the minor diameter. By increasing the beam intersection angle, thereby decreasing the ratio of the major diameter to the minor diameter, the measurement volume may be made smaller. If the minor diameter is then minimized, making it near the sediment grain diameter, the measuring volume becomes small enough to allow fluid velocity measurement. Sediment particles are sometimes absent from the measuring volume. A larger beam intersection angle also reduces the probability of the detection of light scattered by the sediment grains which pass through the beams just outside of the measurement volume. Thus, the scattering from water tracer particles can be detected. However, if the beam intersection angle gets too large, the scattering efficiency of the smaller fluid tracer particles lessens, making them quite hard to detect. Also, for the same particle velocity, a larger scattering angle generates a higher frequency Doppler modulated signal.

Doppler modulation frequencies up to 100 MHz have been successfully amplified and processed, but it is far simpler to process signals less than 1 MHz.

In this study, a beam intersection angle of 21.40 degrees was used. The major diameter of the beam intersection volume is therefore roughly five times the minor diameter. This angle was selected because the resulting beam intersection volume was estimated to be sufficiently small to allow the detection of both the fluid tracer particles and the sediment grains. The particular angle used may not be the most optically efficient. No serious attempt at optimization of the transmitting optical system was made.

Finally, the processing of the photodetector signal must be performed in a careful way due to the bursts of noise, caused by simultaneous scattering from multiple particles. As such bursts are far more likely in sediment-laden flows than in clear fluid flows, they must be identified and discarded prior to data analysis. If they are included in the data analysis, artificial, non-physical, broadening of the measured velocity spectrum will result. Realization of velocity must be made only when a single scattering particle is passing through the measuring volume. Each velocity realization must be independent of every other velocity realization. The photodetector signal must be regular in frequency before being processed. Simultaneous determination of the scattering particle type, whether a fluid tracer particle or a sediment grain, and particle velocity must be performed.

The above criteria imply either the use of a zero-crossing counter-processor or the direct digitization and computer analysis of

the photodetector signal. A frequency tracker should not be used due to the above probable causes of spectral broadening. Digitization of a 1 MHz signal at the Nyquist frequency for a period of several minutes results in excessive amounts of data which then must be reduced. Thus, the counter-processor method is preferable, as it generates far less data. The counter-processor used in this study is detailed in van Ingen (1980). Suggestions for the use of this processor are given in van Ingen (1981).

CHAPTER 5

ANALYSIS OF THE LASER-DOPPLER VELOCIMETRY DATA

This chapter discusses the acquisition and processing of the laser-Doppler velocimetry data presented in Chapter 8. Velocimetry data obtained in sediment-laden flows are quite irregularly spaced in time and care must be exercised in the data reduction and interpretation of the manipulated data. The methods are discussed for the one-dimensional data obtained in this study. Two-dimensional velocimetry data could be processed with an appropriate extension of these methods.

5.1 Data acquisition and preliminary data processing

The velocimetry data are obtained in real time using the laboratory mini-computer and the apparatus described in Chapter 6 and van Ingen (1980). The procedures followed are detailed in van Ingen (1981). Each piece of velocimetry data consists of a set of four numbers: the relative size of the scattering particle which generated the data, two independent realizations of the Doppler heterodyne frequency, and the time of the measurement.

The relative size of the scattering particle is determined by the relative amplitude of the light scattered by that particle. Sediment grains scatter much more light than fluid tracer particles. The velocimetry measurements are sorted into three basic size classes. In order of increasing signal amplitude, the sizes are: fluid measurements, measurements of scattering particles of unidentifiable size, and sediment grain measurements. Unidentifiable scattering

particles are those which scatter too much light to be fluid tracer particles, but not enough light to be sediment grains. The data associated with unidentifiable scatterers are discarded. The amount of such data is quite small.

A zero-crossing counter, described in van Ingen (1980), was used to measure the Doppler heterodyne frequencies. The time required for a preset number of heterodyne signal zero-crossings to occur is determined. The signal frequency is then given by

$$f = \frac{N-1}{\Delta t} \qquad (5.1.1)$$

where f is the signal frequency, N is the preset number of zero-crossings, and Δt is the determined time. Two realizations of the Doppler heterodyne frequency are made to ensure that the observed frequency is regular. As discussed in Chapter 4, light scattered simultaneously from multiple particles, particularly when the flow is sediment-laden, generates velocimetry signals which are not regular in frequency. If the two determined frequencies do not agree and the scattering particle is not identified as a sediment grain, the measurement is discarded. If the particle is identified as a sediment grain, the measurement is retained in the data record, but tagged as unreliable. The detection of a sediment grain, regardless of its velocity, allows for more accurate computation of the sediment transport rate and later analysis for possible conditional sampling errors in the velocimetry process.

The velocity is computed from the heterodyne frequency by

$$u = \alpha f \qquad (5.1.2)$$

where u is the velocity (cm/sec), α is a coefficient determined by the wavelength of the laser light and the optical geometry of the system, and f is the observed heterodyne frequency (KHz).

The data record is then screened for multiple measurements generated by a single scattering particle. The Doppler modulated burst signal generated by a sediment grain is longer in duration and greater in amplitude than that generated by a fluid tracer particle following the same trajectory through the measurement volume. Each sediment grain may generate more than one velocity measurement. The data record is examined and measurements generated by a single scattering particle are consolidated as described in van Ingen (1981).

Thus, the validated data obtained at a single vertical location within the flow field consist of a time series of velocity measurements, each of which is identified as either a fluid measurement or a sediment grain measurement. If the grain velocity is unreliable, it is so denoted. Each data record is not regular in time, nor does it include data from every scattering particle which passed through the velocimetry measurement volume.

5.2 Errors in laser-Doppler velocimetry

This section identifies and quantifies the principal sources of error inherent in the laser-Doppler method of velocimetry. The sources of errors include errors in the determination of the Doppler heterodyne frequency, determination of the velocity from the Doppler heterodyne frequency, and sampling errors.

The first source of error in the velocity measurement is the error in the determination of the Doppler heterodyne frequency. This error is due to the uncertainty in the signal processing electronics. As discussed by Gartrell (1978), the uncertainty in a zero-crossing counter processor system is at most one reference clock period, as a Doppler burst signal may arrive at any time within the clock cycle. The counter system used in this study has a reference clock frequency of 10 MHz, thus the relative error is given by

$$\frac{\Delta f}{f} = 10^{-4} \frac{fm}{N-1} \qquad (5.2.1)$$

where $\Delta f/f$ is the relative error in the frequency measurement, f_m is the measured frequency in KHz, and N is the preset number of zero-crossings. The measured frequencies were in the range 400 to 800 KHz. A minimum of 15 zero-crossings were counted. Therefore, the relative error due to the counter processor is, in the worst case, approximately 0.005. More commonly, 31 zero-crossings were used so that a typical relative error is approximately 0.002.

The uncertainties in the locations and directions of the intersecting laser beams result in a systematic error in the velocity measurement. The coefficient α in equation 5.1.2 is given by

$$\alpha = \frac{\lambda}{2\sin\phi} \qquad (5.2.2)$$

where λ is the wavelength of the laser light and 2ϕ is the beam intersection angle. As discussed in Chapter 6, the error in α was estimated to be 0.025 degrees. Using this value, the relative error in the velocimetry data is found to be 0.002.

The accuracy of the fluid velocity measurements is also dependent on the ability of the fluid tracer particles to follow the small scale fluid flow. Tracer particles which are too large may not follow the fluid particle trajectories. To measure turbulence with significant power at a frequency of 1 KHz in water, fluid tracer particles smaller than 15 μm are required (Durst et al., 1976). The size distribution of particles (excluding sediment grains) found in the flume water was measured (Hunt, 1980). The particles found in the flume water satisfy Durst's criterion as no particles greater than 10 μm were found in the size analysis, and no significant errors in the fluid velocity measurements resulted from this source.

The accuracy of the sediment grain velocity measurements may be affected by rotation of the sediment grains. Each sediment grain is a unique non-spherical, geometric light scattering particle. As each grain passes through the beam intersection volume, laser light is scattered from the illuminated portion of the grain surface. If the grain rotates or spins significantly, the characteristics of the light scattered by the illuminated portion of the grain surface may also change significantly. The detected Doppler burst frequency may not accurately reflect the desired component of the grain velocity. A typical time required in this study for the determination of the Doppler heterodyne frequency was 50 μsec. For a particle to rotate one degree during that time, a 55 rotations per second rate is required. Previous investigations of fluid turbulence indicate little fluid kinetic energy at such frequencies, particularly on length scales on the order of the size of a sediment grain. Significant rotation of a sediment grain during the time required for the determination of the

Doppler heterodyne frequency seems highly unlikely. No significant errors in the sediment velocity measurements were attributed to this source.

Lastly, the data from a laser-Doppler velocimeter do not form a continuous record, even in homogeneous fluid flows. The data record is a series of measurements made over discrete intervals. It has been well documented that such velocimetry measurements of fluid velocities may be statistically biased (Mc Laughlin and Tiederman, 1973, Dimotakis, 1976, Mc Dougall, 1980). The mean fluid velocity as measured is greater than the actual mean fluid velocity. If the fluid tracer particles are homogeneously distributed in the fluid, the probablity that an individual tracer particle will pass through the beam intersection volume is proportional to the local instantaneous volume flux. Relatively fast-moving fluid parcels have higher fluid volume flux, relatively higher numbers of fluid tracer particles, and generate relatively more measurements.

In sediment-laden flows, the fluid velocity data may be biased in a more complicated manner. Whenever sediment grains are within or very near the measurement volume, the generation of a fluid velocity measurement is not possible. A sediment grain which passes sufficiently close to the beam intersection volume scatters enough light to obscure the scattering by a fluid tracer particle passing simultaneously through the volume. The fluid velocity data record is therefore necessarily conditionally sampled. For example, suppose that all relatively fast-moving fluid parcels contain a significantly higher number of sediment grains. Even though such a fluid parcel also has a

relatively high number of fluid tracer particles, the light scattered by the smaller tracer particles will tend to be obscured by the light scattered by the sediment grains. The resultant fluid velocity data record is not biased by measurements of a relatively larger number of fast-moving fluid tracer particles.

Because of this possible conditional sampling of the fluid velocity data record, it is difficult to justify the selection of any one of the existing velocimetry correction procedures. All three of the above correction procedures were applied to the data in this study.

No bias correction procedure need be applied to the sediment grain velocity record. Barring any systematic pre-selection of the grains which generate velocimetry measurements, the mean sediment grain velocity is the mean velocity of the observed grains. Sediment grains are discrete particles; the behavior of a continuous medium is not being inferred.

Even if the grains which generate good velocity measurements are pre-selected in some way, the nature of the correction required is not evident. For example, if sediment grain velocity is positively correlated with the sediment transport rate, the observed mean sediment grain velocity may be less than the actual mean sediment grain velocity. When the sediment transport rate is relatively high, more sediment grains are in the vicinity of the beam intersection volume and the occurrence of simultaneous scattering by multiple particles increases. The likelihood that a given sediment grain which passes through the volume will generate a valid velocimetry data event decreases. There is, however, no physical basis on which to predict, a

priori, a correlation between sediment grain velocity and sediment transport rate. Furthermore, if such a correlation did exist in the flow, it may not be apparent in the observed, biased, velocimetry data record. The character and magnitude of any bias in the sediment grain velocity observations cannot be estimated until more is known about the time-fluctuating characteristics of the sediment grain motion.

5.3 Initial Data Analysis Procedures

This section describes the initial data analysis performed on each of the validated velocimetry data records. Each data record consists of an irregularly spaced time-series of velocity measurements. Each velocity measurement is identified as either a fluid measurement or a sediment grain measurement. If the grain velocity measurement is unreliable, it is so tagged.

Some simple statistics of the fluid and valid sediment grain velocity measurements are first computed. The number of measurements, mean velocity, and velocity standard deviation are determined. The standard deviation of the fluid velocity is the longitudinal turbulence intensity. Note that the number of valid fluid and the number of valid sediment grain measurements will differ in each data record. The three bias correction procedures are applied to the fluid velocity measurements to compute the corresponding corrected mean and standard deviation of the fluid velocity. The probability density functions of the fluid velocity and the sediment grain velocity are determined.

The above statistics obtained for the fluid velocity measurements are compared to those obtained for the sediment grain velocity

measurements at each location. Comparisons are also made between the results obtained at the various measurement locations throughout the water column. Mean velocity and velocity standard deviation profiles for both the fluid and the sediment grains are plotted. The fluid velocity results may be compared to observations in clear water flows by previous investigators to determine the effects of the suspended sediment on the fluid turbulence. The fluid and the sediment grain results will be similiar if the sediment grains are moving with the surrounding fluid and if the grains are not associated with a selected subset of fluid parcels.

Similiar statistics of the computed sediment grain inter-arrival times, the time intervals between successive sediment grain detections, are then obtained for each data record. The determinations are made for those sediment grains which generated valid velocity measurements and for all of the detected sediment grains. The number of measurements, mean inter-arrival time and inter-arrival time standard deviation are determined. Profiles of mean and standard deviation of sediment grain inter-arrival time are plotted. The mean inter-arrival time at each location is compared to the sediment transport rate at that location as measured by suction sampling tube. If the laser velocimeter acts as a grain counter, the mean grain inter-arrival time is inversely proportional to the sediment transport rate. The standard deviation of the sediment grain inter-arrival time gives a measure of the time variability in the sediment transport. The probability density functions of the sediment grain inter-arrival time data are computed for each data record. The physical interpretation of the probability density function is discussed in Section 5.5.

After the initial analysis, the data are then subjected to some time-series analysis procedures. Because of the irregular time spacing of the velocimetry data, the time-series analysis procedures used in this study differ from those applied to regularly spaced data. Additionally, the time spacing of the sediment grain data has a physical meaning. The techniques employed and the subsequent physical interpretation of the results are discussed in depth in the next sections.

5.4 Consequences of irregular time spacing of the fluid velocity data

As noted previously, laser-Doppler velocimetry data is a series of discrete measurements, irregularly spaced in time. If the mean data acquisition rate is rapid with respect to the frequencies of the fluid turbulence with significant energy, this irregularly spaced data may be interpolated to yield regularly spaced data. In homogeneous fluid flows, it is usually possible to construct such a regularly spaced data record. In sediment-laden flows, this is not simply possible. Significant gaps in the fluid velocity data record are created by the passage of sediment grains through or near to the beam intersection volume. Computation of fluid velocity auto-correlations and power spectra must be performed with the irregularly spaced data record. Although such computations are relatively straightforward, the subsequent interpretation of the computed correlations and spectra must be done with care. This section reviews the relevant computation techniques and interpretation guidelines applied in this study. For a detailed discussion of time-series analysis of unequally spaced data, see Deeming (1975), Roberts and Gaster (1980), and Shapiro and

Silverman (1960).

Turbulent flow data are subjected to time-series analysis in an effort to identify and characterize the time-dependent properties of the turbulence. Correlations of velocity fluctuations define the time scales, and by convention, the length scales of the turbulent kinetic energy and shear. The Fourier transforms of these correlations, when properly normalized, show the distribution of turbulent kinetic energy and shear among the various time scales.

Auto-correlations or cross-correlations of a function sampled at random time intervals may be computed by several different methods. The primary difficulty encountered is that the correlation is smeared. At a given lag time, the computed value of the correlation depends on the values of the correlations at the neighboring lag times. Additionally, the error in the computed correlation is a function of the lag time.

Consider the velocity at a point, u(t), sampled at random sample times, t_k. The simple lag velocity correlation coefficients, C(M), are given by

$$C(M) = \frac{1}{N-M} \sum_{k=1}^{N-M} u(t_k)\, u(t_{k+M}) \qquad (5.4.1)$$

where M is the lag index (M=1,2,...) and N is the number of observations. If the sample times are regular, the simple lag auto-correlation is equivalent to the true auto-correlation. In the general case

$$C(M) = \sum_{k=1}^{M} R(\tau j)\ \psi_M(\tau j) \qquad (5.4.2)$$

where t_k is the kth lag time, $R(\tau_*)$ is the true auto-correlation and $\psi_M(\tau_*)$ is the probability density function of lag time τ_* at lag interval M. Thus, given the simple lag correlation coefficients and the relevant inter-arrival time probability density functions, the true auto-correlation may be computed.

The Fourier transform of a continuous-valued function of time differs from the Fourier transform of discrete observations of that function. The discrepancy is due to the finite length and time spacing of the observed data record. The observed Fourier transform, $F_N(\nu)$, is the convolution of the true Fourier transform, $F(\nu)$, with a spectral window function, $\delta_N(\nu)$. Thus,

$$
\begin{aligned}
F_N(\nu) &= F(\nu) * \delta_N(\nu) \\
F_N(\nu) &= \sum_{k=1}^{N} u(t_k) e^{2\pi i \nu t_k} \\
F(\nu) &= \int_{-\infty}^{\infty} u(t) e^{2\pi i \nu t}\, dt \\
\delta_N(\nu) &= \sum_{k=1}^{N} e^{2\pi i \nu t_k}
\end{aligned}
\qquad (5.4.3)
$$

where ν is frequency and $\delta_N(\nu)$ is the spectral window function. It must be noted that, strictly speaking, the fluid velocity at a point within a sediment-laden flow is not a continuous function of time. During the periods when sediment grains pass through that point, the fluid velocity is not defined. At alluvial concentrations, these periods are not that common, less than one per cent of the time. Furthermore, the time of flight of a sediment grain through the measurement volume is small with respect to the turbulent time scales with appreciable kinetic energy. In this study, the fluid velocity at a point is assumed to be a continuous function of time.

The spectral window function is all important in the interpretation of the calculated transform. It pinpoints any pathology of the distribution of the data acquisition times. The spectral window function does not depend on the observed data values but only on the times of observation. The observed Fourier transform may contain aliases, spurious subsidiary peaks which are artifacts of the data sampling. These subsidiary peaks are not physically meaningful, and must be identified prior to the interpretation of the transform. The spectral window function identifies any aliasing in the computed transform.

Similiarly, the observed power spectrum is proportional to the convolution of the true power spectrum with the power spectral window function. Thus,

$$P_N(\nu) = P(\nu) * \gamma_N(\nu)\sigma_u \qquad (5.4.4)$$

$$F_N(\nu)\,\overline{F_N(\nu)} = \sigma_u P(\nu) * [\delta_N(\nu)\overline{\delta_N(\nu)}]$$

where $P(\nu)$ is the true power spectrum, $P_N(\nu)$ is the computed power spectrum, $\delta_N(\nu)$ is the power spectral window function, $\overline{\ }$ denotes complex conjugate, and σ_u is the variance of the function u(t). Again, the power spectral window function identifies any aliasing in the computed power spectrum.

As an example, consider a simple sine wave sampled at regular time intervals. The power spectral window function reduces to

$$\gamma_N(\nu) = \left\{ \sum_{k=1}^{N} e^{2\pi i\nu(k-1)/\nu_s} \right\} \left\{ \sum_{k=1}^{N} e^{\overline{2\pi i\nu(k-1)/\nu_s}} \right\} \qquad (5.4.5)$$

$$= \frac{\sin^2(\pi \frac{\nu N}{\nu_s})}{\sin^2(\pi \frac{\nu}{\nu_s})}$$

where ν_s is the sample frequency. As $N \to \infty$, the spectral window function approaches a set of delta functions equally spaced at intervals of ν_s. Aliasing at integral multiples of the sampling frequency, the familiar result, is predicted. As $\nu \to 0$, the spectral window function approaches N^2. The observed power spectral estimate will be aliased at low frequencies by the finite length of the data record. For a sinusoidal function, $u(t)=\sin(2\pi\eta t)$, the observed power spectral estimate is given by

$$P_N(\nu) = [\sum_{k=1}^{N} \sin(2\pi\frac{(k-1)\eta}{\nu_s})\sin(2\pi\frac{(k-1)\nu}{\nu_s})]^2 + [\sum_{k=1}^{N}\sin(2\pi\frac{(k-1)\eta}{\nu_s})\cos(2\pi\frac{(k-1)\nu}{\nu_s})]^2 \quad (5.4.6)$$

where η is the signal frequency of the sine wave. As $N \to \infty$, the observed spectral estimate approaches a set of delta functions

$$P_N(\nu) = \delta(\eta + i\nu_s) \quad (5.4.7)$$

where i is any integer. The observed spectral estimate is the true spectral estimate, a single delta function located at $\nu=\eta$, convoluted with the spectral window function.

The observed power spectral estimate and the power spectral window function computed for the case of a 2 Hz sine wave sampled at 20 Hz are plotted in Figure 5.4.1. The length of record was 42.5 seconds. The frequencies for the computation were chosen to appear evenly spaced

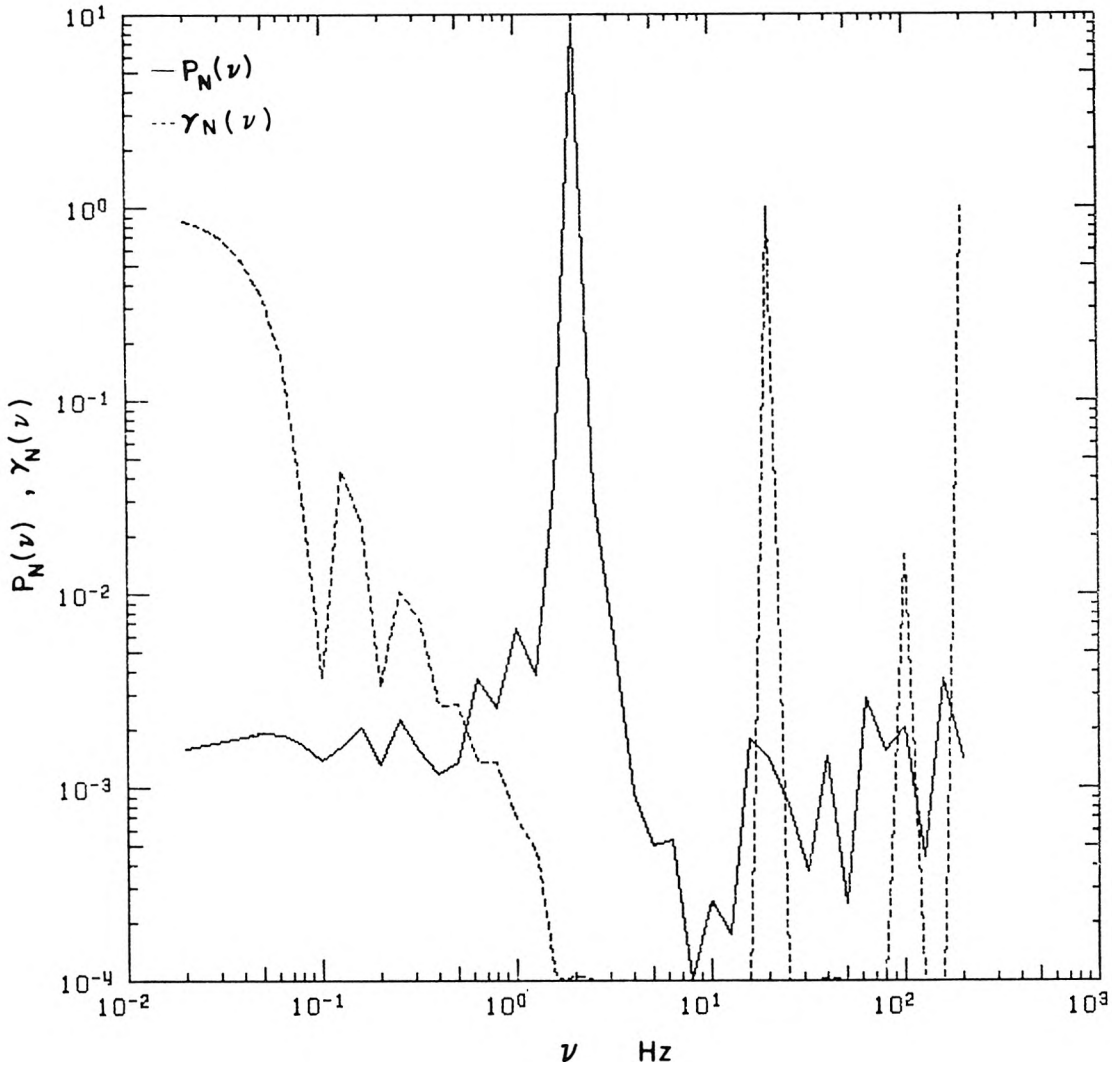

Figure 5.1.1 Sample calculation of power spectral estimate and power spectral window function

when plotted on a logarithmic axis. Forty-one computational frequencies in the range 0.02 to 200 Hz were used. The power spectral estimate appears as the solid curve; the power spectral window function as the dotted curve.

For regularly sampled data, the Nyquist, or cutoff frequency is one-half of the sampling frequency. Any fluctuations existing in the measured system at frequencies higher than the Nyquist frequency cannot be determined from the resultant sampled data record. The Nyquist frequency for the example considered is 10 Hz. Aliasing of the power spectral estimate due to the data record spacing occurs only at frequencies greater than the Nyquist frequency. The example calculation was performed for frequencies greater than the Nyquist frequency so that the aliasing would be apparent. No simple cutoff frequency can be defined for random time sampled data. The reliability of the computed spectral estimate must be gauged by examination of the power spectral window function.

As predicted by Equation 5.4.6, the computed spectral window function exhibits strong peaks at 20, 100, and 200 Hz, all of which are integral multiples of the sampling frequency. However, no such peaks are apparent at 40, 60, or 80 Hz. The peaks are absent because these frequencies were not among the chosen computational frequencies. The computed spectral window function is a discrete function of frequency. The observed spectral window function may change markedly in response to a small shift in the selected computational frequencies, particularly if only a few computational points are used. The number of chosen frequencies is generally limited by the relatively large

computational effort required for each frequency. The spectral window function may sometimes be smoothed by judicious partitioning of the data record, computing the spectral window function for each partition, then averaging the results obtained for each partition. When the sampling times are highly erratic, however, the partitioned, averaged spectra are often less smooth, more variable, than those computed from the entire data record.

All of the above problems in the computation of the spectral window function are encountered in the computation of the power spectral estimate. The expected error in the computed spectral estimate is equal to the value of the estimate. If the signal frequency is not sufficiently close to one of the chosen computational frequencies, the corresponding peak will be lacking in the resultant spectral estimate. Also, all aliasing of the computed spectral estimate may not be predicted by the computed spectral window function. Since aliasing results from a convolution of the spectral window function and the true power spectrum, a spurious peak in the observed spectral estimate is not coincident with its related peak in the spectral window function. The chosen computational frequencies may include the frequency of the spurious peak in spectral estimate, but not the frequency of the related peak in the spectral window function.

Summarizing, time series analysis of irregularly sampled data must be done with care in both computation and interpretation. The spectral window function must be examined when performing spectral analysis. While aliasing can be predicted in advance for regularly sampled data,

it must be analysed after the fact for irregularly spaced data.

5.5 Consequences of irregular time spacing of the sediment grain velocity data

Sediment grain velocity at a point is not a continuous function of time. Rather, it consists of a sequence of discrete values at discrete times. The sediment grain velocimetry record is a subset of these values. The data record is not regular in time. The irregularity in the data spacing has physical significance as it reflects the mechanics of the sediment motions. Thus, sediment grain velocity data are different from fluid velocity data. While it is appropriate to manipulate the sediment velocity data record in the same manner as the fluid velocity data record, the subsequent interpretation of this manipulation differs.

The computed sediment grain inter-arrival times, regardless of the grain velocity, also form a time series of discrete values. If the velocimeter acts as a grain counter, the probability density functions of the sediment grain inter-arrival time reflect the mechanics of the sediment motions. To identify any physical mechanisms which may cause sediment grains to group or cluster, it is desirable to perform some type of time-series analysis on the inter-arrival time data records. The grain inter-arrival time data records may be treated similiarly to the fluid velocity data records, but the meaning of such manipulation differs.

If the passage of each sediment grain through the velocimetry measurement volume is viewed as an independent stochastic event, the time series of sediment grain inter-arrival times might be modeled as a

Poisson process. The probability density function, $\psi(\delta t_g)$, of the sediment grain inter-arrival times, δt_g, would then be given by

$$\psi(\delta t_g) = \nu_g e^{-\nu_g \delta t_g} \qquad (5.5.1)$$

where ν_g is the mean frequency of the sediment grain arrivals. The standard deviation of the sediment grain inter-arrival times would be equal to the mean. Computation of the probability density function for the experimentally observed sediment grain inter-arrival time data records allows this model to be tested. The approach does assume that successive passages of individual sediment grains through the volume are independent events. Time series analysis of the sediment grain inter-arrival times must be performed to check this assumption.

The simple lag correlation coefficients of sediment grain velocity and sediment grain inter-arrival times may be computed as described in Section 5.4. The lag correlation coefficients relate the motion of a given sediment grain to the motion of the Mth successive sediment grain. Just as the auto-correlation of the fluid velocity fluctuations are used to define time scales of the fluid turbulence, the lag correlation of the sediment grain inter-arrival times may be used to define grain number scales of the sediment motions. The number of grains, or lag, at which the grain inter-arrival times are no longer correlated is a measure of the number of grains which move as a group. If little or no correlation is observed, the motion of each sediment grain may be assumed to be independent of the motions of all other sediment grains.

The lag correlation coefficients may also be used to compute the true auto-correlation functions of lag time. Time scales of sediment

grain velocity fluctations and sediment transport rate may be defined by analogy with the time scales of the fluid turbulence. The physical interpretation of such time scales is not exactly analagous to that of the fluid time scales, however. The sediment grain velocity at a point in space can only be defined when a grain is present at that point. Comparison of the time scales of the fluid turbulence and the sediment grain inter-arrival times may give a qualitative description of the time scales of the turbulence which are important in sediment suspension.

The power spectral window function of the sediment grain observations also contains information about the time scales of the sediment motion. The power spectral window function reflects the frequency distribution of mean sediment grain inter-arrival time. A peak in the observed grain spectral window function implies the existence of a dominant sediment grain inter-arrival frequency. The fluid spectral window function has no such direct physical significance. The time spacing of the fluid velocity measurements is an artifact of the measurement technique. The time spacing of the detection of sediment grains reflects the transport of the sediment.

Interpretation of the time-series analysis of a function which is discontinuous in time is not straightforward. Suspended sediment, when viewed on the granular scale, is not a continuum. Sediment grain velocity measurements are recorded at random time intervals because sediment transport is an inherently intermittent process.

5.6 Summary

This chapter has presented the errors inherent in the technique and the methods of data analysis used in this study. Careful analysis and interpretation of laser-Doppler velocimetry data obtained in sediment-laden flows is not simple. Each velocity realization must be validated and multiple realizations of the same scattering particle must be eliminated. The resultant data record is irregular in time, and the any physical interpretation of such data must be done with care. With such care, the small scale, time varying mechanics of sediment-laden flows may be observed without flow disruption.

CHAPTER 6

EXPERIMENTAL APPARATUS

The experiments on turbulence and sediment grain transport in open channel flow reported in Chapter 8 were performed in the W. M. Keck Laboratory of Hydraulics and Water Resources. Most of the hydraulic apparatus used is similiar to that used in several previous experimental investigations of sediment transport in the Keck Laboratory. In addition, a laser-Doppler velocimeter was developed for use in sediment-laden flows. This chapter describes all of the apparatus used in this study.

6.1 The 13-meter flume

The experiments were conducted in the 13-meter tilting flume located in the Keck Laboratory. A schematic diagram of the flume is shown in Figure 6.1.1. The flume has been described in detail in Taylor (1971).

The flume is 26.7 cm (10.5 in) wide and 25.4 cm (10.0 in) deep. The flume discharge (sediment and water) is recirculated from the outlet section to the inlet section through a 10.2 cm (4.0 in) return pipe by an axial flow pump. The pump is connected to a two-speed electric motor through a variable-speed drive. The flume, pump, motor and return pipe are mounted on a tiltable truss.

The truss is supported at two points: on a pivot point near the downstream end and on a manually operated, screw-type jack near the upstream end. Thus, the flume slope may be varied continuously from

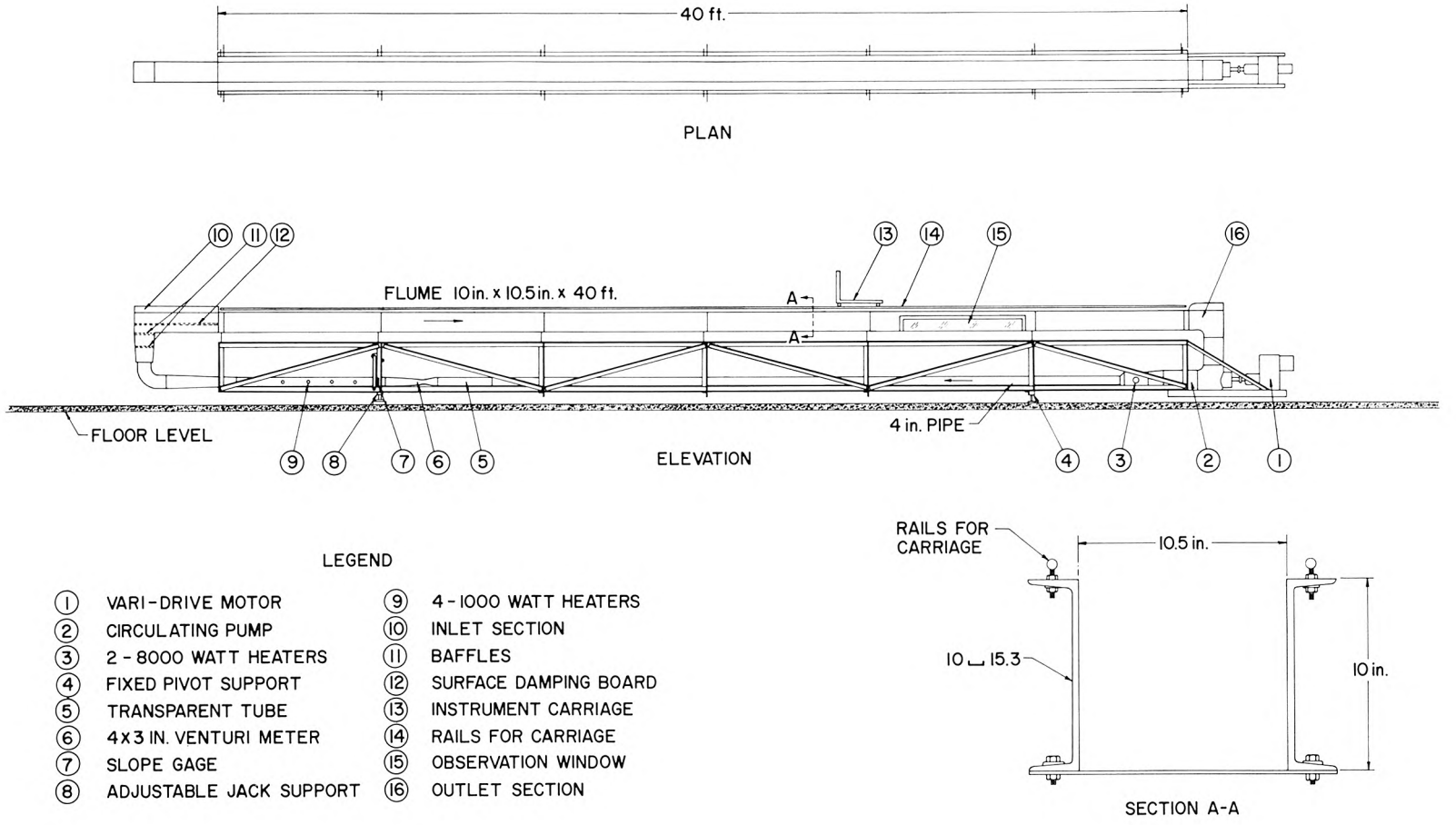

Figure 6.1.1 13-meter flume schematic drawing

-0.001 to +0.038 and is read directly from a scale (with vernier) located near the jack.

The flume consists of two steel channel beams bolted to a bed plate. The inside surfaces are painted with a bitumastic paint and are nearly hydrodynamically smooth. A window, 1.47 m in length, is installed 8.6 m from the inlet box and 2.1 m from the outlet box. Two precision stainless steel round bars mounted on top of the flume side wall beams act as rails for a metal instrument carriage. Gearing of the instrument mount on the carriage allows positioning of the mounted instrument to within 0.2 mm in the vertical or transverse directions. A point gage, Pitot tube, and sediment sampler were interchangeable on the instrument mount.

At the flume inlet, a series of baffles was used to damp large scale turbulence and secondary currents generated in the return pipe, and in the inlet and outlet sections. Two rectangular grids made from glued lucite strips (strip width=1.27 cm; opening=1.27 cm) were placed horizontally in the vertical portion of the inlet section. Two 0.30 cm mesh and two 0.16 cm mesh screens were placed vertically across the end of the inlet section at the upstream end of the flume. A plywood board was floated just downstream of the screens to damp surface disturbances. A 0.16 cm mesh screen was located at the downstream end of the flume.

The original flume truss was modified to accommodate the carriage for the laser-Doppler velocimeter. The cross brace located under the glass window was cut and replaced by two braces to provide the necessary clearance for the velocimeter carriage. Panels of lucite and

wood were made to cover the top of the flume to prevent dust from the laboratory ventilation system from entering the flume.

6.2 Sand characteristics

The sand used in this study has a geometric mean grain size, d_g, of 0.245 mm, a geometric standard deviation, σ_g, of 1.22, and a density, ρ_s, of 2.65 g/cm . The size analysis is shown in Figure 6.2.1. The material is one of the size fractions obtained by Taylor (1971) in a fall velocity separation of a natural alluvial sand. The sand was discharged into a water flume flow (mean velocity=12 cm/sec, depth=56 cm) using a dry sediment hopper. Slot dividers were positioned along the flume bed downstream of the hopper. The sediment which accumulated between each pair of slot dividers was removed. The resulting separated sands have size distributions which are not strictly log-normal, but are slightly bimodal as seen in Figure 6.2.1. The deviation from log-normal is not large and was judged not important in this study.

6.3 Measurements of time-averaged flow characteristics

Although these experiments were directed at observing the time-fluctuating characteristics of a sediment-laden flow, measurements of time-averaged flow quantities of the more traditional type were also made.

Flume discharge was measured by a Venturi tube connected to an air-water differential manometer. The Venturi was located in the return pipe near the upstream end. The manometer can be read to the

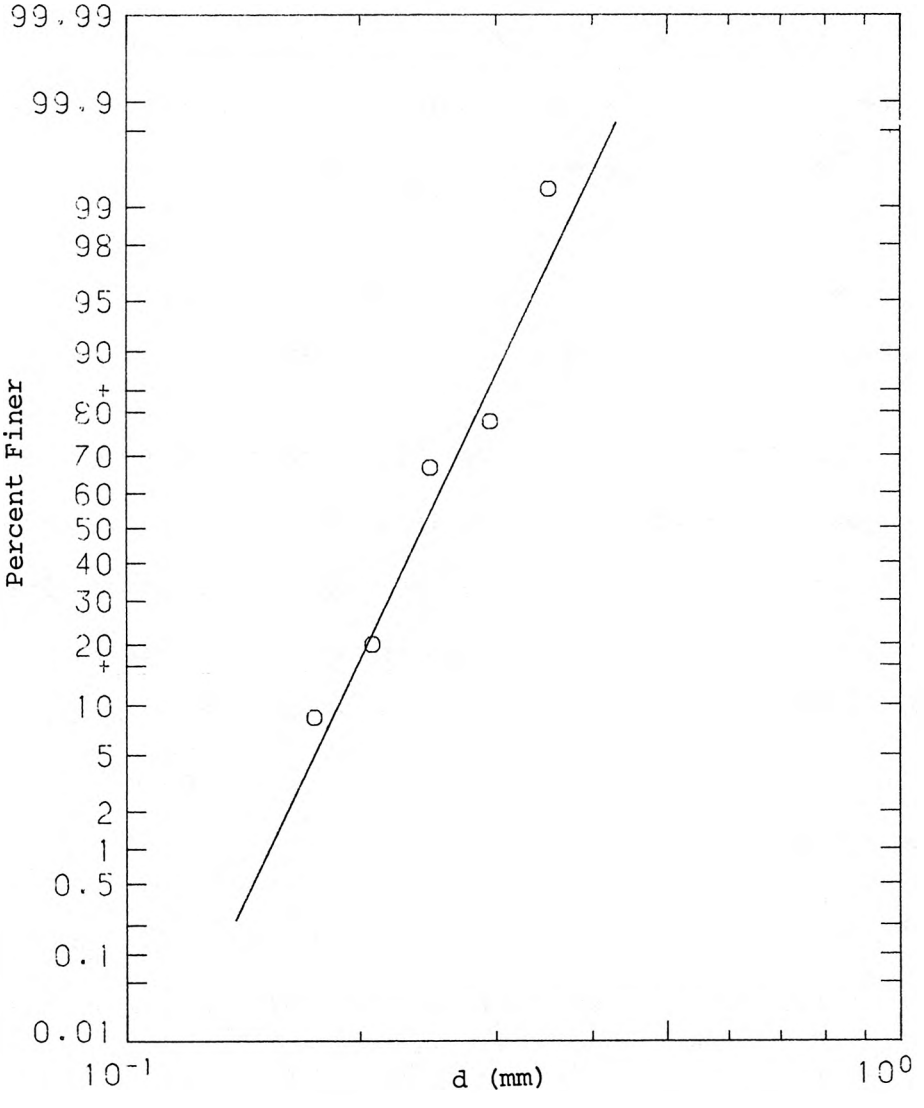

Figure 6.2.1 Sediment grain size distribution

nearest 0.2 mm with a vernier. The Venturi tube was calibrated prior to this study using clear water. The maximum error in the discharge measurement was judged to be approximately three per cent.

The mean water surface slope and sediment bed slope were determined from a series of point gage measurements at twenty locations along the flume. Measurements of the quiescent water surface were used as a horizontal reference. The reported surface slope, S=0.00275, is the average of ten sets of point gage measurements. The error in the reported slope measurement is judged to be approximately five per cent.

Local mean velocities were measured by a 0.63 cm (0.188 in) O.D. Prandtl-type Pitot tube. An air-water manometer was connected to the Pitot tube. The manometer can be read to the nearest 0.2 mm with a vernier. Due to the Froude number of the flow used in this study, Fr=0.75, small surface standing waves were often present. The mean velocity at a fixed point was observed to vary as much as eight per cent over several minutes.

Local mean sediment concentration measurements were made with the point sediment sampler shown in Figure 6.3.1. The sampler was made from 0.95 cm (0.375 in) O.D. brass tubing. The tip opening was flattened as shown. Samples were withdrawn at the local flow velocity (isokinetically) by a siphon arrangement as described by Brooks (1954).

Total load measurements were also made. A second brass sampling tube, shown in Figure 6.3.2, was suspended vertically in the outlet section throat. Sampling was again isokinetic as described by Vanoni and Brooks (1957).

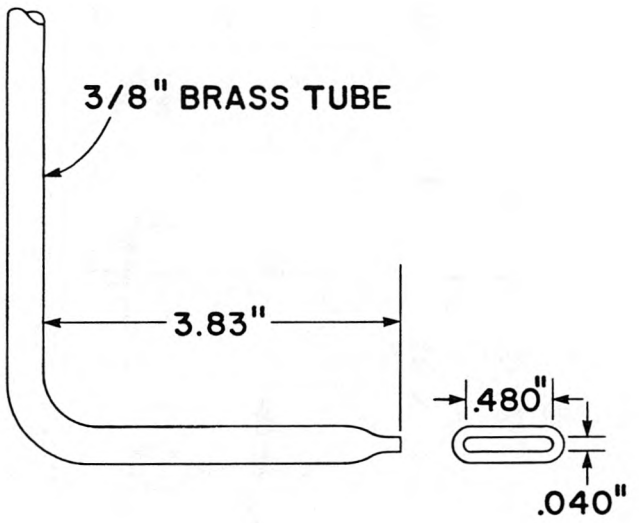

Figure 6.3.1. Sediment concentration point sampling tube

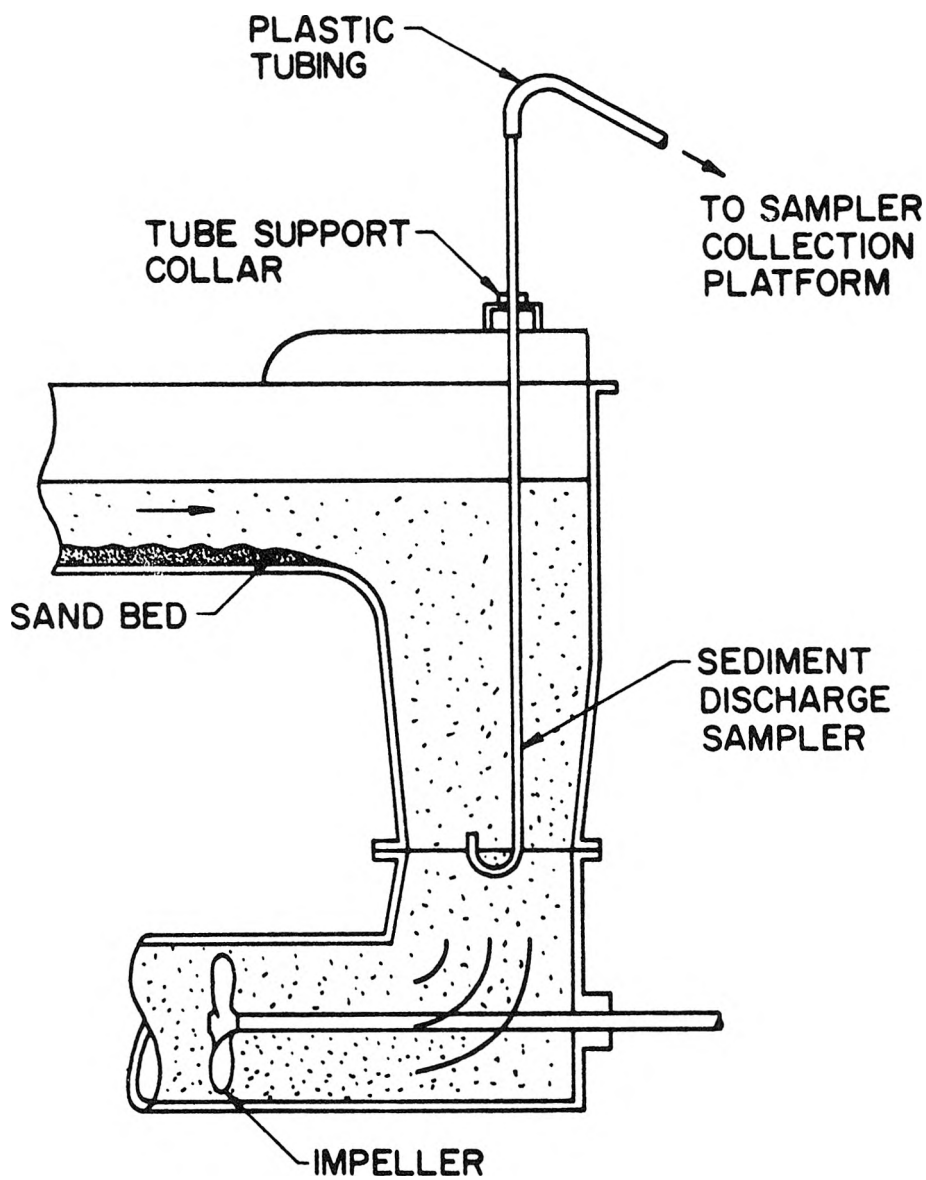

Figure 6.3.2 Sediment concentration total load sampling tube

6.4 Measurements of time-fluctuating flow characteristics

A laser-Doppler velocimeter, shown in Figures 6.4.1 and 6.4.2, was developed to measure the one-dimensional, time-varying characteristics of the flow at a fixed point. Direct, instantaneous measurements of fluid velocity, sediment grain velocity, and sediment grain inter-arrival time were made. The dual-scatter method was used. Some non-standard optics and processing electronics were developed due to the special problems inherent in applying the basic technique to sediment-laden flows, as described in Chapter 4 and van Ingen (1980).

The light source for the system was a Spectra-Physics Model 162, argon ion laser. The laser was tuned to the 5145 Angstrom line. The output power was approximately 15 mW. As shown in Figure 6.4.2, the laser light was first passed through a cube beam splitter. Three resultant beams were produced, two of which have forty-five per cent of the intensity of the initial beam and one which has ten per cent. The two equal stronger beams were made parallel by two mirrors. The dimmer beam was not used. The beams were focused and made to intersect by a lens.

The transmitting optics were aligned as follows. The optical components were first firmly attached to a 1.25 cm (0.5 in) thick aluminum carrier plate. The plate was leveled using a precision level. The two beams were then made parallel to the carrier plate and to each other by adjusting the position of the two mirrors. The directions of the beams were checked by shining them across the laboratory to a wall 10 m from the carrier plate. The transmitting lens (250 mm diameter, 450 mm focal length) was then installed. The vertical position of the

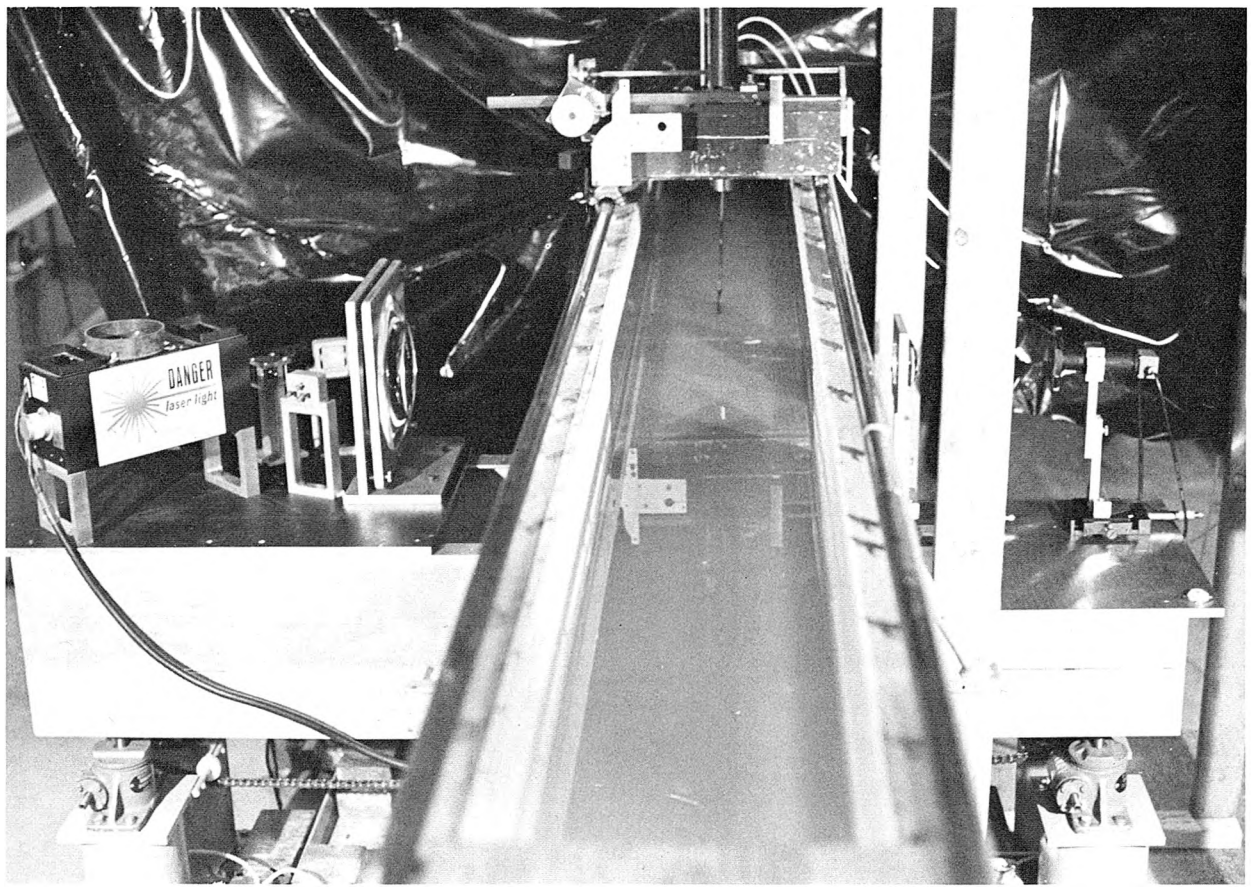

Figure 6.4.1 Photograph of the laser-Doppler velocimeter

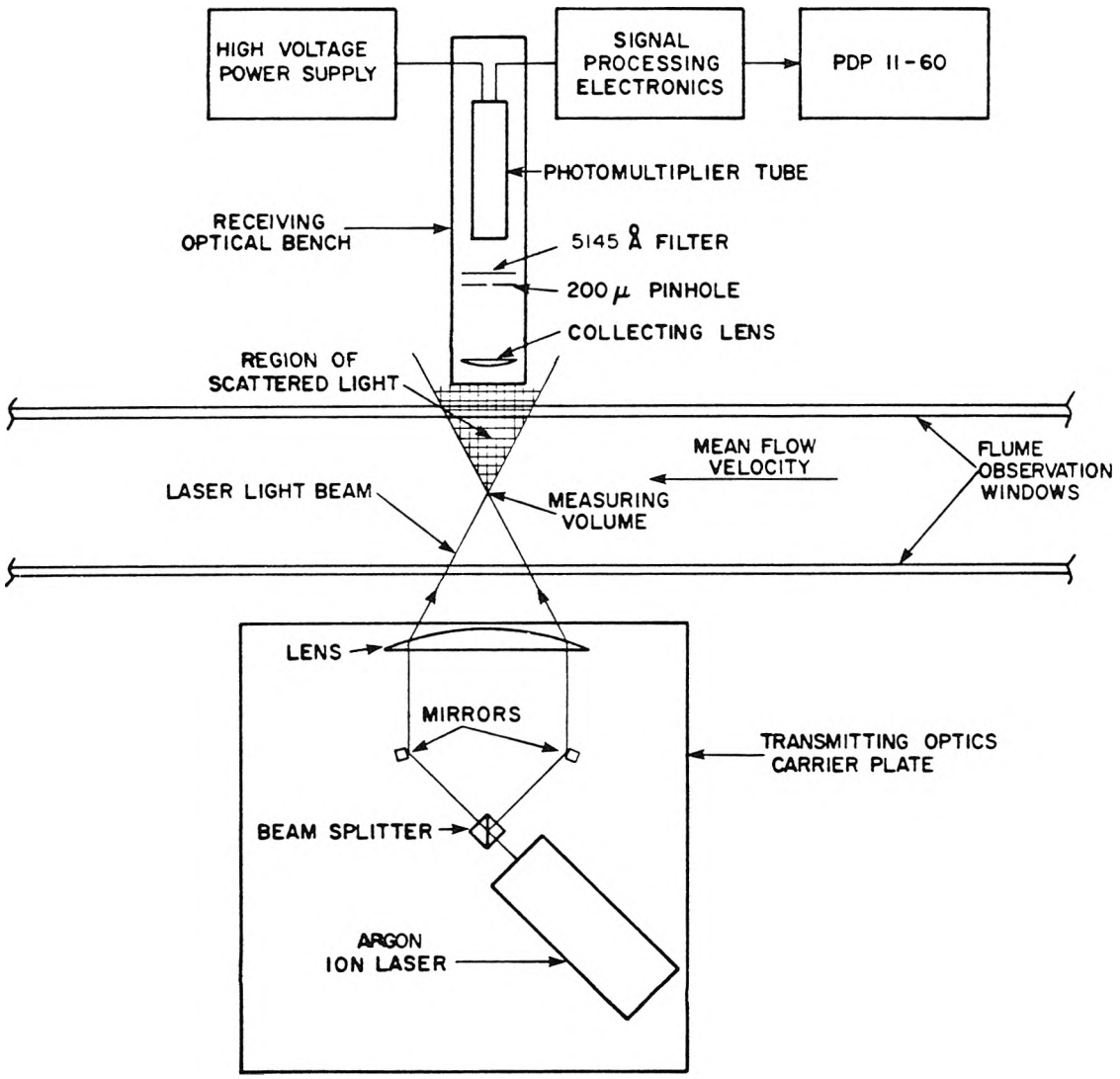

Figure 6.4.2 Laser-Doppler velocimeter plan-view schematic

lens was adjusted until the beams were not vertically refracted. As is likely in a lens of such size, some spherical aberration was noted. The beam separation distance was adjusted to achieve the desired beam intersection angle. The intersection angle was determined by measuring the resulting beam separation at the wall. The beam intersection angle was determined to be 10.70 degrees; the error was judged to be 0.025 degrees. The mean velocity determined by the laser-Doppler velocimeter was correlated to the velocity determined by a Pitot tube as a check on the beam survey. Good agreement was noted.

The diameters of the beams at the beam intersection volume and at the transmitting lens were measured using a precision optical slit. Using these measurements and the procedures given by Durst et al (1976), the minor diameter of the intersection volume was judged to be 0.6 mm. The length of the intersection volume was computed to be 3.2 mm and the maximum number of fringes contained within the volume was estimated at 216.

The receiving optical system consisted of a lens, a pinhole, a laser line filter and a photomultiplier. The lens collected a portion of the light scattered by each particle which passed through the laser beam intersection volume. The unscattered laser beams were masked and not collected by the receiving lens. The photocathode surface was placed at the image point of the laser beam intersection. The pinhole acted as an aperture, blocking light scattered from places other than the beam intesection. Additional apertures in combination with the pinhole were tried, but did not seem to improve the signal quality. The filter excludes the collection of the background lighting in the

laboratory. The mercury line from the fluorescent lighting in the laboratory is quite close to the argon line used, hence a narrow band pass filter was necessary. The photodetector, a RCA 8645 photomultiplier, converted the collected light intensity into an electrical current.

The transmitting and receiving optics were aligned as follows. The transmitting optics plate was mounted on one side of the special carriage described later in this chapter. The components of the receiving optics were mounted to a second aluminum plate which was then mounted to the carriage on the opposite side of the flume (see Figure 6.4.1). The receiving lens was placed as close as possible to the flume. This was done to minimize the total receiving optical pathlength. The pinhole and filter were fixed in place on the housing of the photomultiplier. The photomultiplier was positioned as accurately as possible at the calculated image point of the beam intersection volume. By trial and error, the position of the photomultiplier was adjusted to give the best signal.

The photomultiplier output current was amplified, filtered and processed electronically to yield digital velocimetry data. These data were sent to the laboratory mini-computer in real time for later analysis. The data from each particle consisted of three sixteen bit numbers. The relative size of the scattering particle, whether the scattering particle was a sand grain or a fluid tracer particle, is the four higher order bits of the first data word. The lower twelve bits of the first data word and the entire second data word are two independent measurements of the Doppler heterodyne frequency. Two

measurements are made to ensure the validity of the data as explained in Chapter 4. The velocity of a scattering particle is computed from the measured heterodyne frequency by

$$u = \frac{\lambda f}{2\sin\theta} \tag{6.4.1}$$

where u is the streamwise component of particle velocity, f is the heterodyne frequency, λ is the laser light wavelength, and 2ϕ is the angle of the beam intersection. The time of measurement, as timed by the internal computer clock, is the fourth word. The processing electronics are described in detail in Appendix A. The subsequent analysis of the data has been discussed in Chapter 5.

6.5 The laser velocimetry carriage

A special carriage for the laser-Doppler velocimeter was designed and built to facilitate the velocity measurements. The carriage held the transmitting and receiving optics plates in rigid alignment and allowed the vertical positioning of the laser beam intersection volume within the water column. The carriage is shown in Figure 6.5.1. The carriage passed underneath and through the flume support truss near the flume window.

The transmitting and receiving optics mounting plates were fixed with aluminum channel spacers to an aluminum box beam. The flume support truss was altered to allow this beam to pass through the truss, just underneath the flume channel. The beam was supported by four precision screw jacks which were rigidly mounted on a steel plate which also passed underneath the flume support truss. The box beam, with the attached optical plates, can be raised and lowered smoothly by the

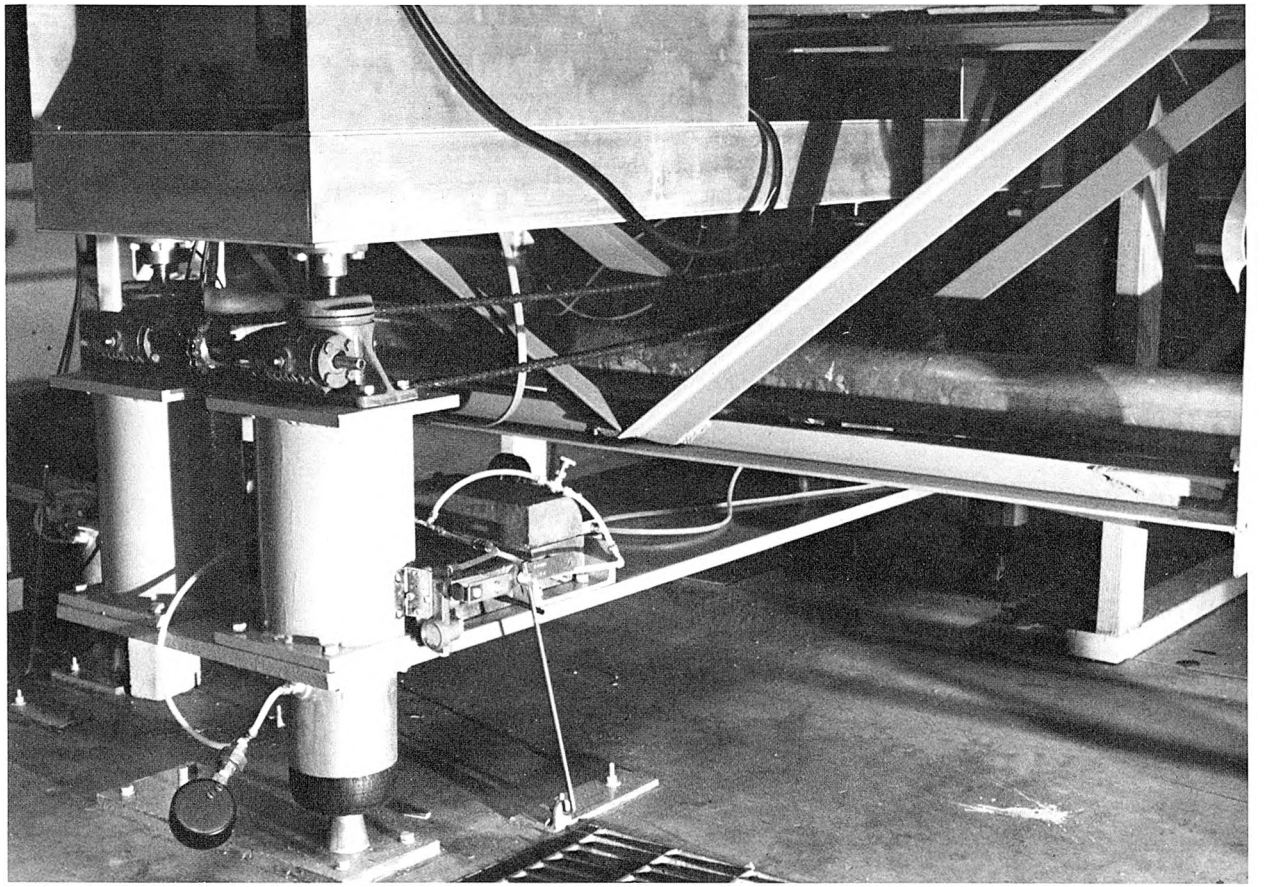

Figure 6.5.1 Photograph of the laser velocimetry carriage

jacks. The four jacks were connected and could be moved simultaneously by manually turning a master drive handle. The velocimeter measuring volume was positioned vertically within the water column by determining its location with the flume point gage.

The steel plate is supported by four Firestone Model IX84D Air Mount vibrational isolators. The flume glass, hence the velocimeter measuring volume, was located near the downstream flume pivot point. Using a Kinemetrics Model SS-1 Ranger Seismometer, it was found that the pump produces local vibrations in the laboratory floor at the pivot point. At the pump speeds commonly used in this study, the local floor vibrations had significant energy in the range of 5 to 15 Hz. Unfortunately, the laser velocimeter is a superior vibration detector, as it is incapable of distinguishing the scattering caused by a particle fixed in space seen from a vibrating carriage and the scattering caused by a moving particle seen from a fixed carriage. As the expected turbulence frequencies were of the same order as the floor vibrations, it was necessary to vibrationally isolate the velocimeter carriage from the floor. Using the isolators and weighting the carriage with lead bricks to give added mass, a 99.4 percent reduction in the amplitude of vibration of the velocimeter was achieved.

CHAPTER 7

EXPERIMENTAL PROCEDURE

A general description of the laboratory flow in which the velocimetry results were obtained is given in this chapter. Visual observations and conventional measurements of relevant flow properties are discussed. The laser-Doppler velocimetry data records are introduced.

7.1 General description of the flow conditions

The velocimetry results were obtained in a steady, uniform sediment-laden flow over a natural sand bed. The flow conditions, corrected for the side-wall effect following Vanoni and Brooks (1957), are summarized in Table 7.1.1. The flow was chosen to be in the high transport, flat bed regime to minimize flow disturbances due to sediment bed forms.

The sediment bed was flat in the center portion of the flume; small ripples projected from either side wall approximately four centimeters into the flume. Intermittently, the bed became undular. The undulations were approximately forty centimeters in length and less than one centimeter in height. These bed waves, when present, traveled slowly downstream. Sporadic surface waves, usually in phase with the bed waves, were also noted. These disturbances are primarily due to the relatively small size of the experimental flume. However, the waves were small with respect to large amplitude ripples or dunes found in other flow regimes.

Table 7.1 Mean flow conditions

Fluid discharge	Q	12.94	l/sec
Mean velocity	u	64.41	cm/sec
Mean depth	d	7.54	cm
Hydraulic radius	R	4.82	cm
Bed shear velocity	u_{*_b}	3.88	cm/sec
Bed friction factor	f_b	0.029	
Energy slope	S	0.00275	
Sediment discharge	Q_s	4.92	g/sec
Mean sediment concentration	$\bar{c}$	0.380	g/l
Geometric mean sediment size	d_g	0.245	mm
Geometric standard deviation	σ_g	1.22	
Sediment fall velocity	v_s	3.2	cm/sec
Water temperature	T	21	°C
von Karman constant	k	0.26	
Rouse exponent	z	1.67	
Froude number	Fr	0.75	
Reynolds' number	Re	1.24×10^5	

The suspended sediment concentration profile was measured by suction sampling tube. Three samples were obtained at each measurement location. The volume of each sample was one liter; the sample time on the order of three minutes. The results are shown in Figure 7.1.1. The mean of the samples is indicated by the plotting symbol; the range of the samples by the solid line. The variation noted is of the order of that commonly reported in similiar laboratory measurements.

Laser-Doppler velocimetry is dependent on the presence of a dilute concentration of small fluid tracer particles. If the particle number density of tracer particles becomes too large, the velocimetry signal deteriorates. The laser beams are diffused by repeated light scattering along the beam path. Multiple fluid tracer particles pass simultaneously through the beam intersection volume. The velocimetry signal is obscured.

Fluid tracer particles were continuously generated in the flume system by abrasion of sand grains and the flume return pipe. After several hours of recirculation in the flume, the flume water became visibly cloudy. Thus, it was repeatedly necessary to stop the circulating pump and change the water in the flume system. With care, it was possible to reproduce flow conditions to within the error inherent in measurement by point gage or pitot tube. That is, the errors which result from a change of the flume water were indistinguishable from the uncertainties which result from the repetition of a given measurement without disturbing the flowing flume.

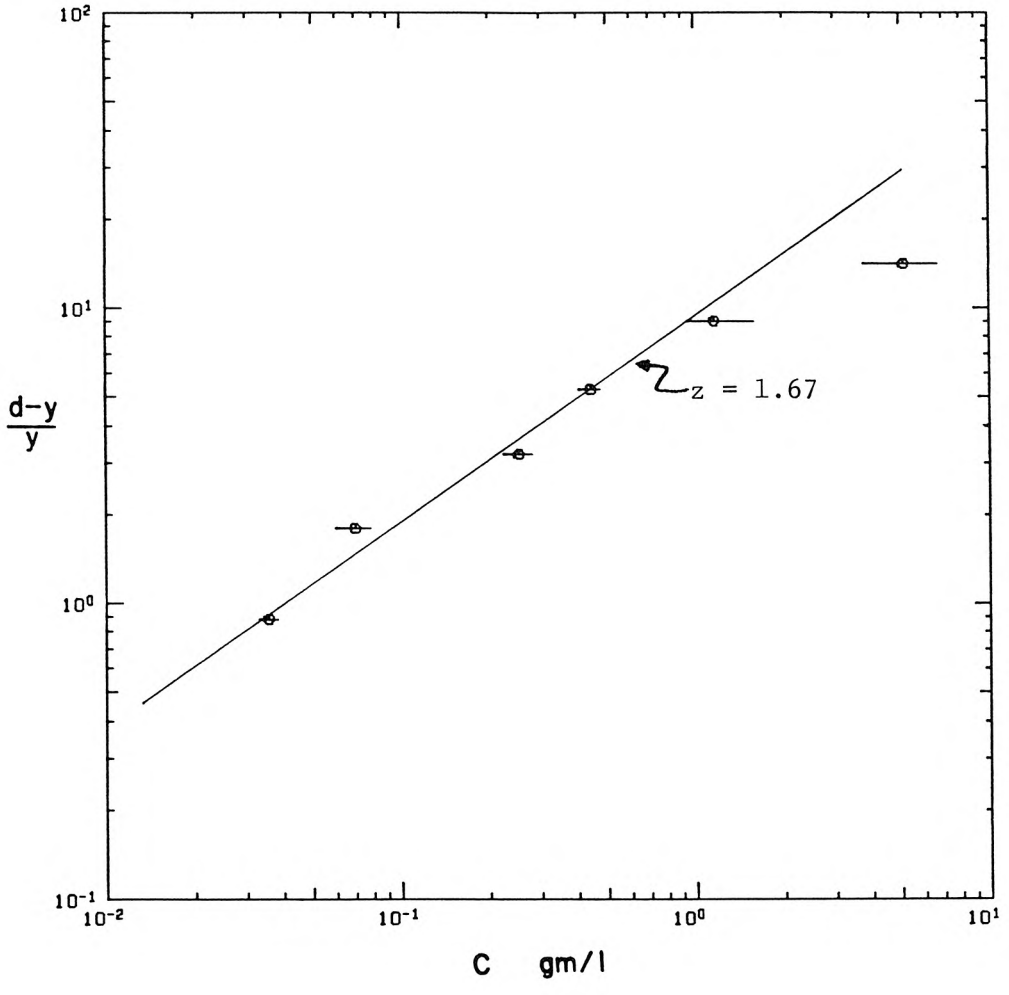

Figure 7.1.1 Suspended sediment concentration profile

7.2 Description of velocimetry procedures

A total of twenty-four velocimetry data records were obtained at six different vertical locations in the water column. The velocimetry measurements were all one-dimensional in the streamwise direction. Twelve data records were retained for later analysis; seven data records were discarded due to the dubious accuracy of the velocimetry data and five data records were discarded due to possible ambiguities in the identification of fluid and sediment grain measurements. The sampling procedure followed is detailed in van Ingen (1981).

At each location in the water column, the laser beam intersection was positioned with the point gage. Several short exploratory test data records were taken with various combinations of the band-pass filter setting, the Doppler burst threshold level, and the preset number of zero-crossings. It is necessary to obtain and screen sample data records before a valid combination of the above instrumentation settings can be assured. After preliminary screening, the final instrumentation settings were selected. Long time sampled data records were then obtained at all chosen instrumentation settings. The sampling period of the long time sampled records ranged from five minutes to twenty minutes. Some duplicate data records, records with identical instrumentation settings, were taken as a check on the time variability of the data acquisition.

The flume water was changed before moving the velocimeter to the next vertical measurement location. All measurements at a given elevation were obtained without altering the flume flow in any manner. After refilling, the flow was allowed to stabilize for approximately

thirty minutes prior to the acquisition of new exploratory test data records. Velocimetry data were obtained at elevations of 6.00, 4.00, 2.70, 1.80, 1.20, and 0.75 cm above the sediment bed reference level. Beneath 0.75 cm, the laser beams were, more often than not, blocked by the sediment bed; no measurements were possible.

During the subsequent analysis, a data record was discarded if it was found to have an anomalously high fraction of invalid data events or if the probability density function of the Doppler burst signal frequency was markedly skewed with respect to the frequency pass band of the filter. The discarded records were generally obtained as the flow became overseeded with fluid tracer particles. The variability noted in the remaining data records is judged to be due to fluctuations in the flow, not to the velocimetry data acquisition. The measurement location, the number of measurements of each type of scattering particle, and the length of record of each of the twelve retained validated data records are summarized in Table 7.2.1.

Table 7.2.1 Velocimetry Data Records

Location (cm above the bed)	Record Name	Period (min:sec)	Number of Fluid Velocity Measurements	Number of Valid Sediment Grain Velocity Measurements	Total Number of Sediment Grains
6.00	SQ600	9:06	29883	422	1597
	SQ601	15:10	13352	551	5733
4.00	SQ401	12:01	14607	1213	12538
2.70	SQ271	10:31	12776	1737	15593
	SQ272	18:35	14808	3112	29366
1.80	SQ180	5:37	21203	1403	5405
	SQ181	6:53	9916	1143	9655
	SQ182	7:02	23585	1880	7881
1.20	SQ120	9:09	9763	1584	16115
	SQ121	9:17	9118	2131	19661
	SQ122	8:58	9566	2047	20967
0.75	SQ750	25:04	9320	1181	12997

CHAPTER 8

PRESENTATION OF THE RESULTS

The one-dimensional laser-Doppler velocimetry data are presented in this chapter. The fluid and sediment grain velocity records are discussed first. Sediment grain inter-arrival time data are then shown. Finally, sediment grain velocity and inter-arrival time correlation statistics are presented.

8.1 Representative velocimetry data records

Portions of one of the validated velocimetry records obtained at each of the vertical measurement locations are presented in Figures 8.1.1 through 8.1.6. The measurement locations are identified by their respective elevations in centimeters above the sediment bed reference level. The fluid velocity measurements are connected by a solid curve; the sediment grain velocity measurements are indicated with plotting symbols. The plotted fluid velocity measurements have been filtered by a running average technique. In Figure 8.1.1, location 6.00, the effect of water surface waves on the data may be clearly seen. These waves, when present, were visually observed to shift slowly downstream. Also note that the sediment grains are, more often than not, moving faster than the fluid. No such wavy character is evident in the sample record from location 4.00, Figure 8.1.2. The sediment grains occasionally move faster than the surrounding fluid. The data records at location 2.70, exemplified by Figure 8.1.3, show little or no wavelike motion. The sediment grains move at a velocity comparable to that of the surrounding fluid. The data records at

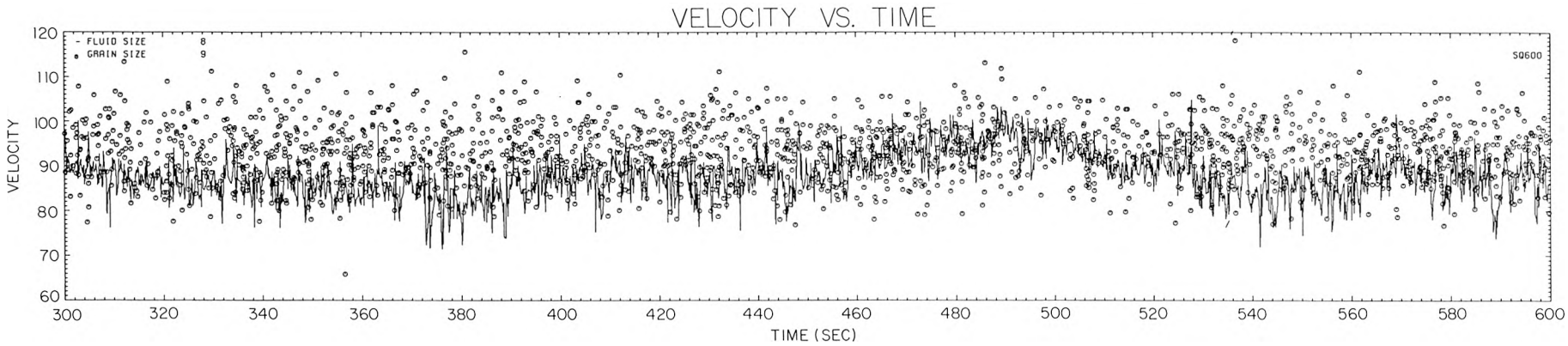

Figure 8.1.1 Sample velocimetry data record, location 6.00

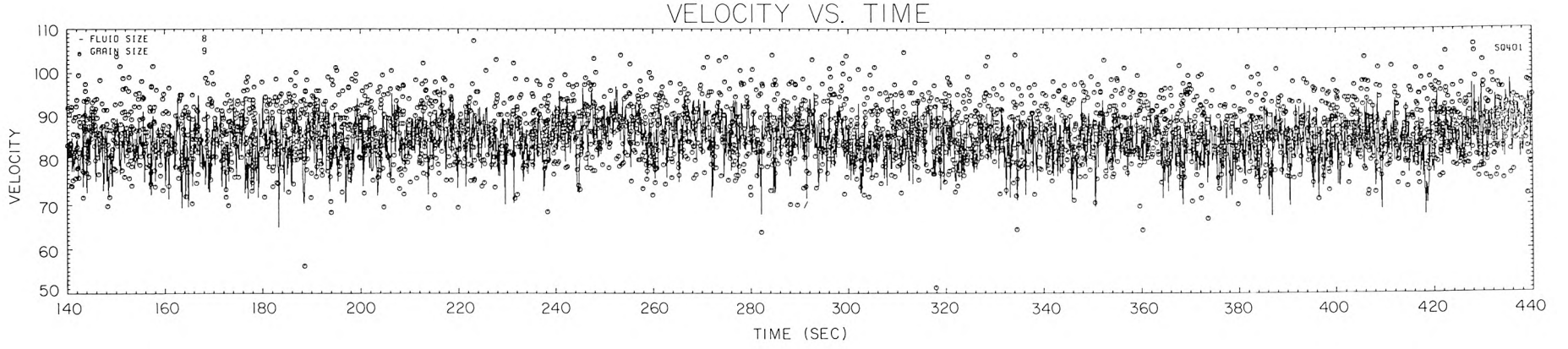

Figure 8.1.2 Sample velocimetry data record, location 4.00

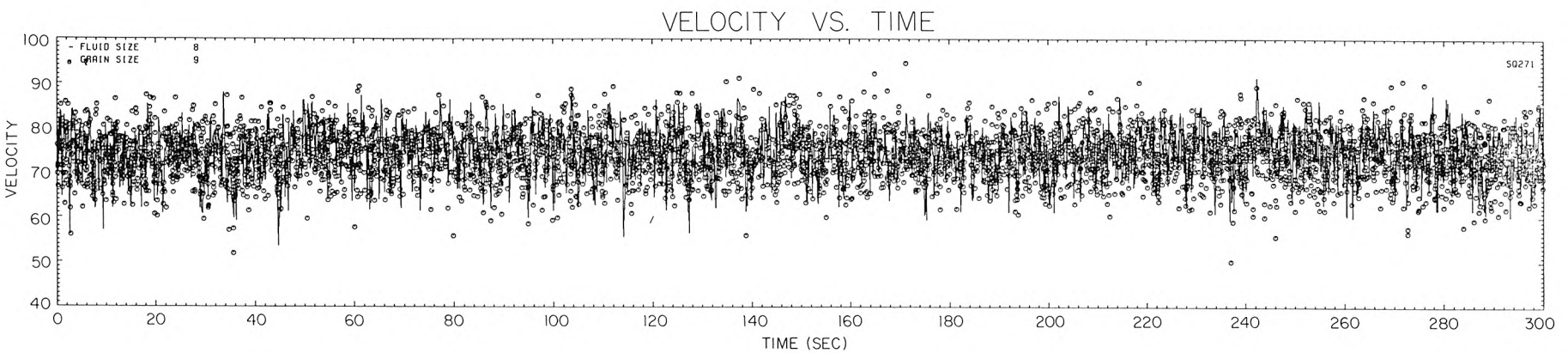

Figure 8.1.3 Sample velocimetry data record, location 2.70

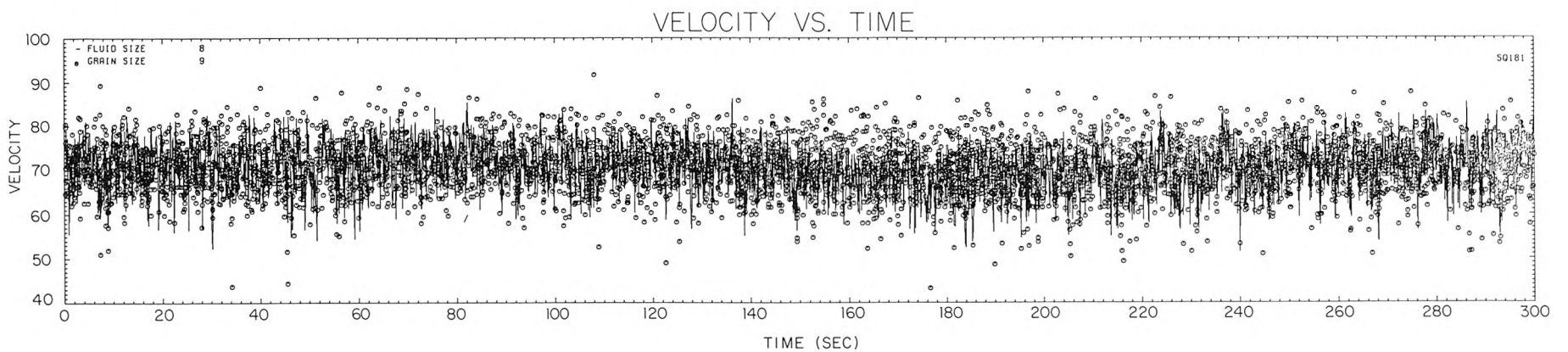

Figure 8.1.4 Sample velocimetry data record, location 1.80

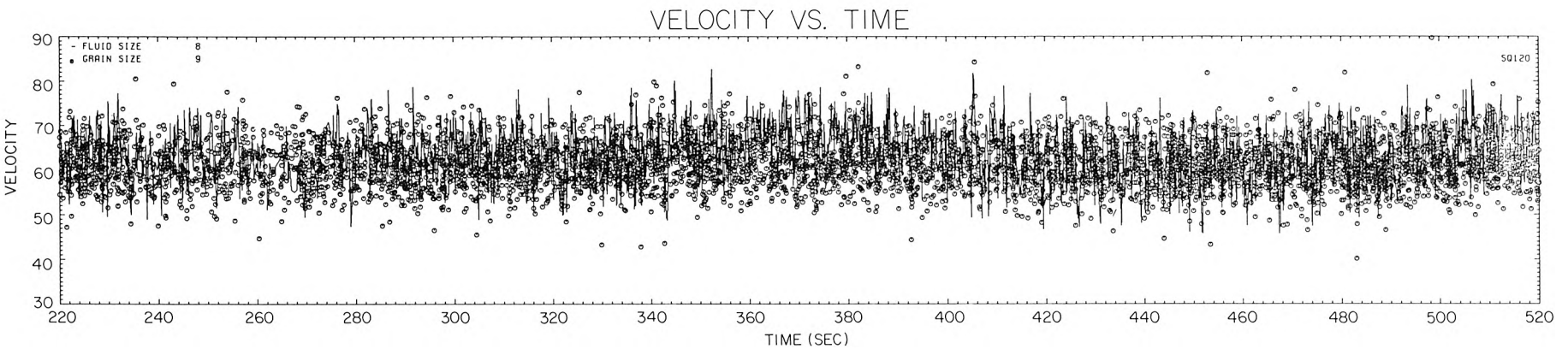

Figure 8.1.5 Sample velocimetry data record, location 1.20

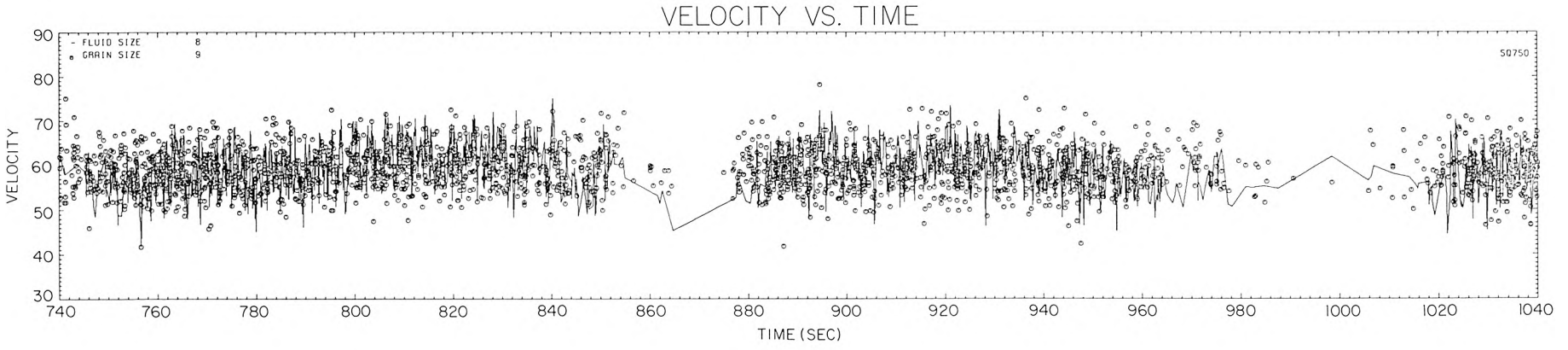

Figure 8.1.6 Sample velocimetry data record, location 0.75

location 1.80, Figure 8.1.4, are very similiar to those obtained at location 2.70. At location 1.20, Figure 8.1.5, a wavy character is again observed. The oscillations are now due to intermittent undulations in the sediment bed. Many of the sediment grains lag the nearby fluid. The effect of bed undulations is seen most clearly in Figure 8.1.6, location 0.75. The velocimetry record contains periods in which little or no data was collected. The gaps in the data are caused by undulations in the sediment bed which completely blocked the laser light beams.

Figures 8.1.7 and 8.1.8 illustrate the effects of the filter used on the fluid velocity measurements in the preceding figures. The unfiltered data appear in the lower plot of each figure. Trends in the fluid velocity data record are more easily seen in the filtered plot. The filtered plots must be viewed with care, however, when comparing the fluid and the sediment grain velocity. The velocity of some of the sediment grains seems very different from the nearby filtered fluid velocity measurements. Filtering the fluid velocity removes many of the extreme fluctuations. Comparison of the filtered plots to the unfiltered plots shows that this apparent difference in the sediment grain and fluid velocity is primarily due to the filtering. The sediment grain velocity is seen to be quite similiar, in most cases, to the nearby fluid velocity.

Some grains are observed to have a velocity different from that of the surrounding unfiltered fluid, but this still may not be the case within the flow. The fluid velocity data record may lack measurements of the "surrounding" fluid velocity. Portions of the unfiltered data

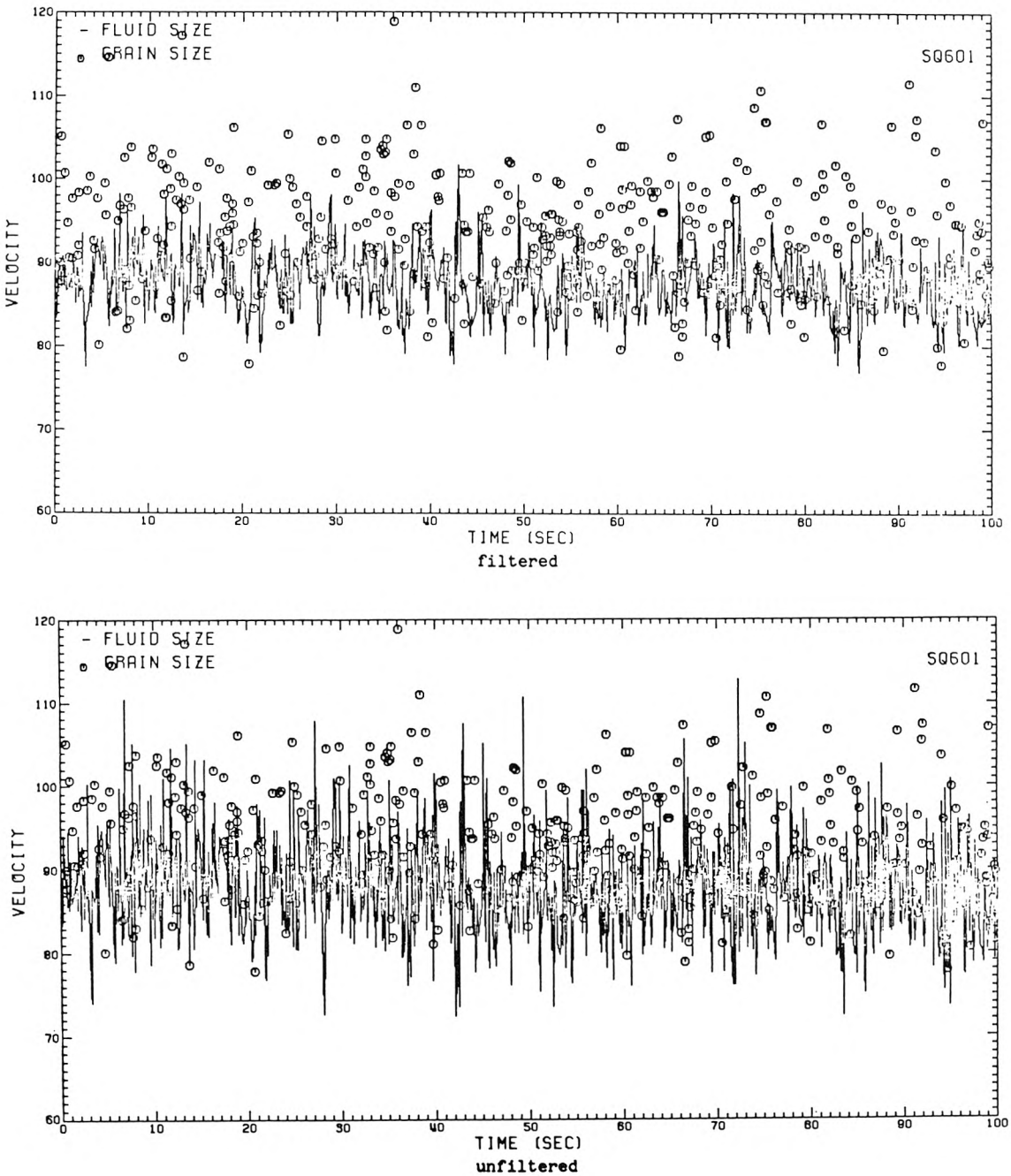

Figure 8.1.7 Sample velocimetry data record, filtered and unfiltered, location 6.00

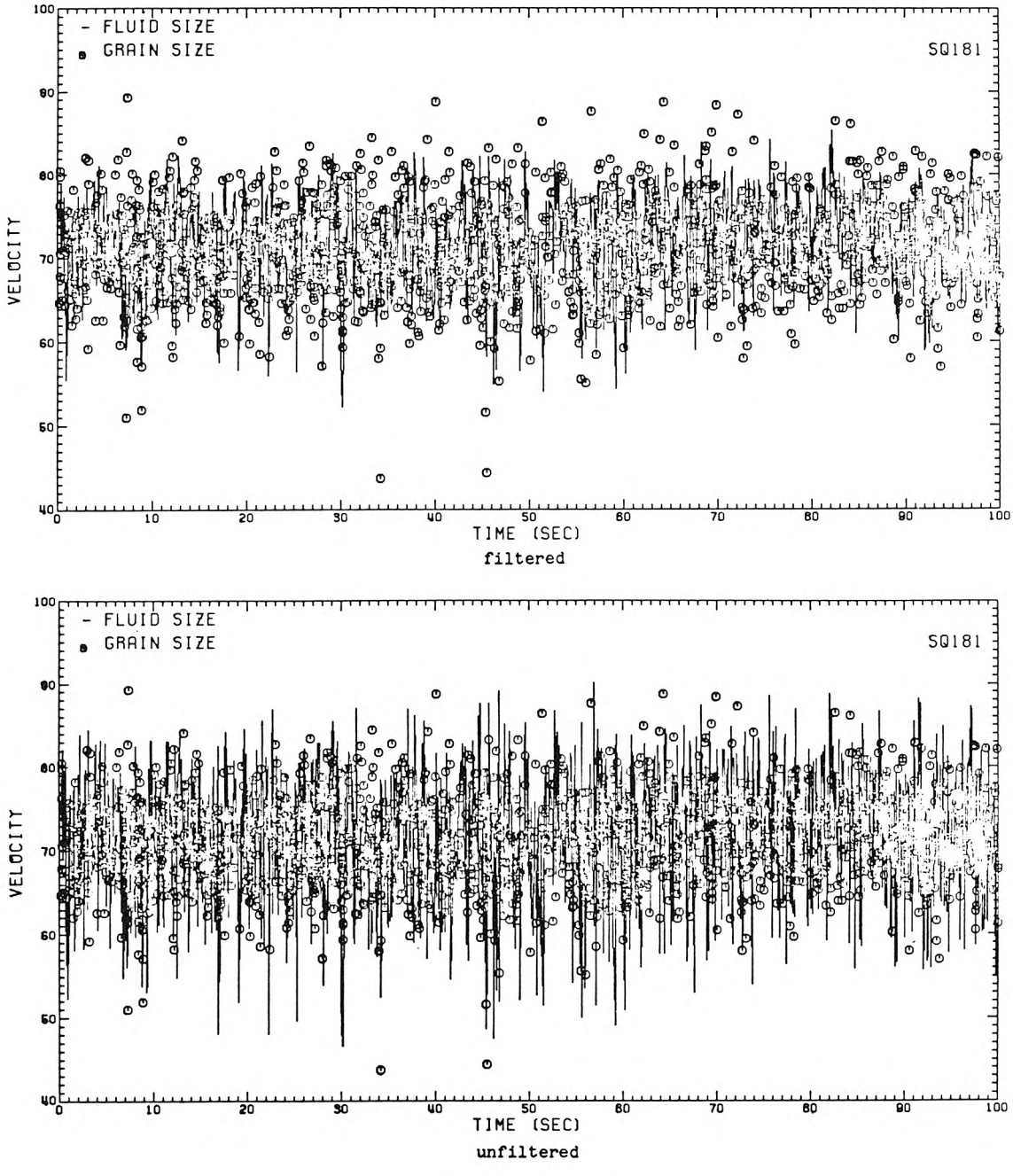

Figure 8.1.8 Sample velocimetry data record, filtered and unfiltered, location 1.80

records shown in the previous Figures are expanded in Figure 8.1.9 to allow each fluid velocity measurement to be identified with a second plotting symbol. At approximately t=17 seconds the fluid velocity data record from location 6.00 contains a gap. No measurements of the fluid velocity were made. The sediment grain velocity recorded at this time seems to differ from the plotted fluid velocity, but there are no measurements of the fluid velocity very near to the grain. The times of measurement of fluid and sediment grain velocity are not coincident and the resulting data records are not continuous.

8.2 Measurements of fluid and sediment grain velocity

Profiles of the mean velocity of the fluid, $\overline{u}$, and the sediment grains, $\overline{u}_g$, are shown in Figure 8.2.1. The mean velocities computed from the different data records obtained at a single location are noted to vary. This is most probably due to slow, long time-scale fluctuations in the flow. A comparison of $\overline{u}$ and $\overline{u}_g$ is presented in Figure 8.2.2. In the lower portion of the flow, $\overline{u}_g$ is less than $\overline{u}$. At location 6.00, near the water surface, the sediment grains are observed to move significantly faster, in the mean, than the fluid.

Profiles of the standard deviation of the velocity of the fluid, $\sqrt{\overline{u'^2}}$, and the sediment grains, $\sqrt{\overline{u_g'^2}}$, are shown in Figure 8.2.3. Profiles of the relative velocity fluctuation, the local value of the standard deviation expressed as a percentage of the local mean, are given in Figure 8.2.4. The fluid velocity observations are in accordance with existing experimental measurements. Comparisons of $\sqrt{\overline{u'^2}}$ and $\sqrt{\overline{u_g'^2}}$ are given in Figure 8.2.5 and Figure 8.2.6. Throughout

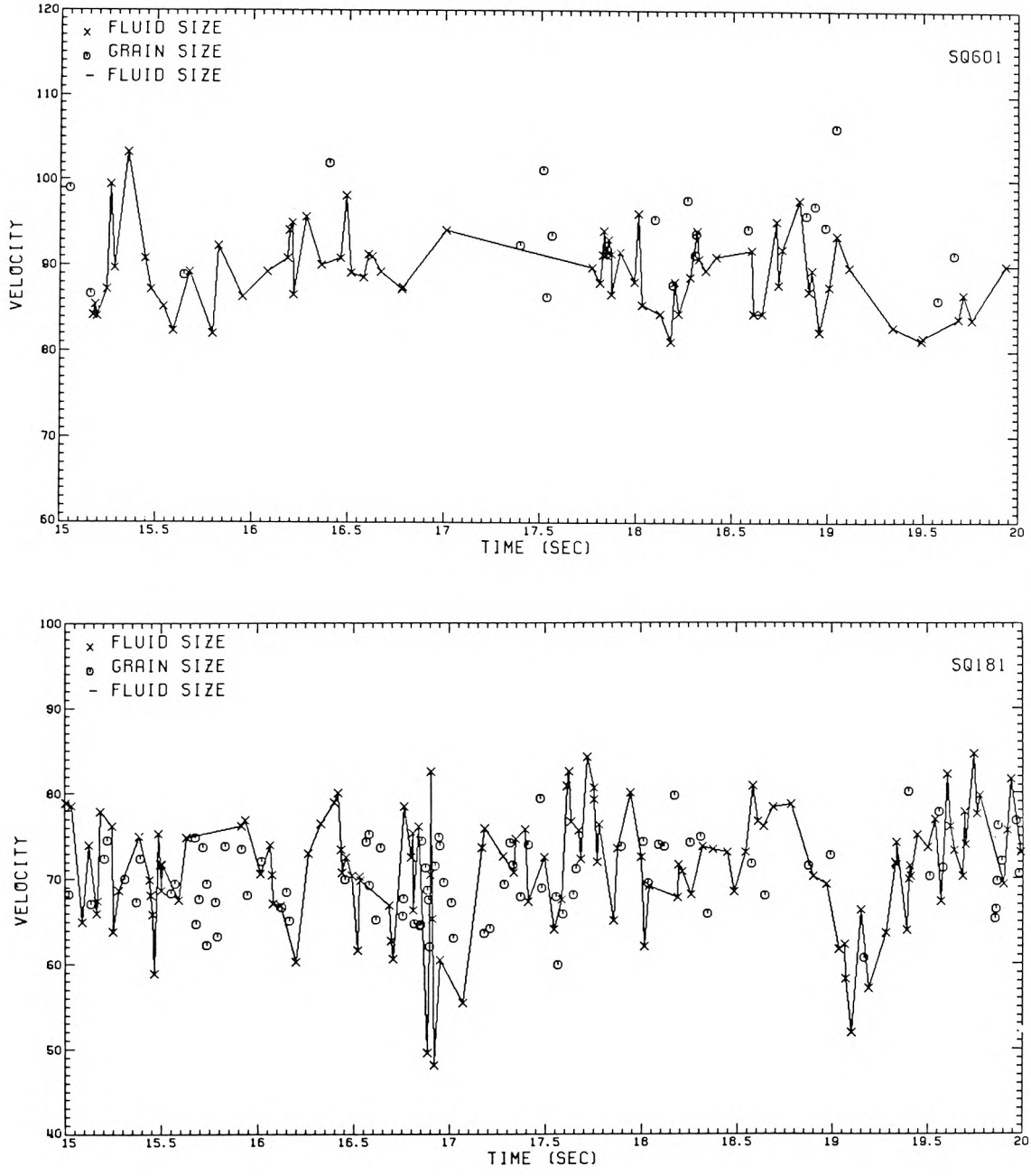

Figure 8.1.9 Sample expanded scale velocimetry data records, locations 6.00 and 1.80

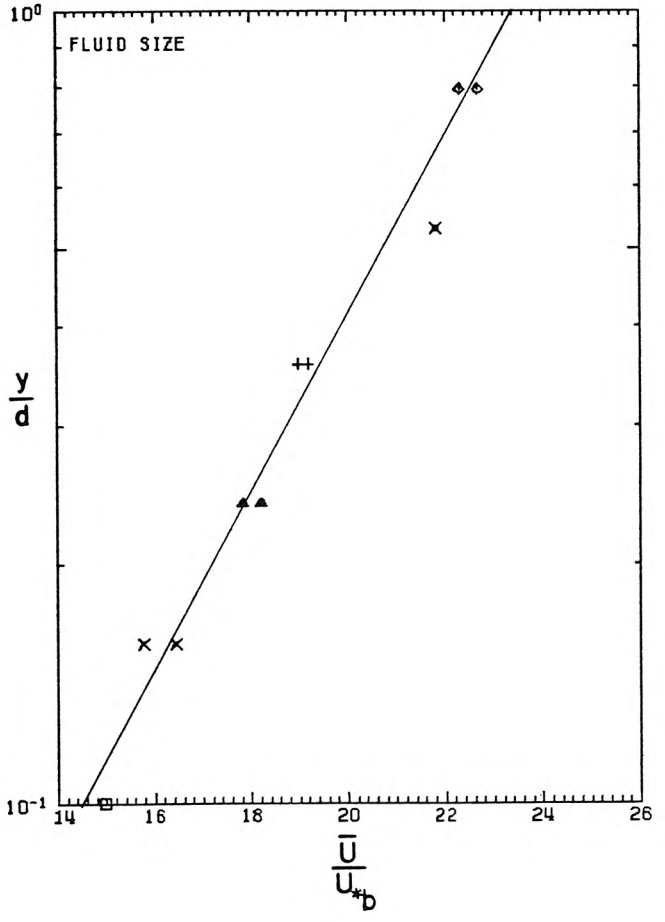

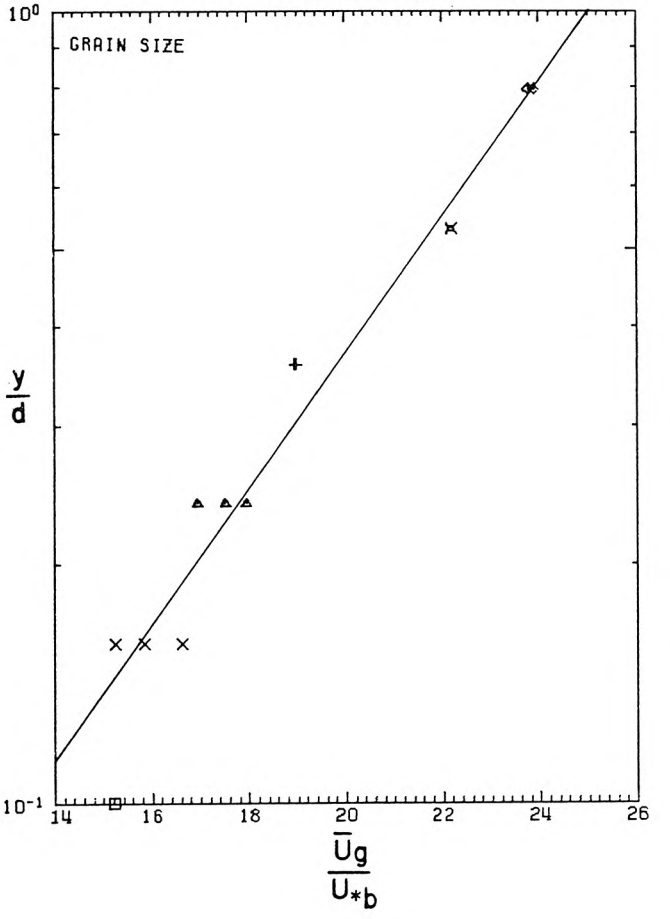

Figure 8.2.1 Profiles of mean velocity

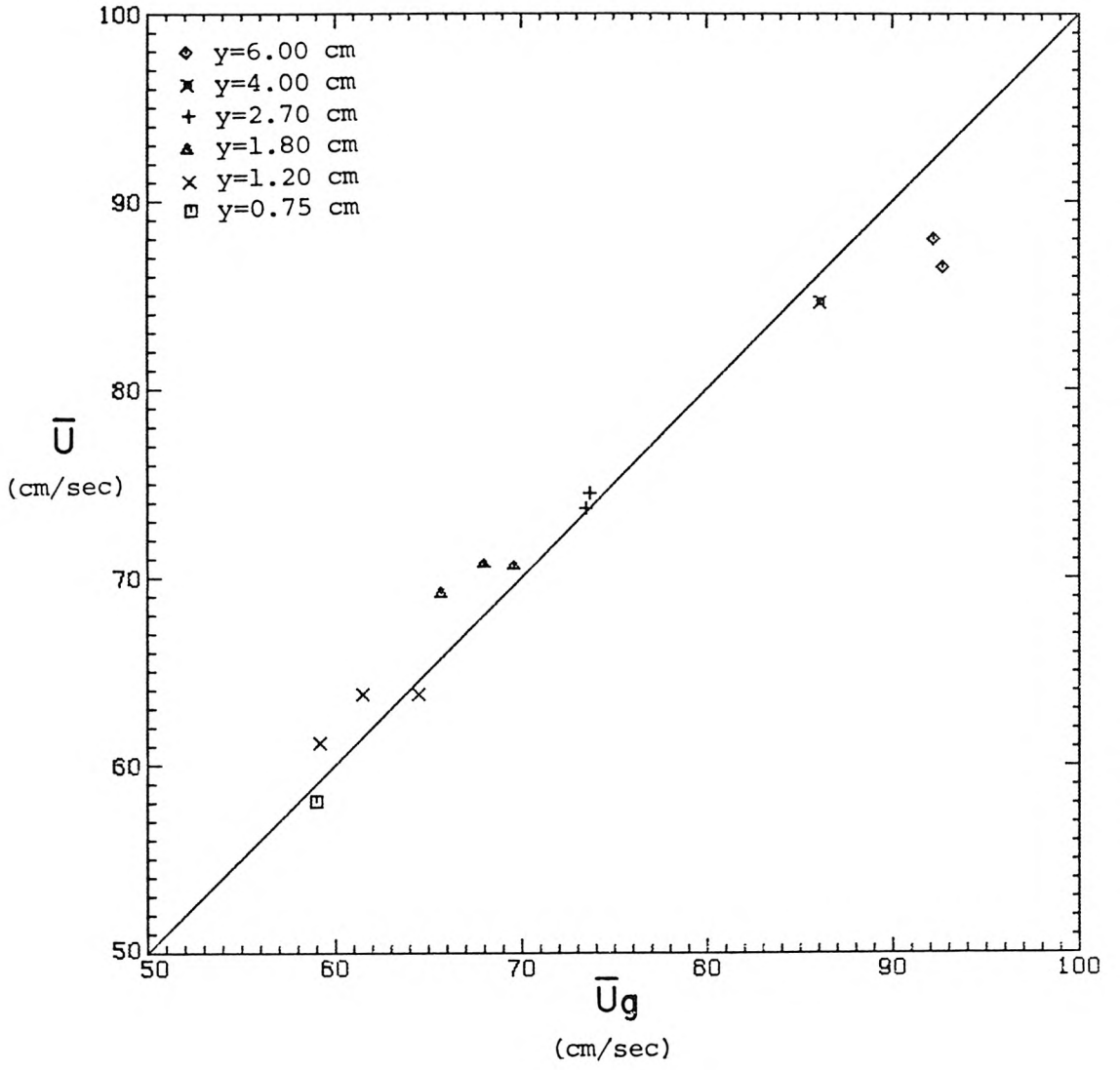

Figure 8.2.2 Comparison of fluid and sediment grain mean velocity

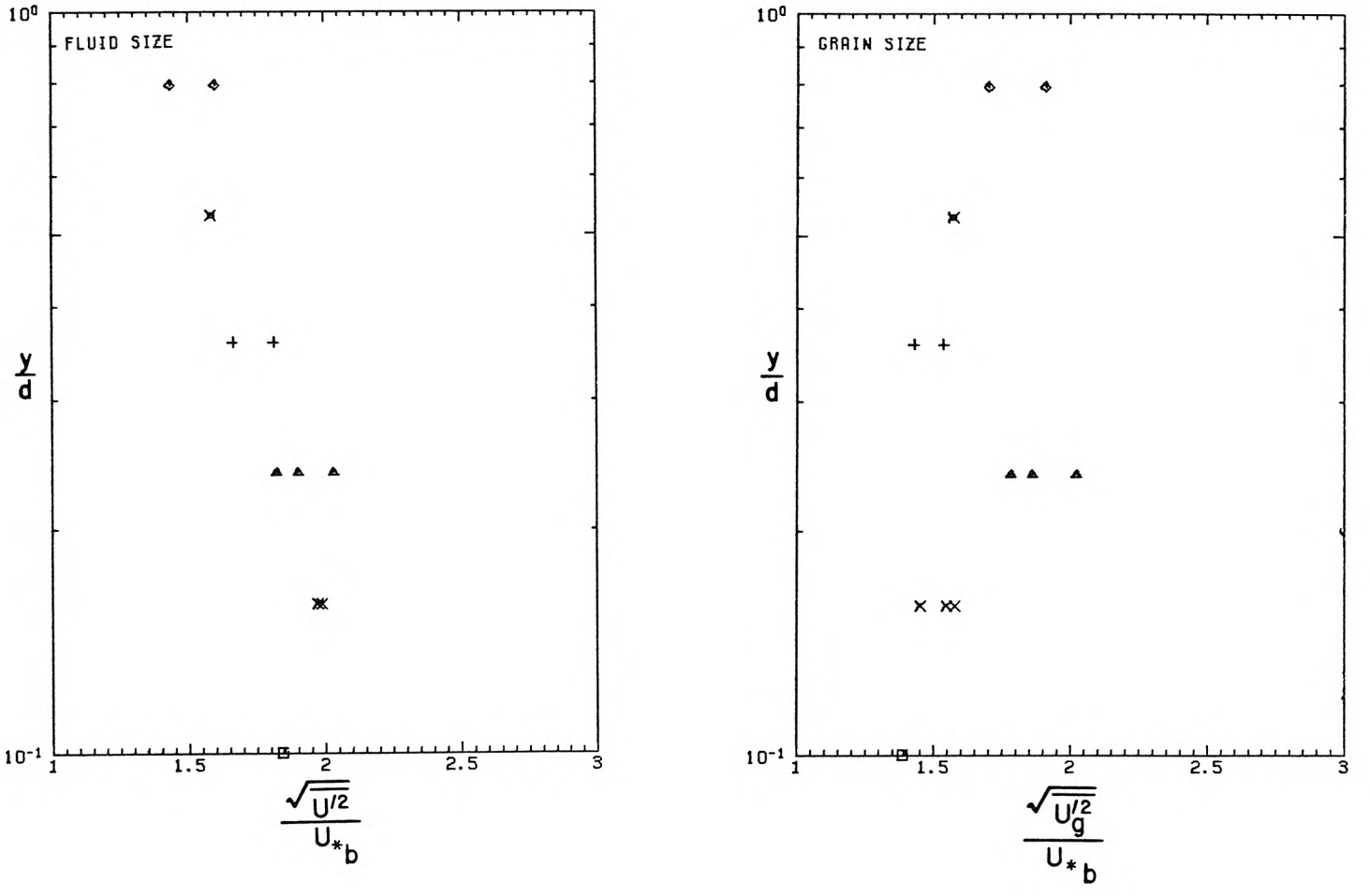

Figure 8.2.3 Profiles of velocity standard deviation

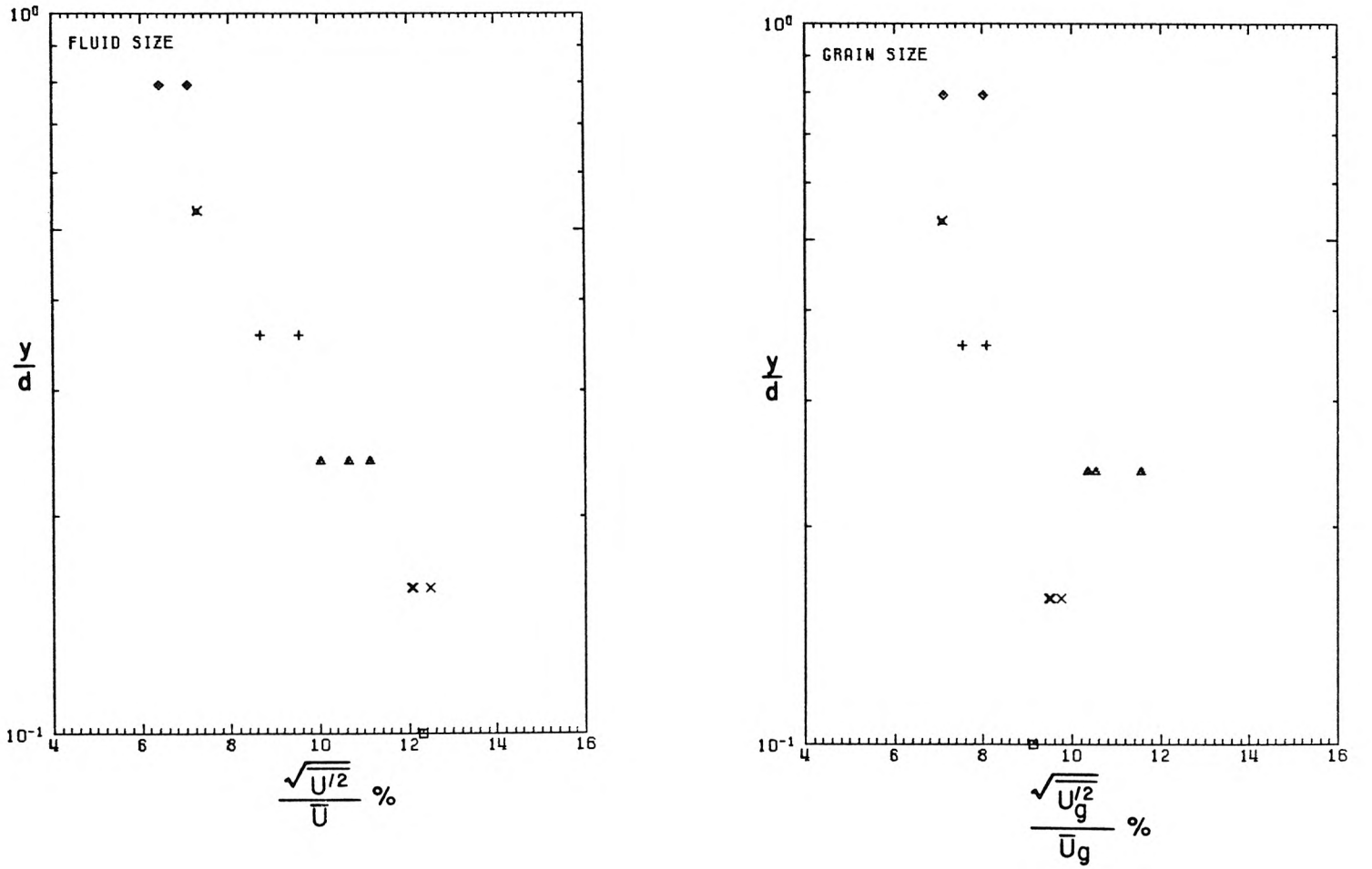

Figure 8.2.4 Profiles of relative velocity fluctuation

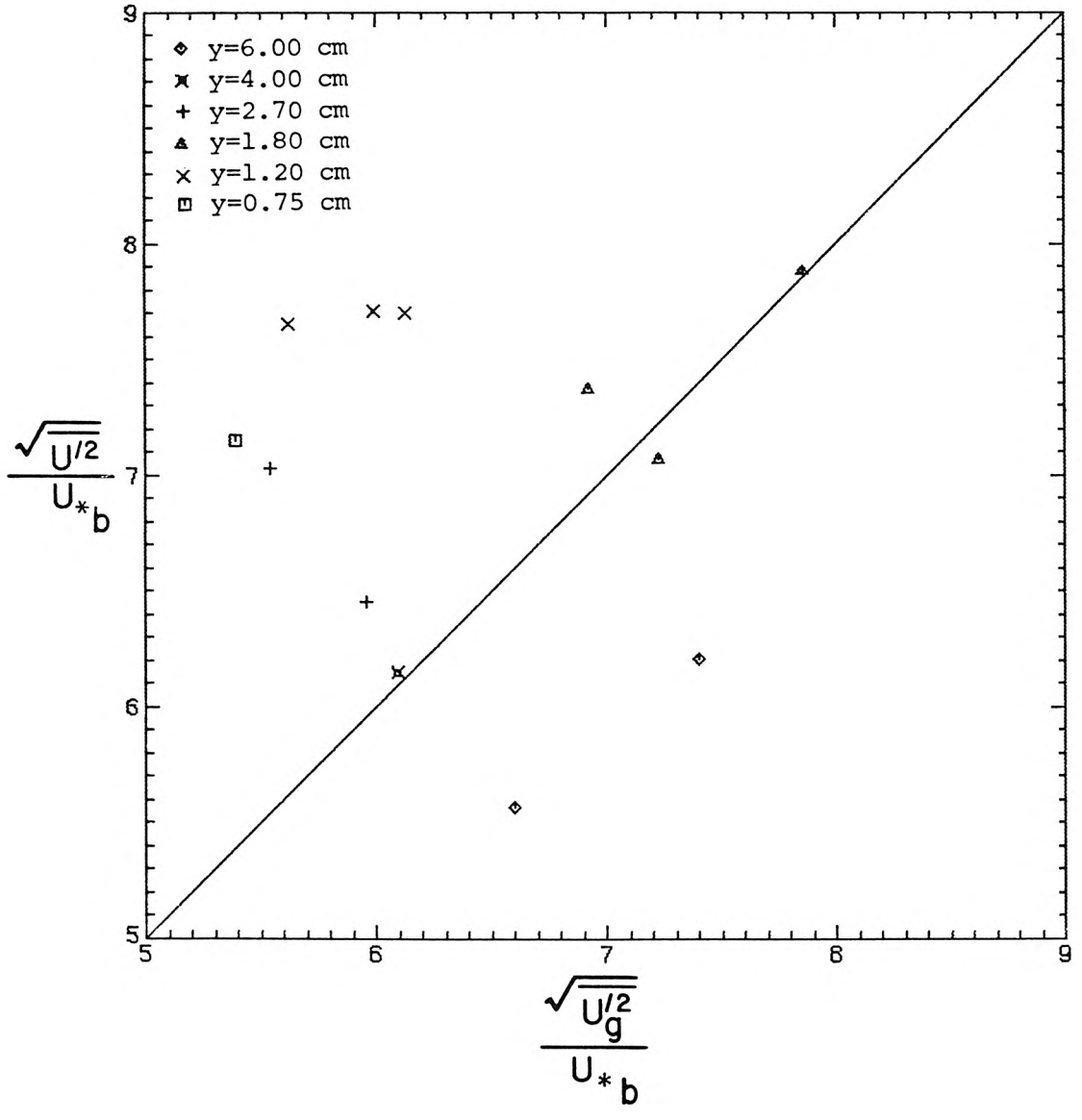

Figure 8.2.5 Comparison of fluid and sediment grain velocity standard deviation

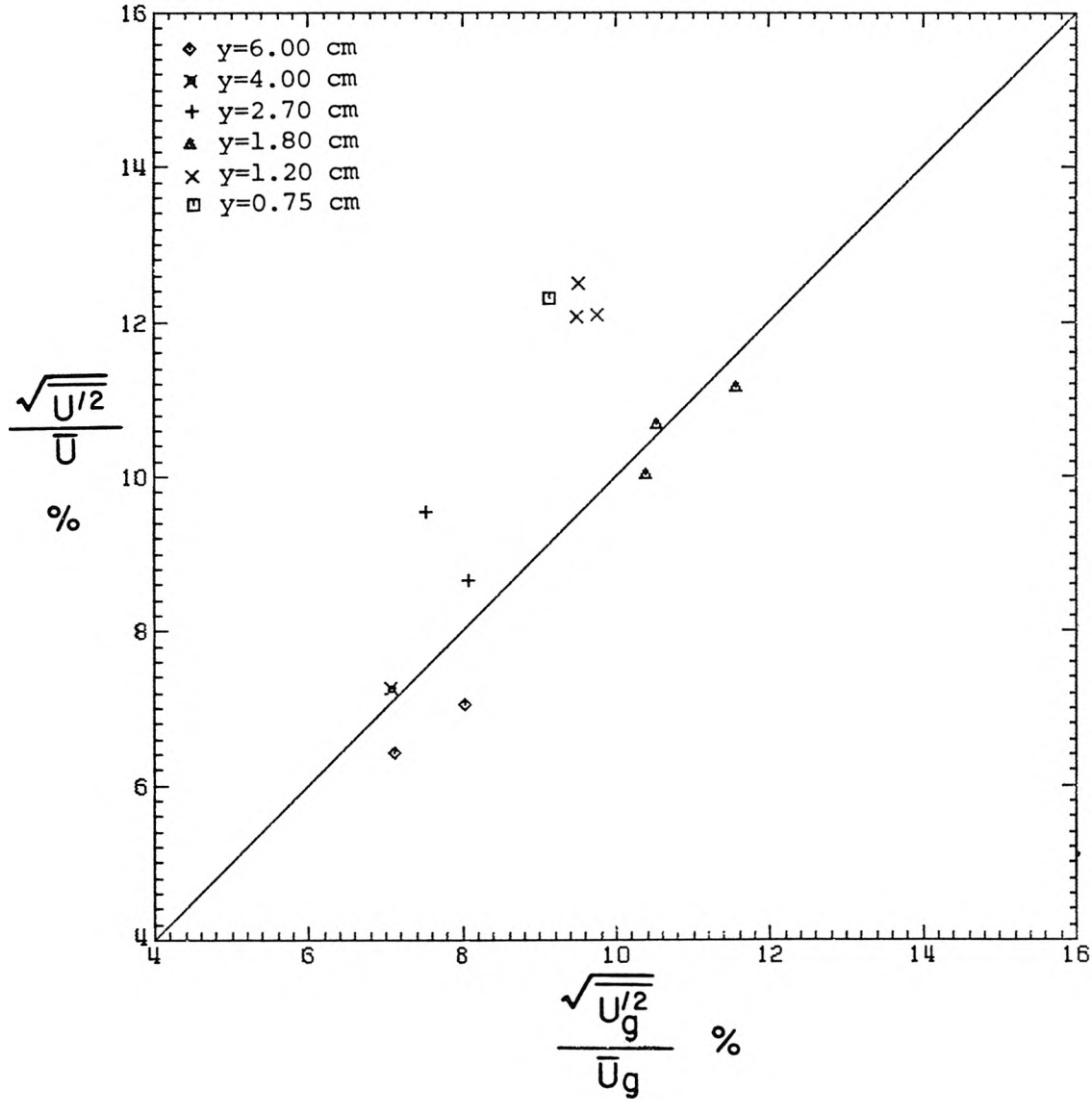

Figure 8.2.6 Comparison of relative fluid and sediment grain velocity fluctuation

most of the water column, $\sqrt{\overline{u'^2}}$ is greater than $\sqrt{\overline{u'^2}_g}$. Near the sediment bed, $\sqrt{\overline{u'^2}}$ and the relative fluctuation in the fluid velocity is much greater than $\sqrt{\overline{u'^2}_g}$. Near the water surface, $\sqrt{\overline{u'^2}_g}$ is much greater than $\sqrt{\overline{u'^2}}$, but their relative fluctuations are nearly equal.

The velocity probability density functions for each data record are shown in Figure 8.2.7. The fluid velocity probability density function is given by the solid line; that of the sediment grains by the dashed line. The mean fluid velocity and the mean sediment grain velocity are noted with plotting symbols. The probability density function of the fluid velocity near the sediment bed is broader than that near the free surface. The sediment grain velocity distribution does not exhibit such a trend. The sediment grain velocity tends to be less than the fluid velocity at locations 1.20 and 1.80. Also, at locations 1.20 and 0.75, the distribution of the fluid velocity is broader than distribution of the sediment grain velocity. The fluid velocity is clearly less than the sediment velocity at location 6.00. At the remaining locations, the probability density functions of the fluid velocity and the sediment grain velocity are quite similiar.

The simple lag correlation coefficients of velocity fluctuations computed for one of the data records from location 1.80 are shown in Figure 8.2.8. Similiar results were obtained for each of the remaining data records. No correlation in the velocity of successive sediment grains was found in any of the data. Unfortunately, the subsequent calculation of the true auto-correlation function proved unreliable. This calculation requires the inversion of a matrix with elements

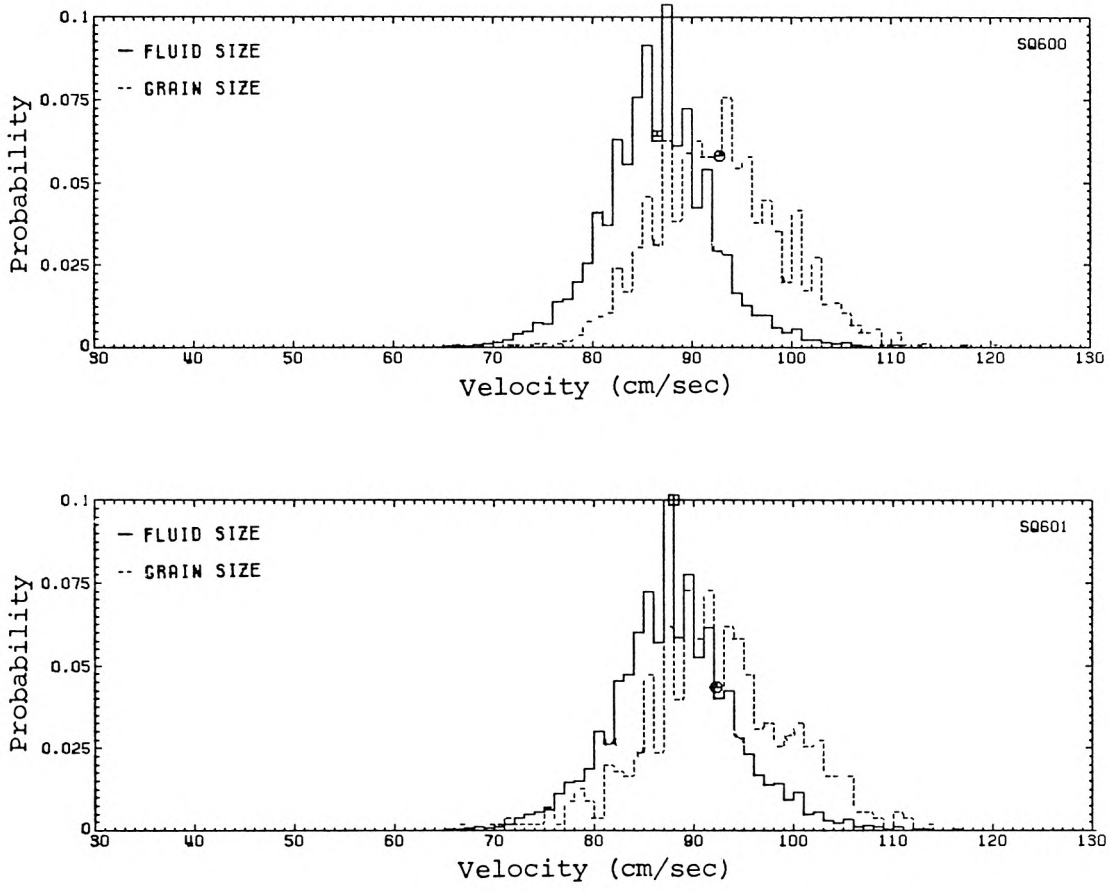

Figure 8.2.7.a Velocity probability density functions, location 6.00

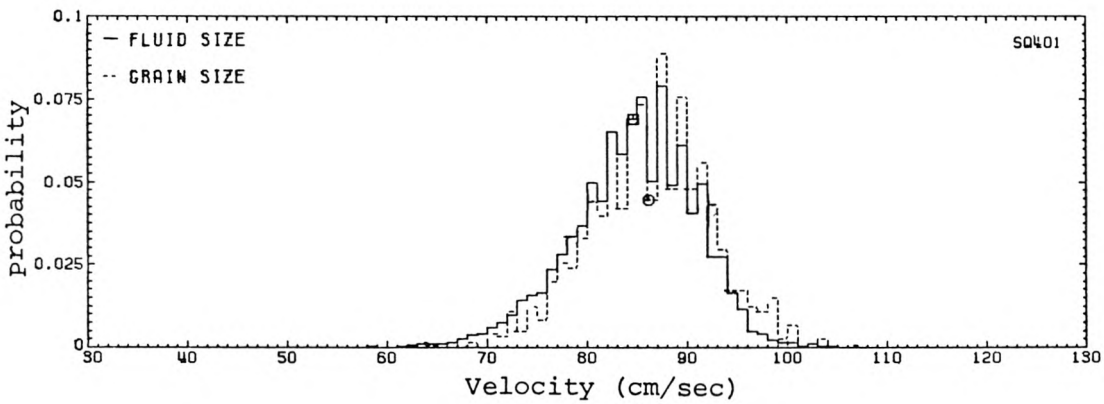

Figure 8.2.7.b Velocity probability density function, location 4,00

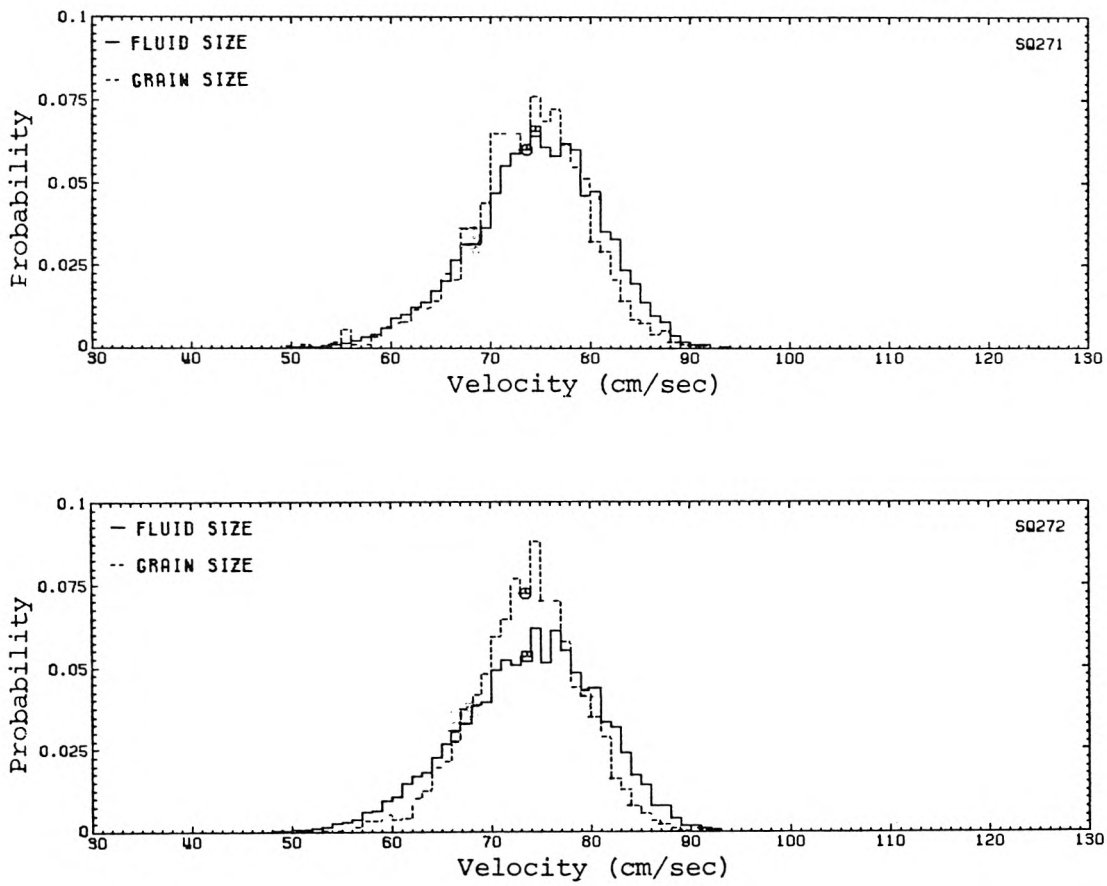

Figure 8.2.7.c Velocity probability density functions, location 2.70

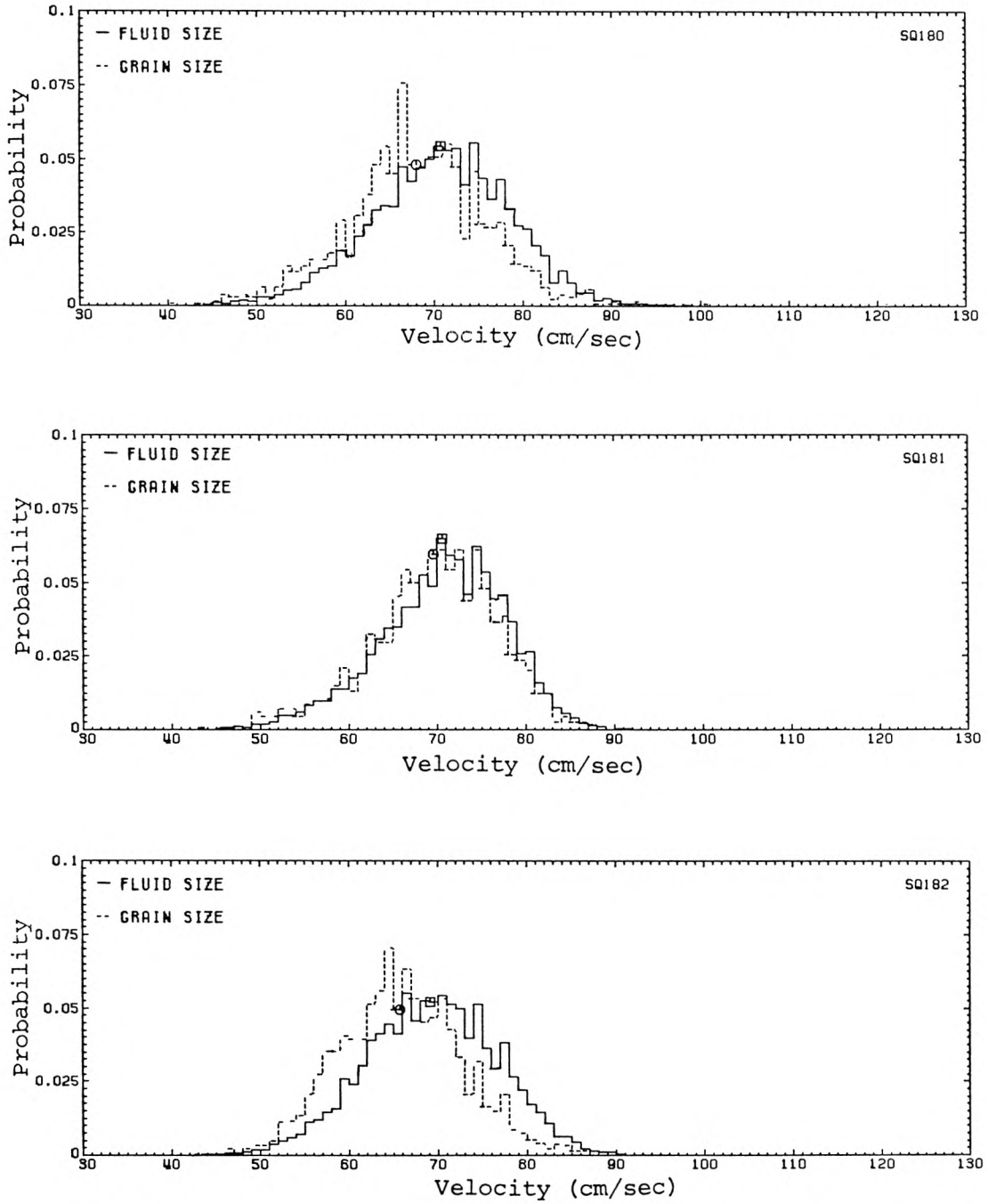

Figure 8.2.7.d Velocity probability density functions, location 1.80

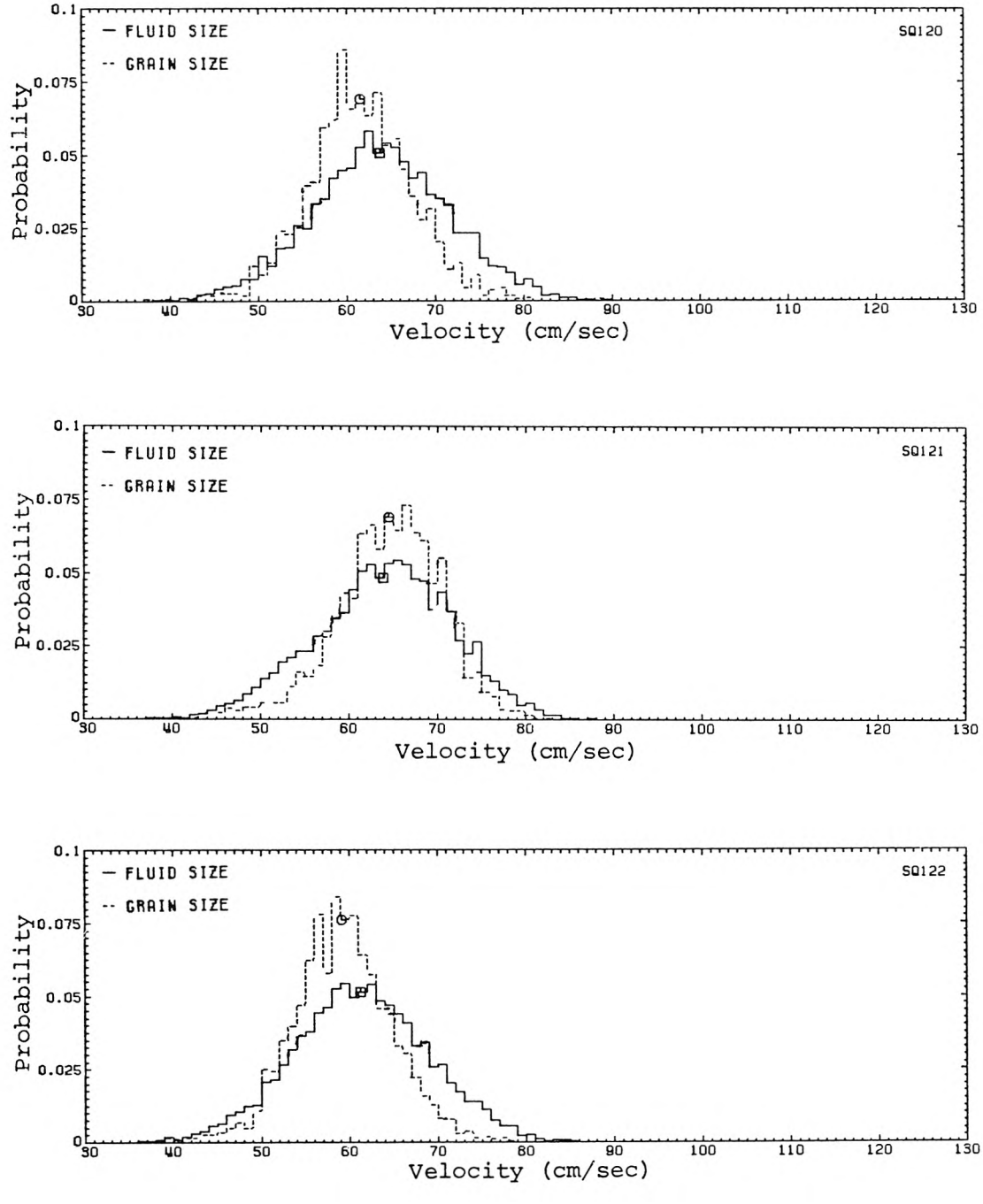

Figure 8.2.7.e Velocity probability density functions, location 1.20

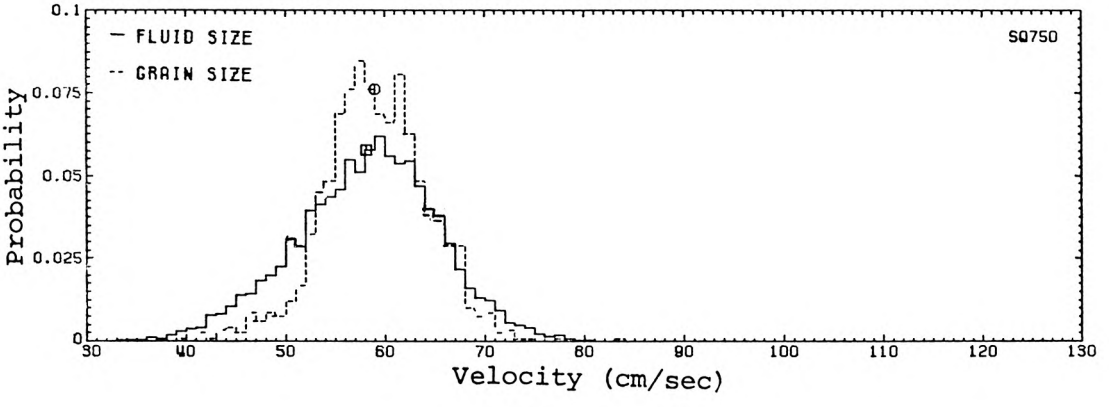

Figure 8.2.7.f Velocity probability density function, location 0.75

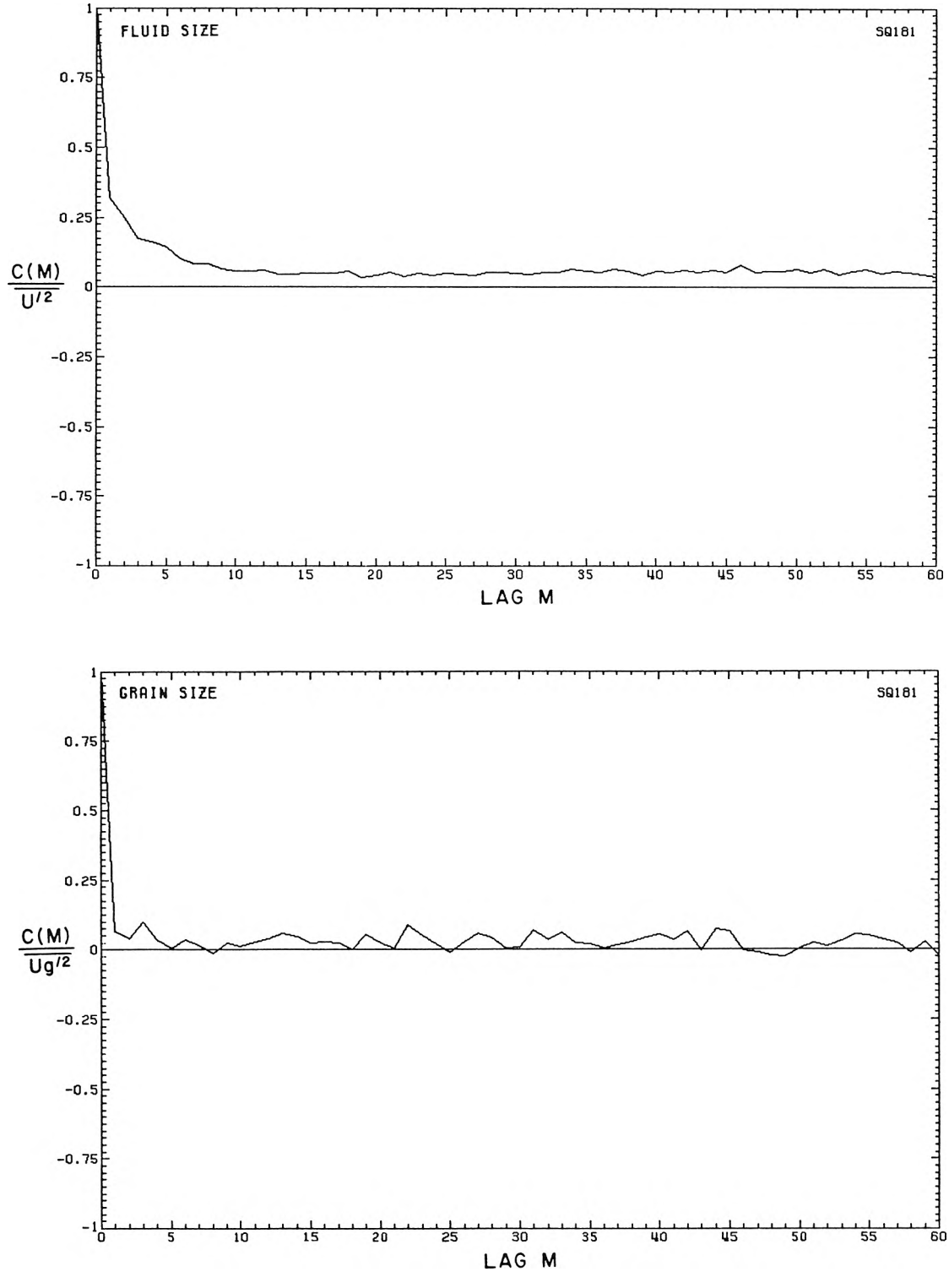

Figure 8.2.8 Sample simple lag correlation coefficients of velocity fluctuation, location 1.80

determined by the probability density functions of lag time τ at lag M. Such a matrix becomes more nearly singular as the sampling becomes more irregular in time. The numerical inversion of a nearly singular matrix is plagued by numerical instability. The computed inverted matrix, if obtained at all, bears little or no resemblance to the inverse of the initial matrix. The velocimetry events obtained in this study are quite irregularly spaced in time. The resulting matrices of lag time probability density for both the fluid and the sediment grain measurements in each data record are nearly singular. The computed true velocity auto-correlation functions were overwhelmingly dominated by the numerical errors and were physically meaningless.

The normalized power spectral estimate of the fluid velocity fluctuations and the relevant power spectral window function as computed for two of the data records are shown in Figure 8.2.9. The power spectral estimate is given by the solid line; the spectral window function is given by the dashed line. The mean sampling frequency is indicated with a plotting symbol. The results are presented for two of the data records with the most similiar time sampling characteristics.

The futility of the spectral computations is apparent. While the power spectral estimate generally decreases with increasing frequency, the expected error in the power spectral estimate is equal to the value of the estimate. There is no smoothing inherent in the direct computation of the power spectral estimate. The spectral window function does indicate a lower bound on the frequency for which the computation of the power spectral estimate should be performed. For

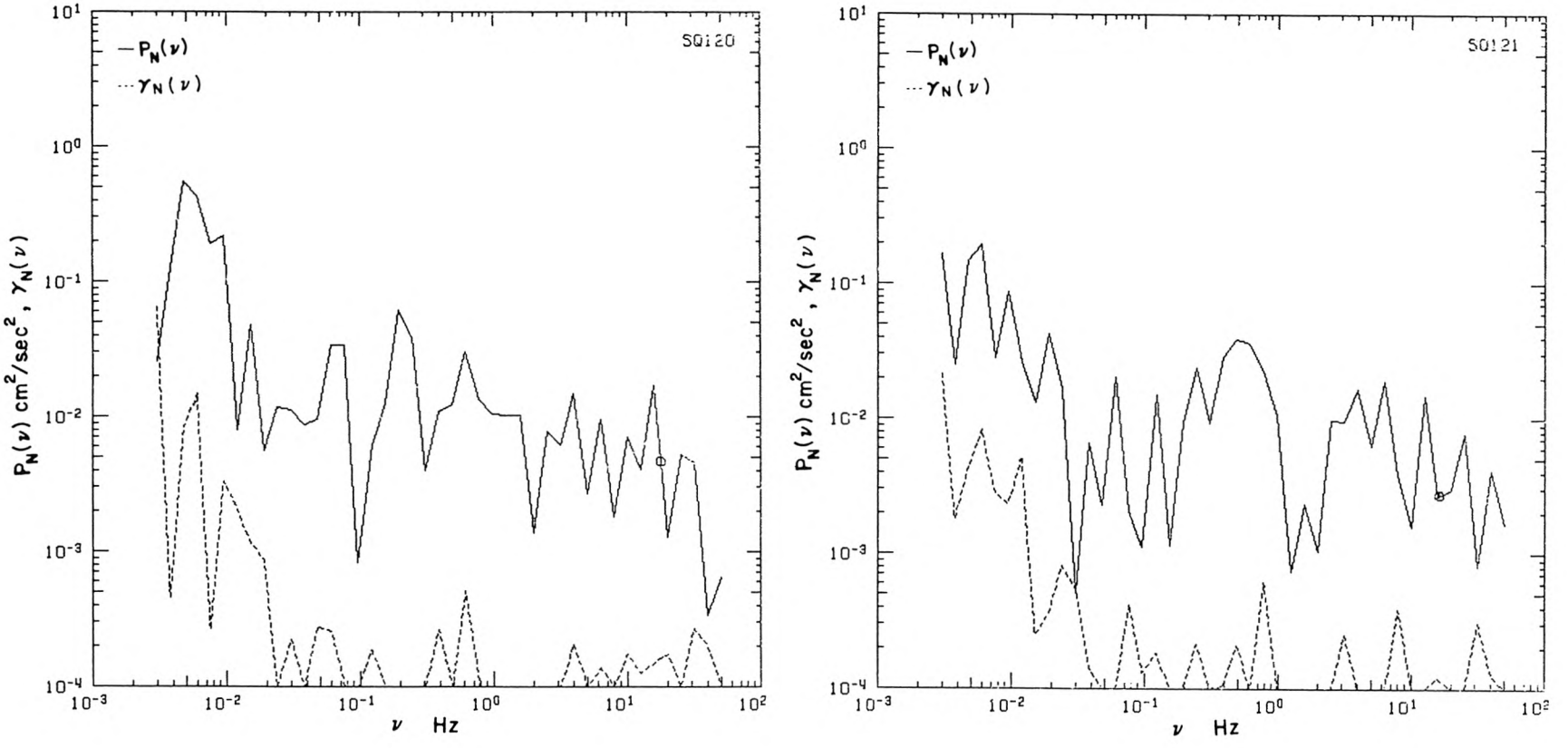

Figure 8.2.9 Sample fluid velocity fluctuation power spectral estimates and power spectral window functions, location 1.20

the presented data records, this lower bound is seen to be approximately 0.02 Hz, which corresponds to roughly one-tenth of the total sampling period.

The results of the spectral calculations of the sediment grain velocity fluctuations are still less instructive. Figure 8.2.10 shows the power spectral estimate and the power spectral window function corresponding to the fluid results shown in Figure 8.2.9. No trend in the power spectral estimate is at all apparent. The mean sampling frequency of the sediment grain velocity in the data records shown is approximately 4 Hz. Thus, at best, only long-time fluctuations in sediment grain velocity can be considered. The expected error in the sediment grain velocity spectral calculations is greater than that of the fluid velocity spectral estimates due to the relatively smaller number of sediment grain velocity measurements.

The effects of the bias correction procedures on the computed mean and standard deviation of the fluid velocity are shown in Figure 8.2.11. The result of the Mc Laughlin-Tiederman (1973) correction is given in Figure 8.2.11.a. The trapezoidal bias correction suggested by Dimotakis (1976) was applied to give Figure 8.2.11.b. Figure 8.2.11.c illustrates the effect of the procedure developed by Mc Dougall (1980). Little change in $\bar{u}$ results from any of the correction procedures. All of the bias corrections tend to increase $\sqrt{\overline{u'^2}}$ slightly. The trapezoidal averaging correction yields a slightly larger change in $\sqrt{\overline{u'^2}}$ than the other correction procedures; however, no significant difference among the three correction procedures is apparent.

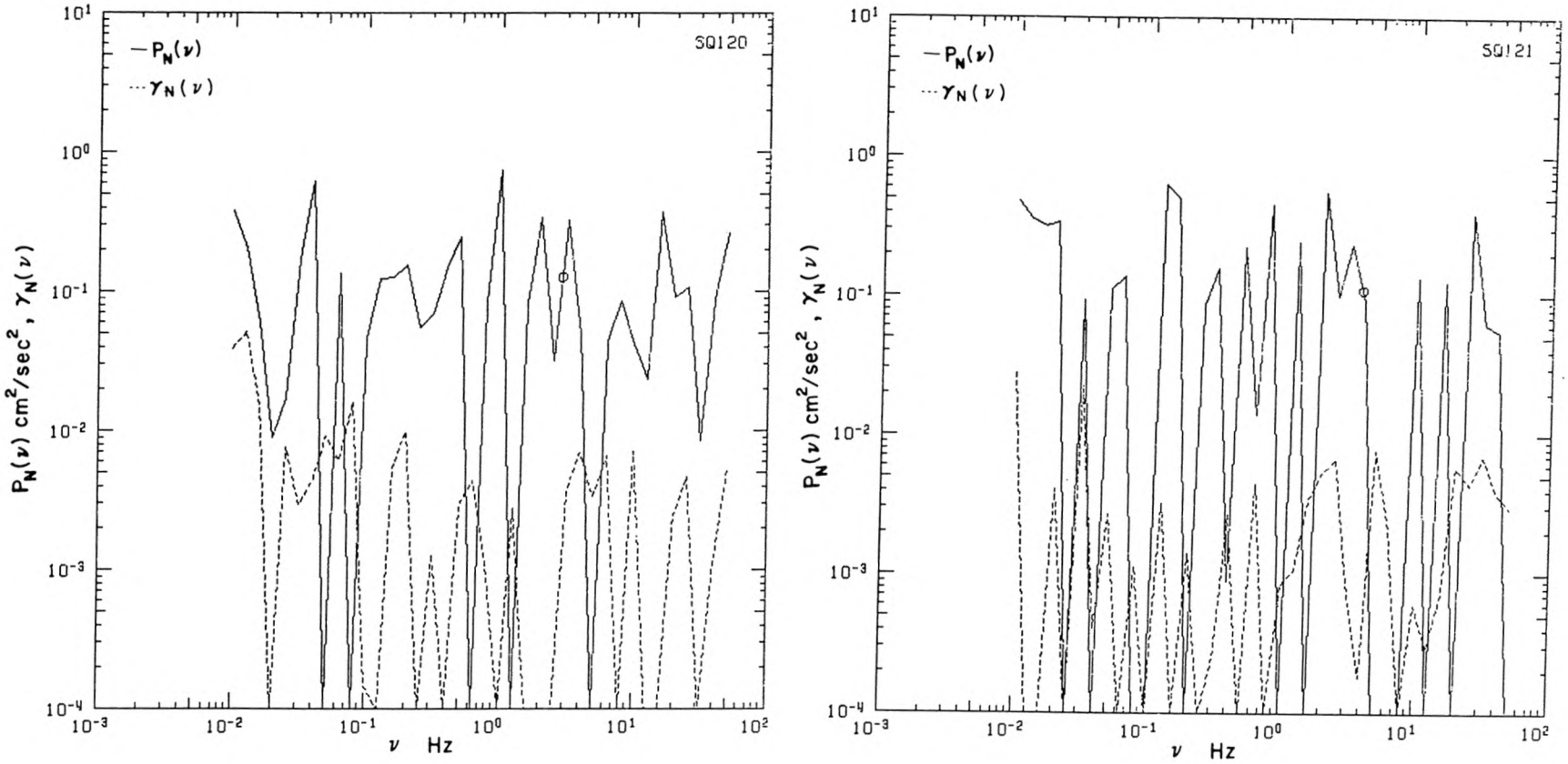

Figure 8.2.10 Sample grain velocity fluctuation power spectral estimates and power spectral window functions, location 1.20

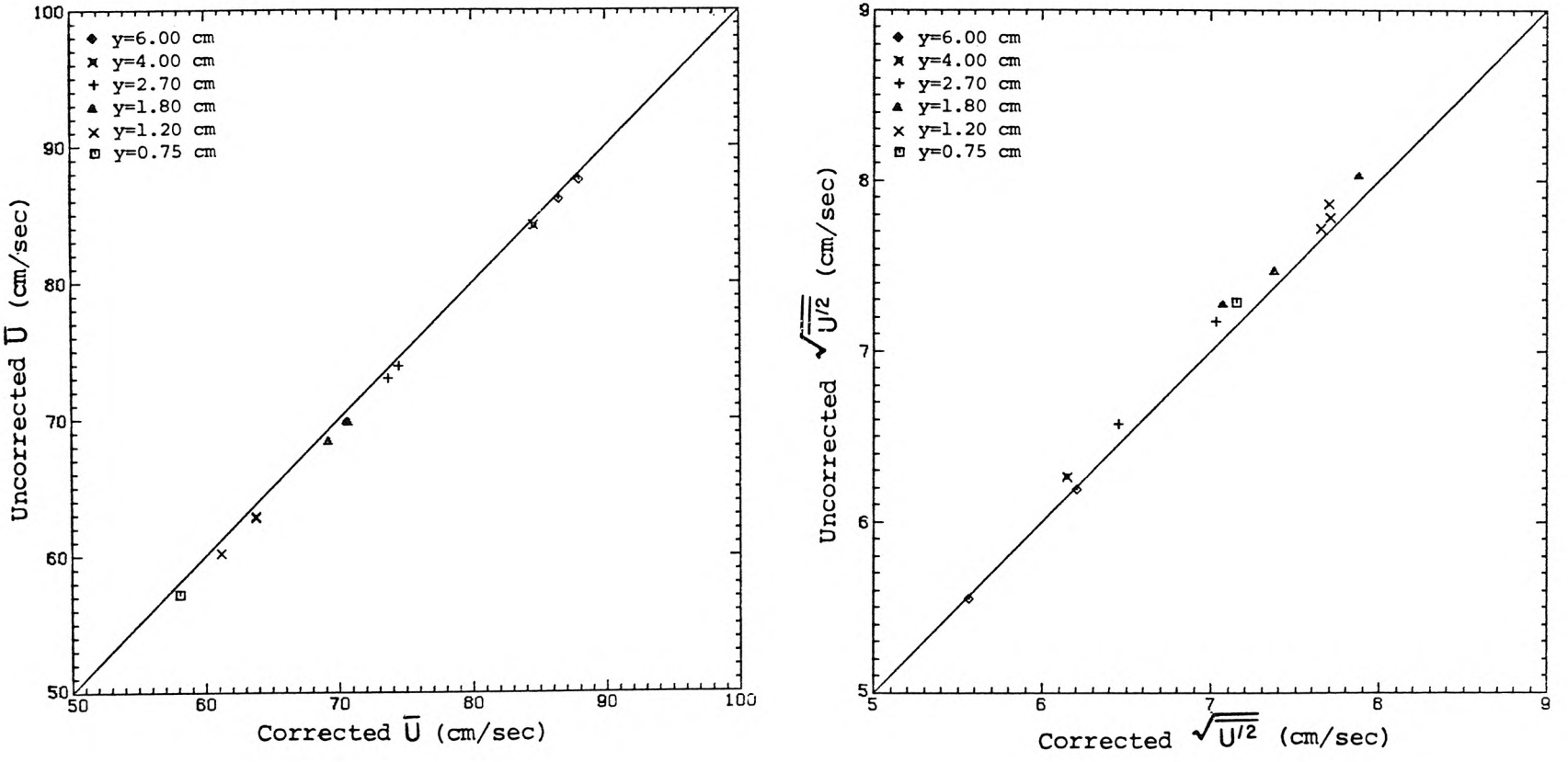

Figure 8.2.11.a Comparison of uncorrected and corrected fluid velocity mean and standard deviation, Mc Laughlin-Tiederman procedure

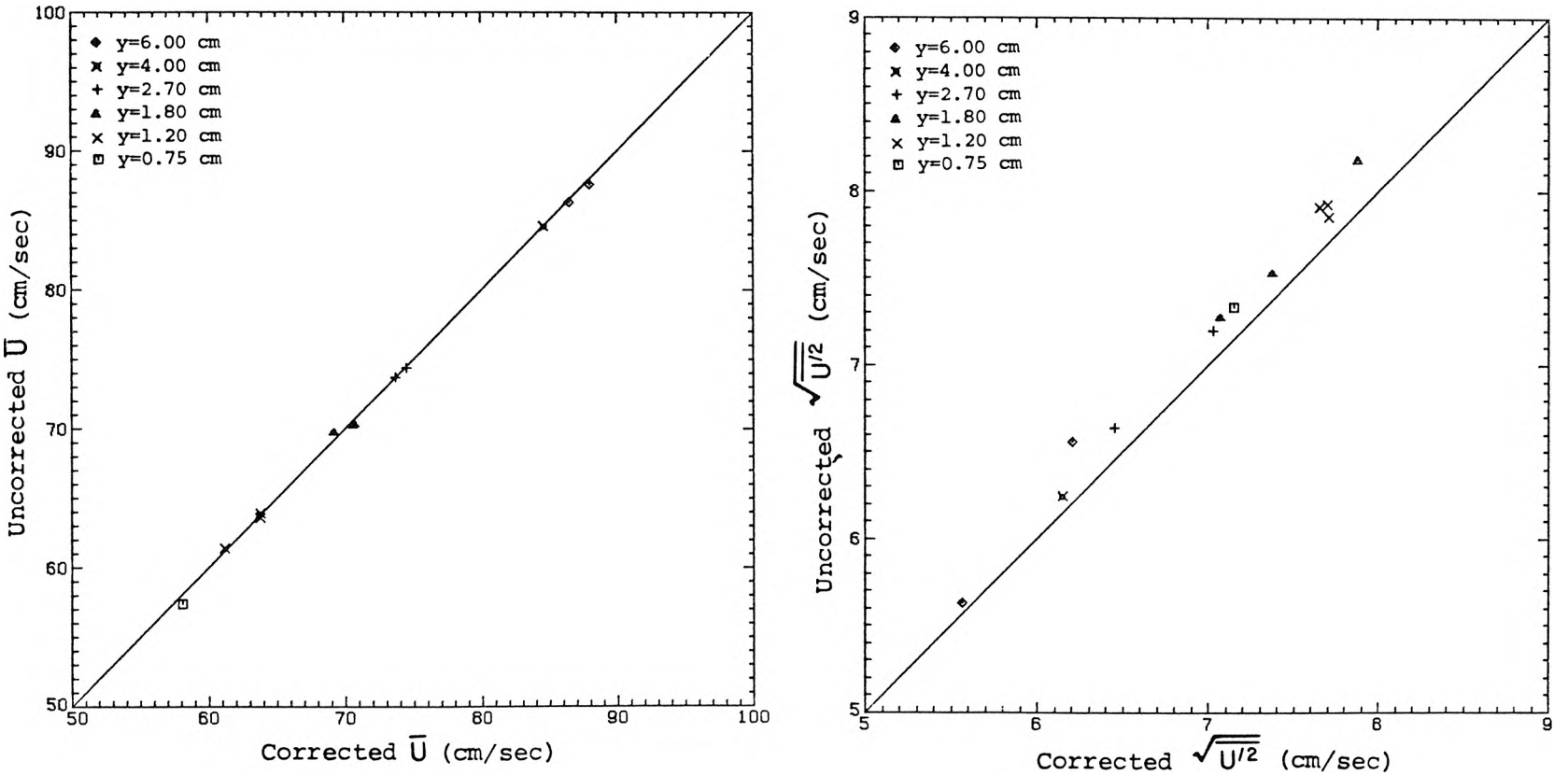

Figure 8.2.11.b Comparison of uncorrected and corrected fluid velocity mean and standard deviation, Dimotakis procedure

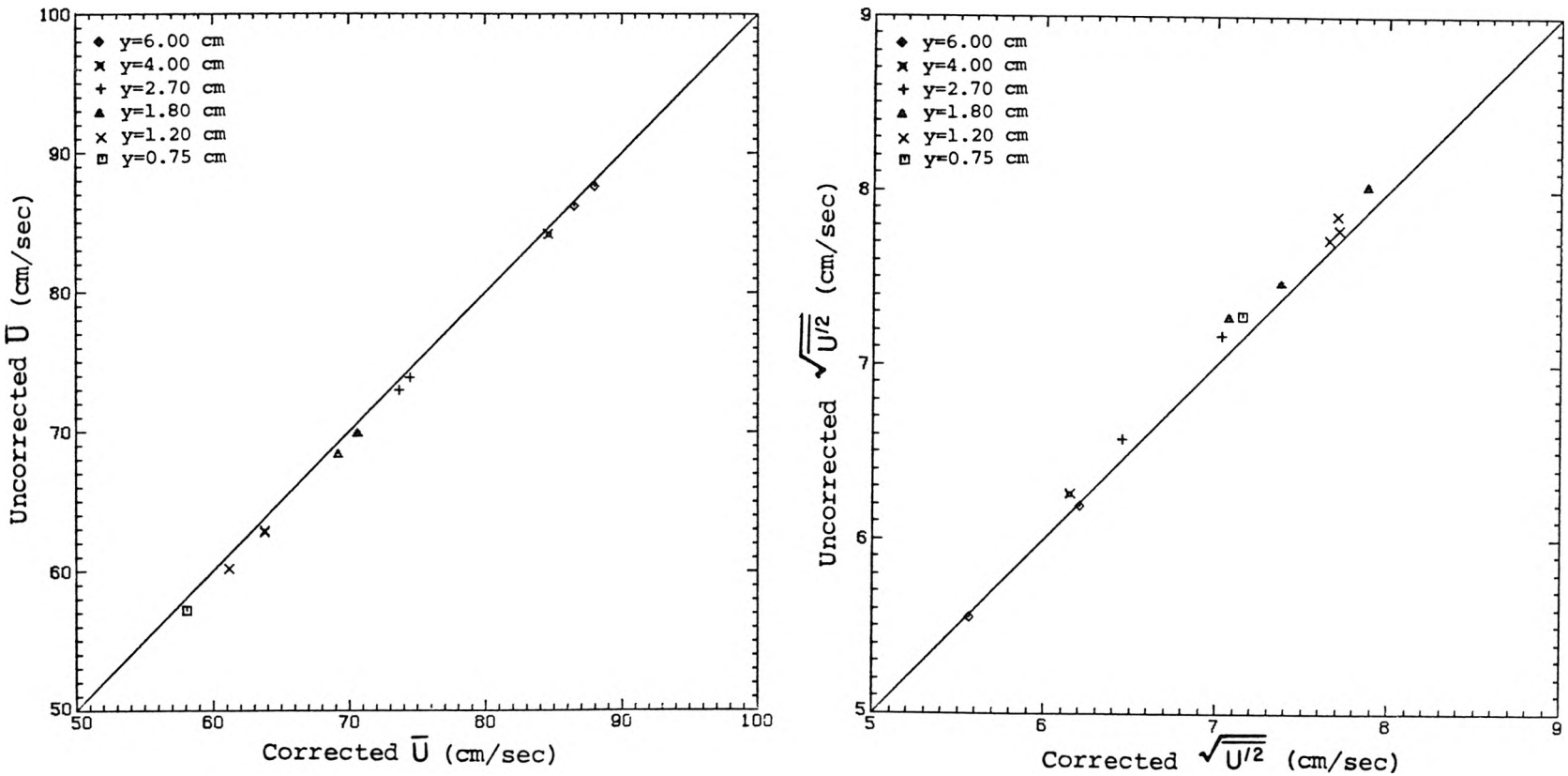

Figure 8.2.11.c Comparison of uncorrected and corrected fluid velocity mean and standard deviation, Mc Dougall procedure

The Mc Laughlin-Tiederman and the Dimotakis procedures procedures were also used to compute corrected velocity probability density functions. The results for one of the data records from each location are shown in Figure 8.2.12. The corrected velocity probability density functions are only very slightly broadened. Again, the two correction procedures are very similiar and have only minor effect compared to the uncorrected velocity distribution.

8.3 Representative sediment grain inter-arrival time records

Associated with each velocimetry data record is a sediment grain inter-arrival time data record. As discussed in Chapter 3, sediment transport rate is inversely related to the sediment grain inter-arrival time. The fluctuations in grain inter-arrival times give a measure of the small time-scale fluctuations in the sediment transport rate. The inter-arrival time data records corresponding to each of the previously given velocimetry data records are shown in Figures 8.3.1 through 8.3.6. The inter-arrival times for all detected the sediment grains, size class 4 G, are connected with a solid line; those sediment grains which generated good velocimetry signals, size class 9, are indicated with plotting symbols. Note that the inter-arrival time values for size class 9 are not plotted; only the occurrence of a valid velocimetry measurement at a given time is implied.

The time variability in sediment grain inter-arrival time at any one of the measurement locations is readily apparent from the figures. Also, the occurrence of a valid velocimetry data does not seem to be obviously correlated with long inter-arrival times.

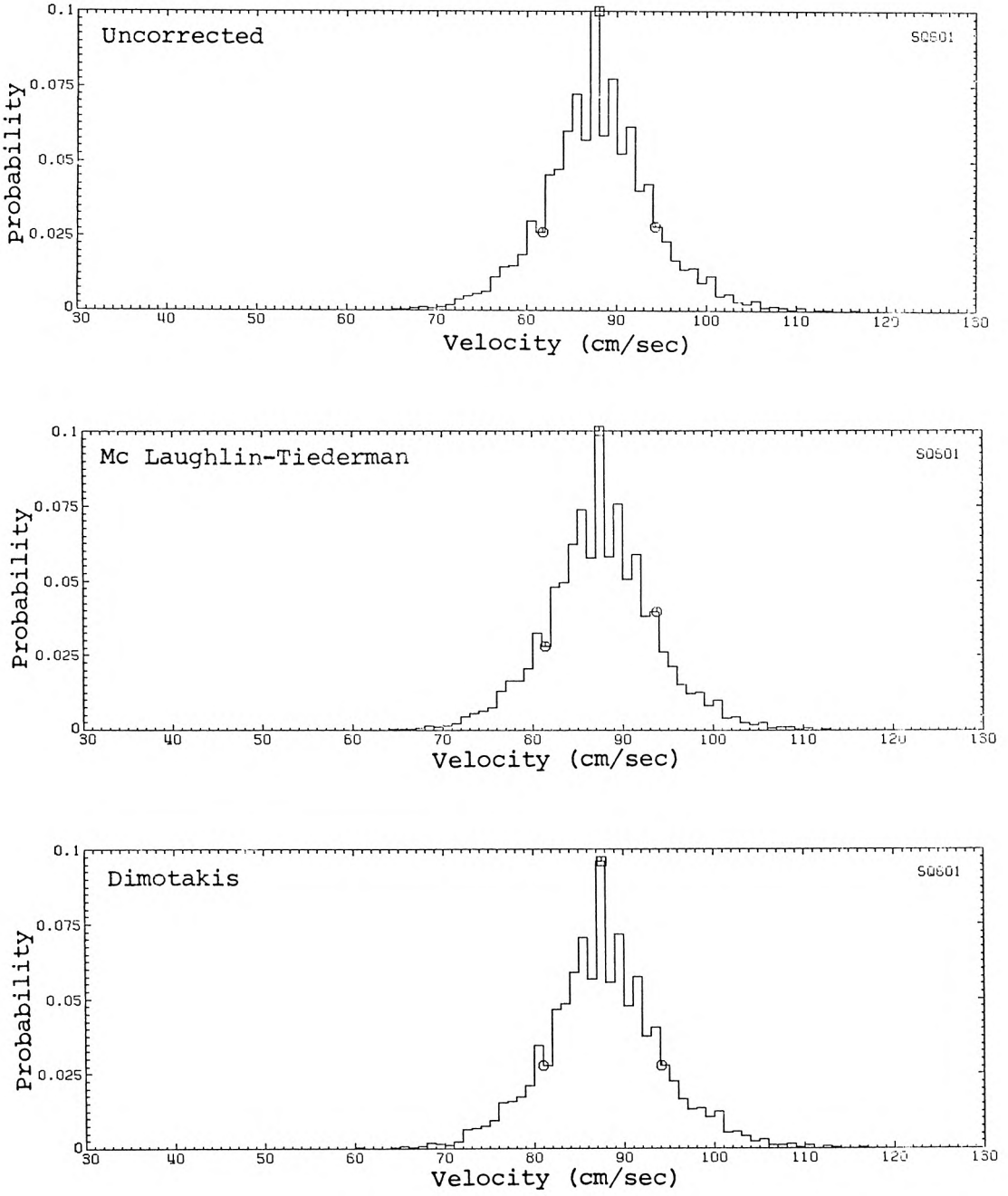

Figure 8.2.12.a Sample comparison of uncorrected and corrected fluid velocity probability density function, location 6.00

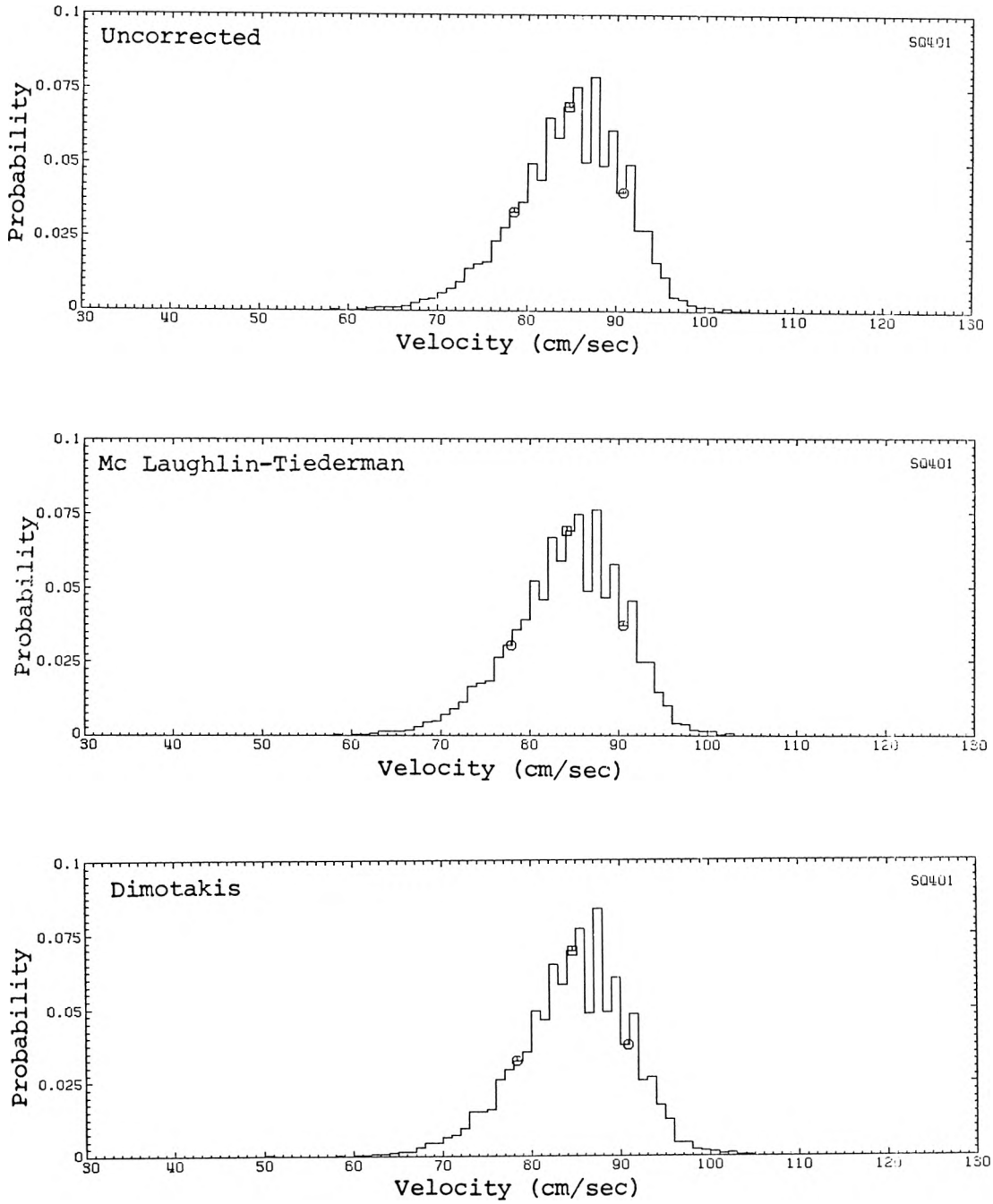

Figure 8.2.12.b Sample comparison of uncorrected and corrected fluid velocity probability density function, location 4.00

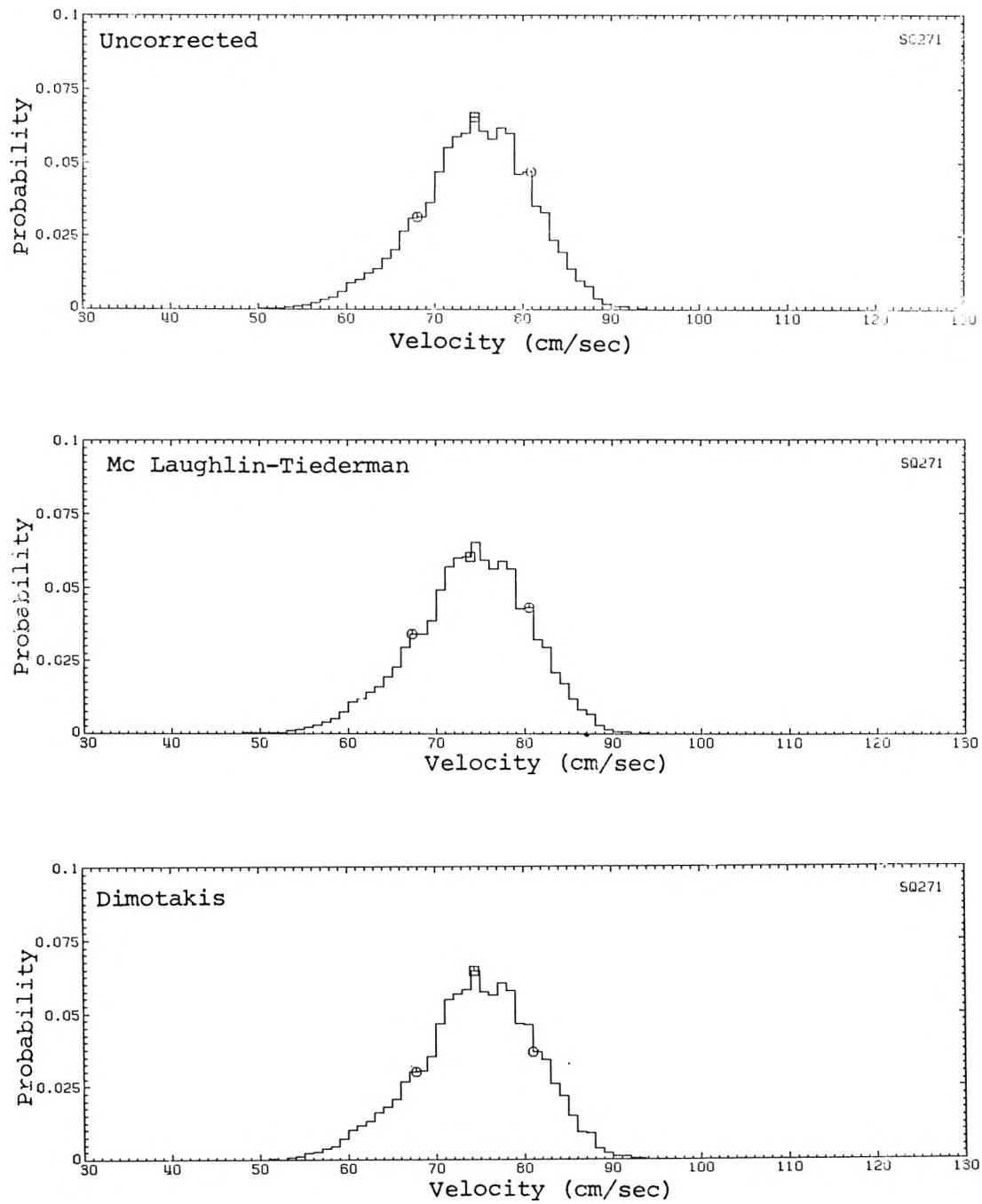

Figure 8.2.12.c Sample comparison of uncorrected and corrected fluid velocity probability density function, location 2.70

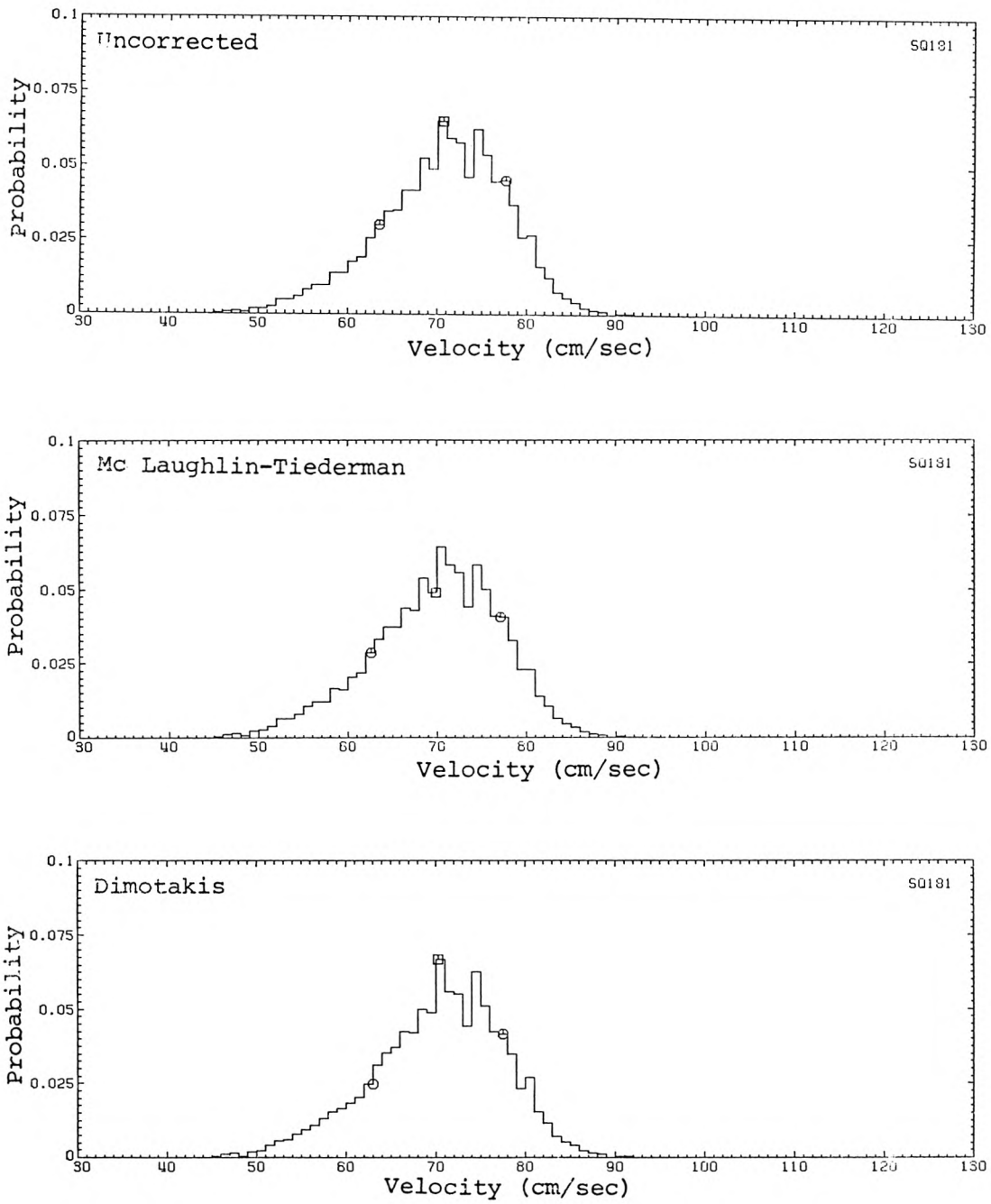

Figure 8.2.12.d Sample comparison of uncorrected and corrected fluid velocity probability density function, location 1.80

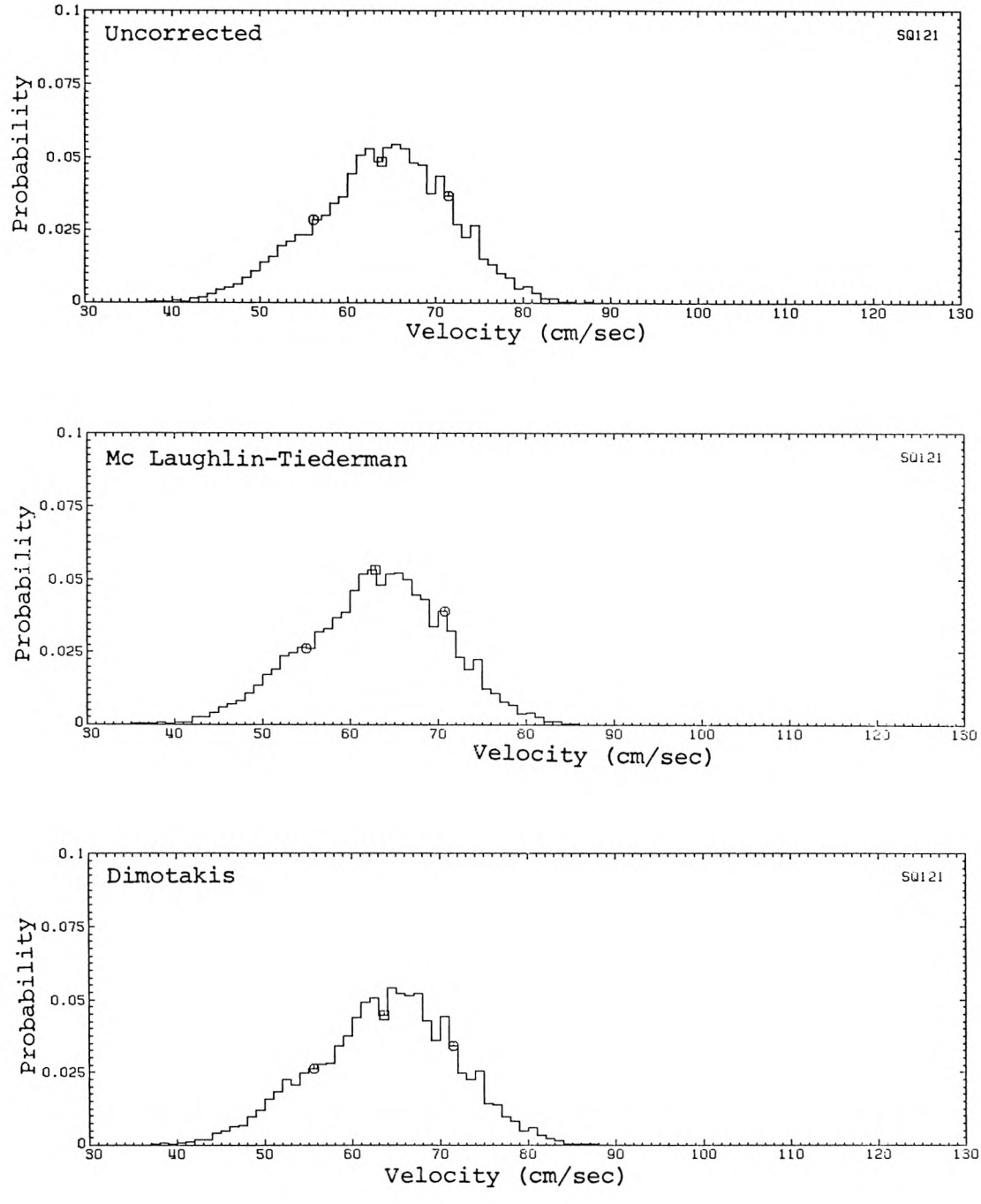

Figure 8.2.12.e Sample comparison of uncorrected and corrected fluid velocity probability density function, location 1.20

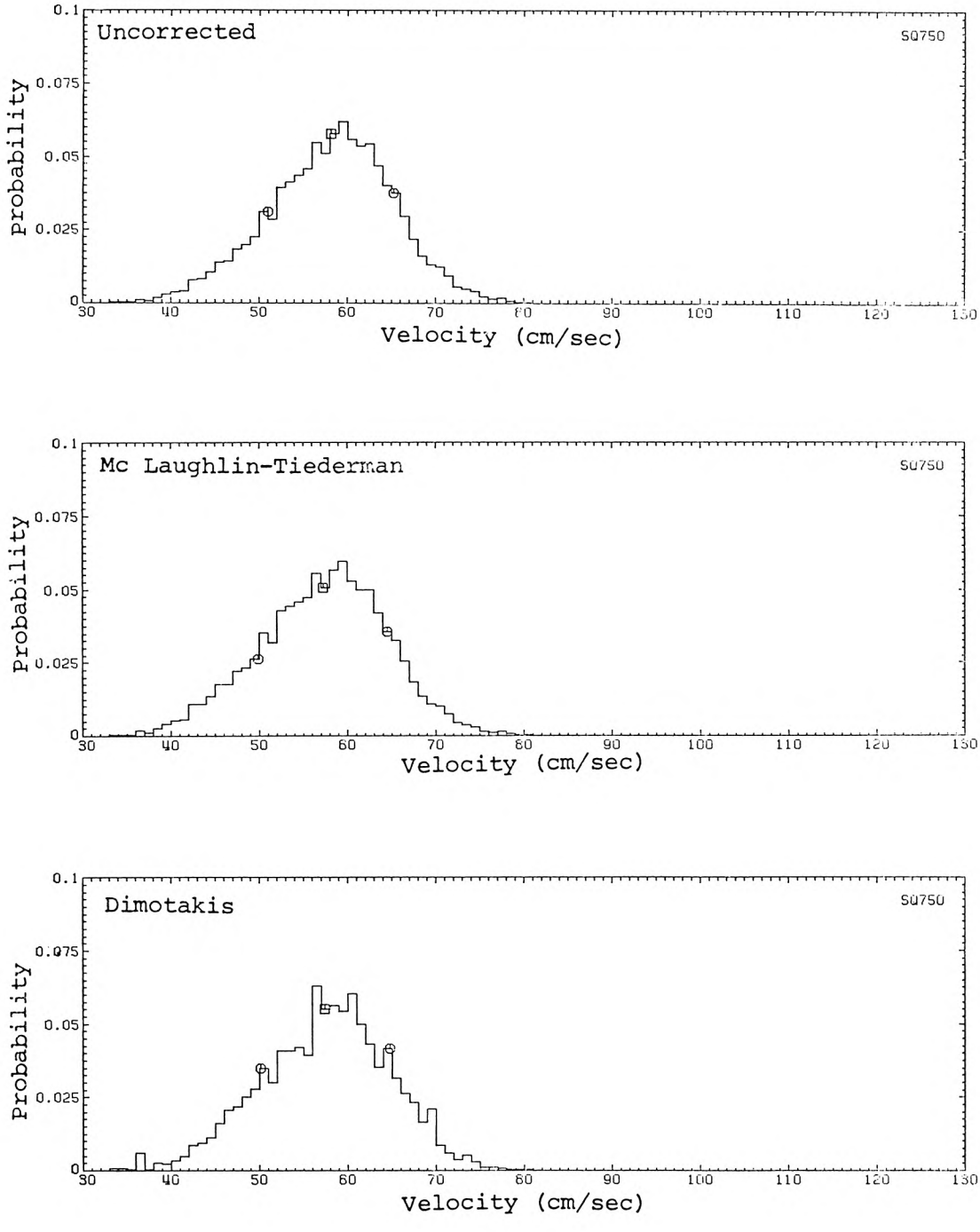

Figure 8.2.12.f Sample comparison of uncorrected and corrected fluid velocity probability density function, location 0.75

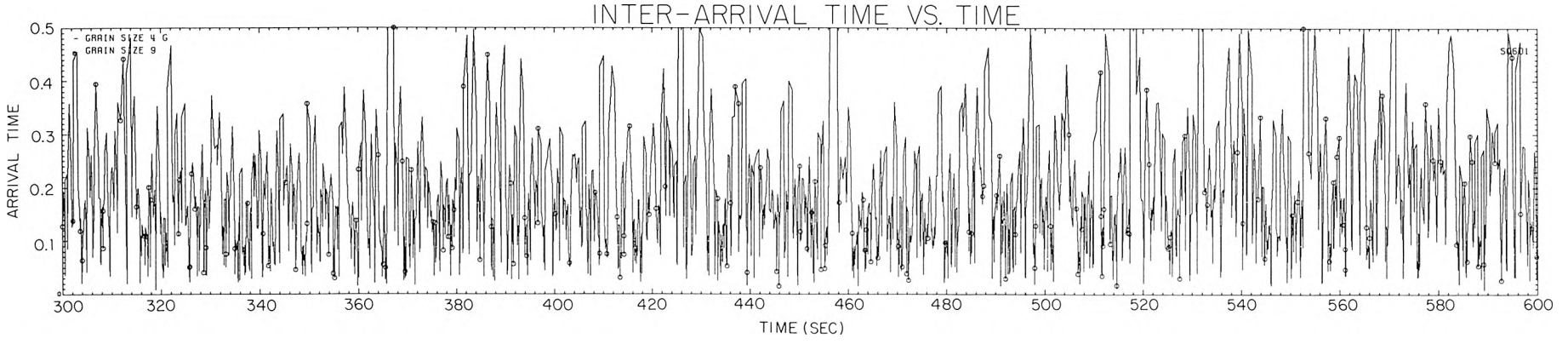

Figure 8.3.1 Sample sediment grain inter-arrival time data record, location 6.00

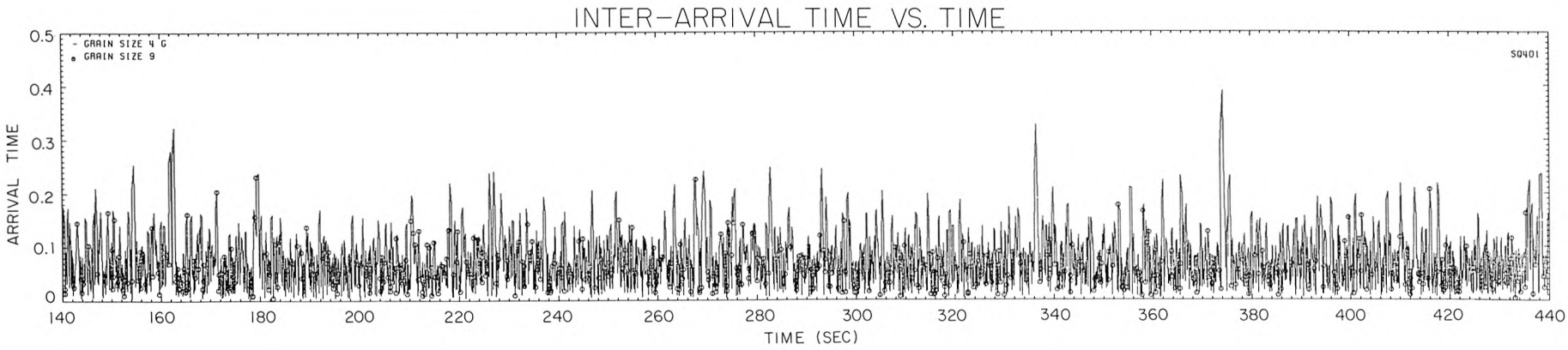

Figure 8.3.2 Sample sediment grain inter-arrival time data record, location 4.00

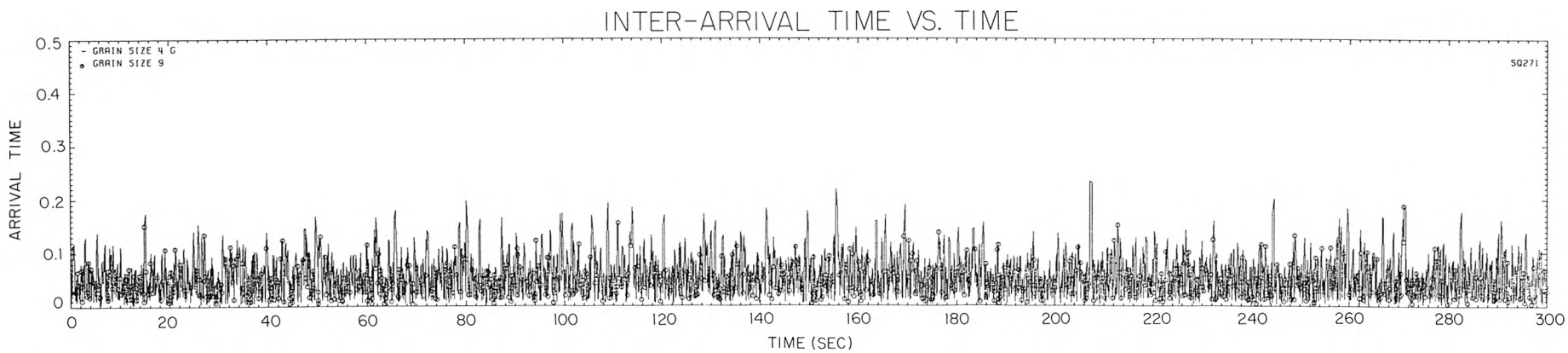

Figure 8.3.3 Sample sediment grain inter-arrival time data record, location 2.70

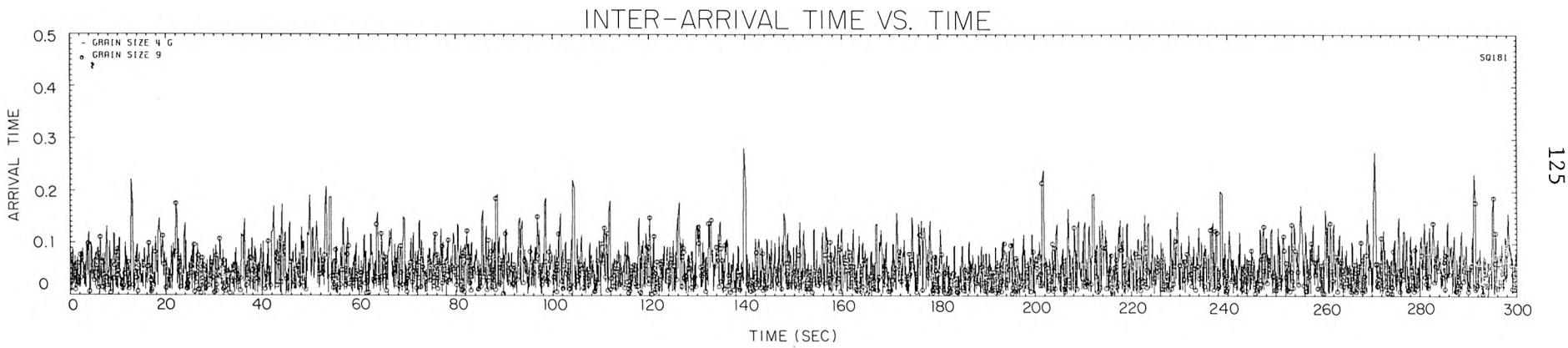

Figure 8.3.4 Sample sediment grain inter-arrival time data record, location 1.80

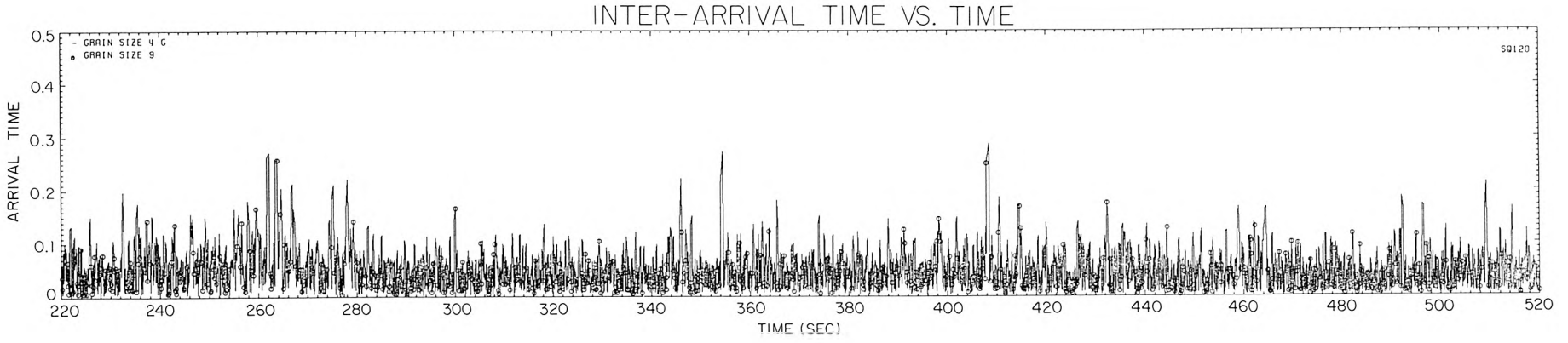

Figure 8.3.5 Sample sediment grain inter-arrival time data record, location 1.20

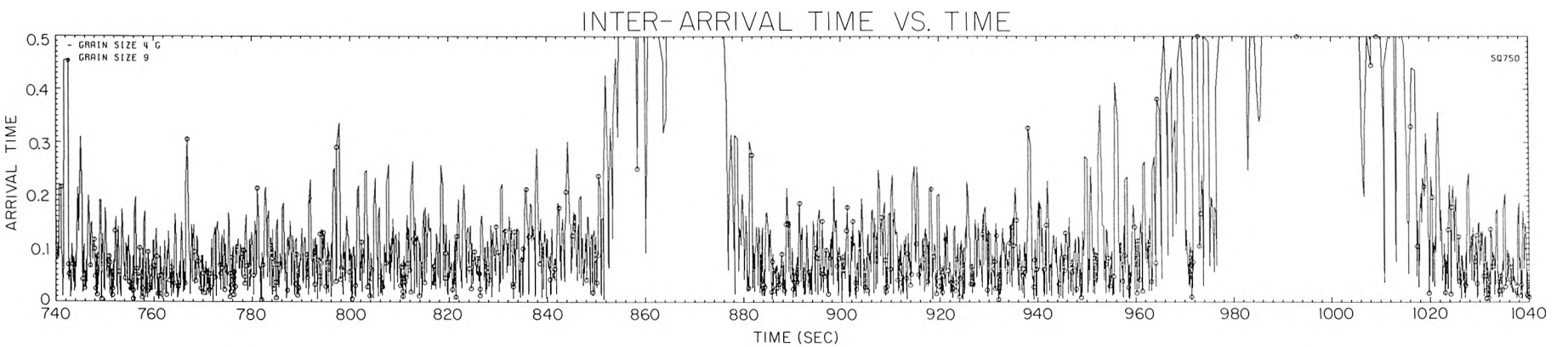

Figure 8.3.6 Sample sediment grain inter-arrival time data record, location 0.75

8.4 Measurements of sediment transport

Profiles of the mean sediment grain inter-arrival time, $\overline{\delta t_g}$, are shown in Figure 8.4.1 for size class 9 and size class 4 G. Some variations are noted in the different data records obtained at a single location. The inter-arrival time tends to decrease with proximity to the sediment bed, as the sediment grain inter-arrival time is inversely related to the sediment transport rate. Exceptions to this trend are noted in size class 4 G at location 1.80, in both size classes at location 0.75, and in size class 9 at location 1.20. No clear explanation for the observed value of $\overline{\delta t_g}$ in size class 4 G at location 1.80 is apparent.

The computed value of $\overline{\delta t_g}$ for location 0.75, appears to be anomalously high. As shown in Figure 8.1.6, the data record at this location contains periods in which no data events were collected. The gaps in the data record are associated with very long grain inter-arrival times as seen in Figure 8.3.6. The computed $\overline{\delta t_g}$ is biased by these long grain inter-arrival times. During the gaps, the actual sediment grain inter-arrival times are quite small; the laser beams are blocked by the sediment bed. A more representative value of $\overline{\delta t_g}$ may be computed by excluding those grain inter-arrival times caused by the record gaps. Determination of the true $\overline{\delta t_g}$ is not possible, however, as the number of sediment grains passing through the measurement volume during the gaps in the data record remains unknown.

In Figure 8.4.1.a, $\overline{\delta t_g}$ does not decrease from location 1.80 to location 1.20. Instead, a slight increase is observed. This may be caused by a decrease in the probability that a given sediment grain

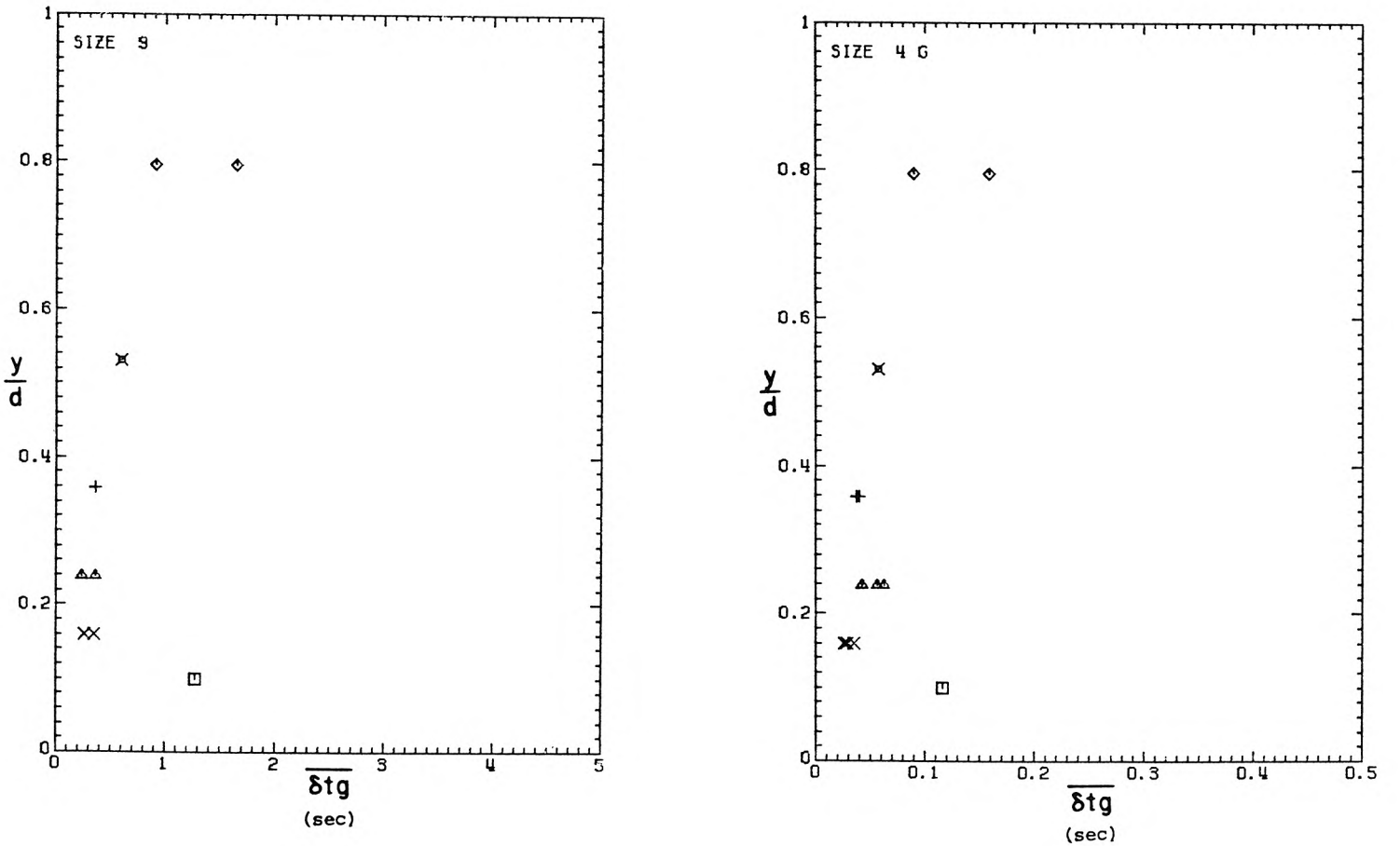

Figure 8.4.1 Profiles of mean sediment grain inter-arrival time

will generate a valid velocimetry data event. If the sediment transport rate becomes sufficiently high, multiple grains may simultaneously pass near the beam intersection volume. While the number of grains which pass through the volume increases, the number of grains which generate valid velocimetry events decreases. The time between good velocimetry events tends to increase.

Profiles of the standard deviation of the sediment grain inter-arrival times are shown in Figure 8.4.2. The mean and the standard deviation of the inter-arrival times are approximately equal. Examined on a granular scale, the fluctuations in the sediment transport are on the order of the mean sediment transport.

The mean sediment transport rate is compared to the mean sediment grain inter-arrival time in Figure 8.4.3. The transport rate, q_s, is computed as $\bar{u}\bar{c}$, where $\bar{u}$ is the mean fluid velocity and $\bar{c}$ is the local suspended sediment concentration as measured by suction tube sample. The range of the suction tube samples are indicated with error bars.

As discussed in Chapter 3, if at most one sediment grain passed through the beam intersection volume at any given instant, the velocimeter would be, effectively, a particle counter. The mean sediment transport rate would be inversely related to the mean sediment inter-arrival time by

$$q_s = \frac{m}{\overline{\delta t_g}\, dA} \qquad (8.4.1)$$

where m is the mean mass of the sediment grains and dA is the effective frontal area of the scattering volume. For size class 9, dA was

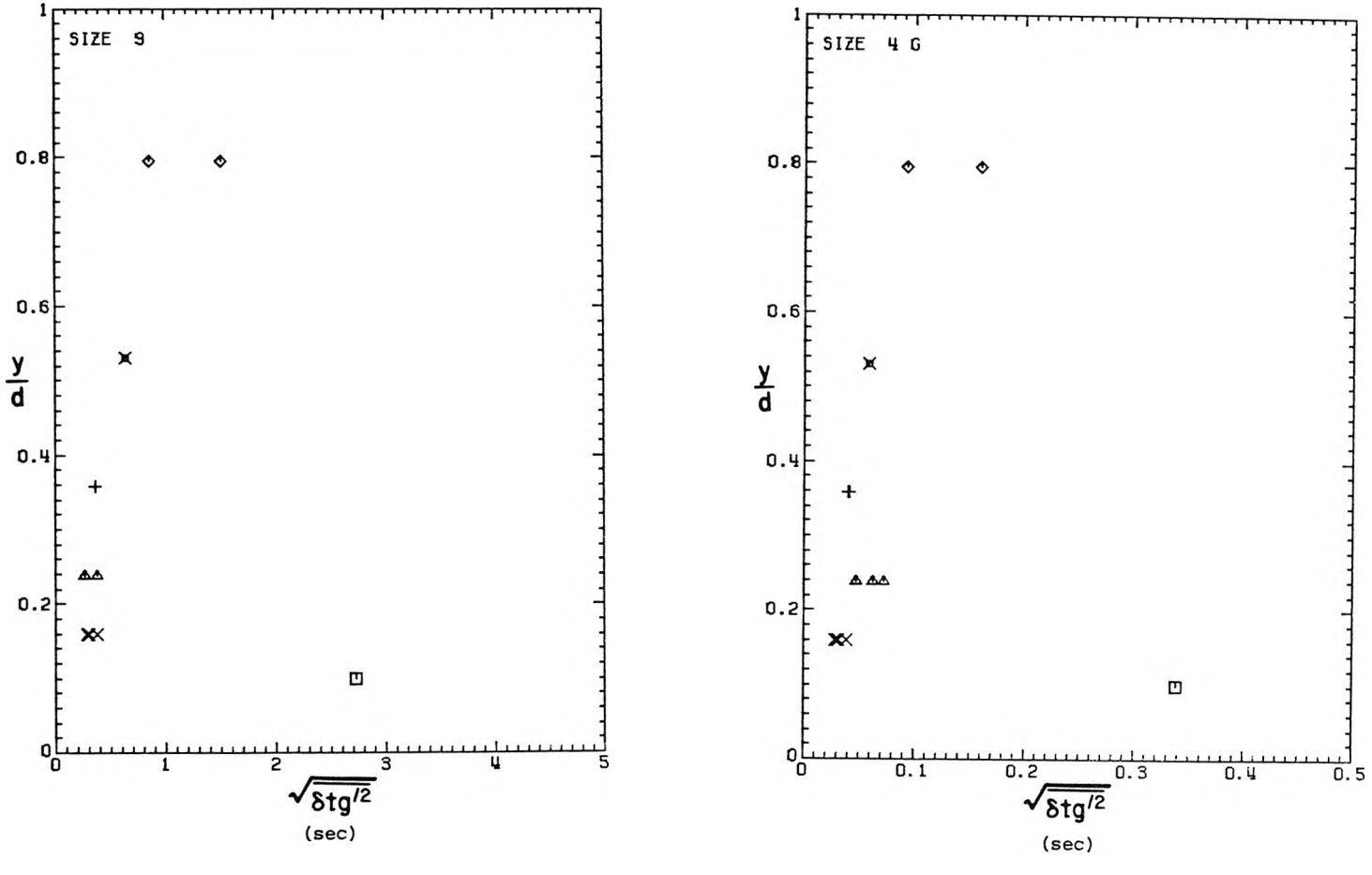

Figure 8.4.2 Profiles of sediment grain inter-arrival time standard deviation

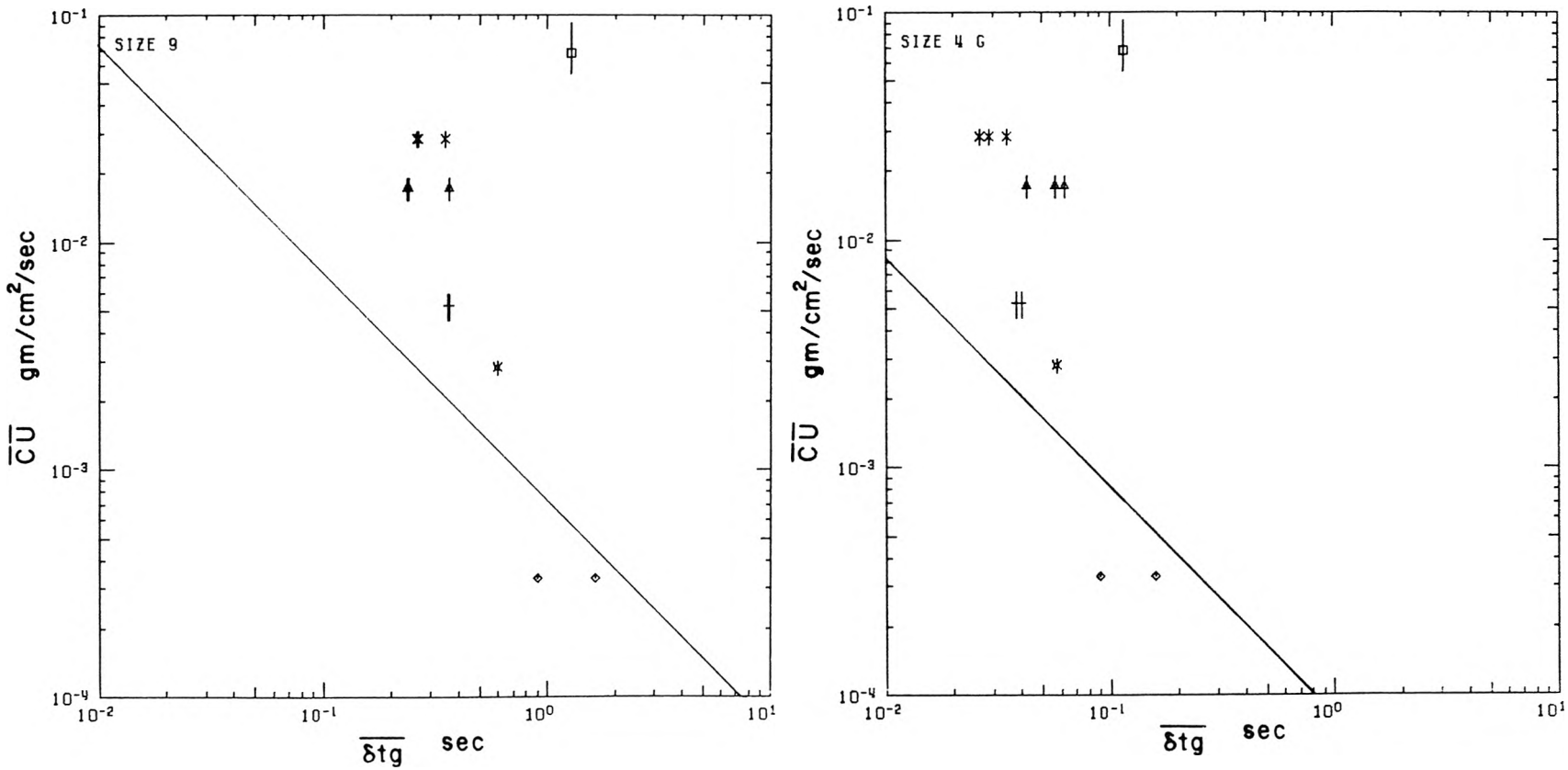

Figure 8.4.3 Comparison of mean sediment transport rate and mean sediment grain inter-arrival time

estimated to be 1.3 mm^2, based on the computed frontal area of the laser beam intersection volume and the sediment grain size. The area was estimated to be ten times larger for size class 4 G. The resulting estimated calibrations are plotted in Figure 8.4.3 with solid lines. Values near the water surface are in reasonable agreement with the crude estimated calibration. The values in the lower portion of the flow are in error by at least an order of magnitude. The sediment grain inter-arrival time is much too large, implying that the number of grains detected is much too small. The velocimeter is far from a simple particle counter.

Figure 8.4.4 gives the sediment grain inter-arrival time probability density functions for each data record. The mean inter-arrival time is indicated with a plotting symbol. The probability density functions are observed to be exponential in character. Little change in the probability density functions with elevation is noted in the lower portion of the flow. The velocimeter is failing to detect many, or even most, of the particles which pass through the beam intersection volume.

The simple lag correlation coefficients of the sediment grain inter-arrival times for two of the data records are shown in Figure 8.4.5. Similiar results were obtained for each of the remaining data records. Again, as discussed in Section 8.2, it was not possible to compute the true arrival time auto-correlation functions. While the sediment grain inter-arrival time data in the lower portion of the flow are not reliable due to the inability of the velocimeter to detect all sediment grains, the observations in the upper portion of the flow seem

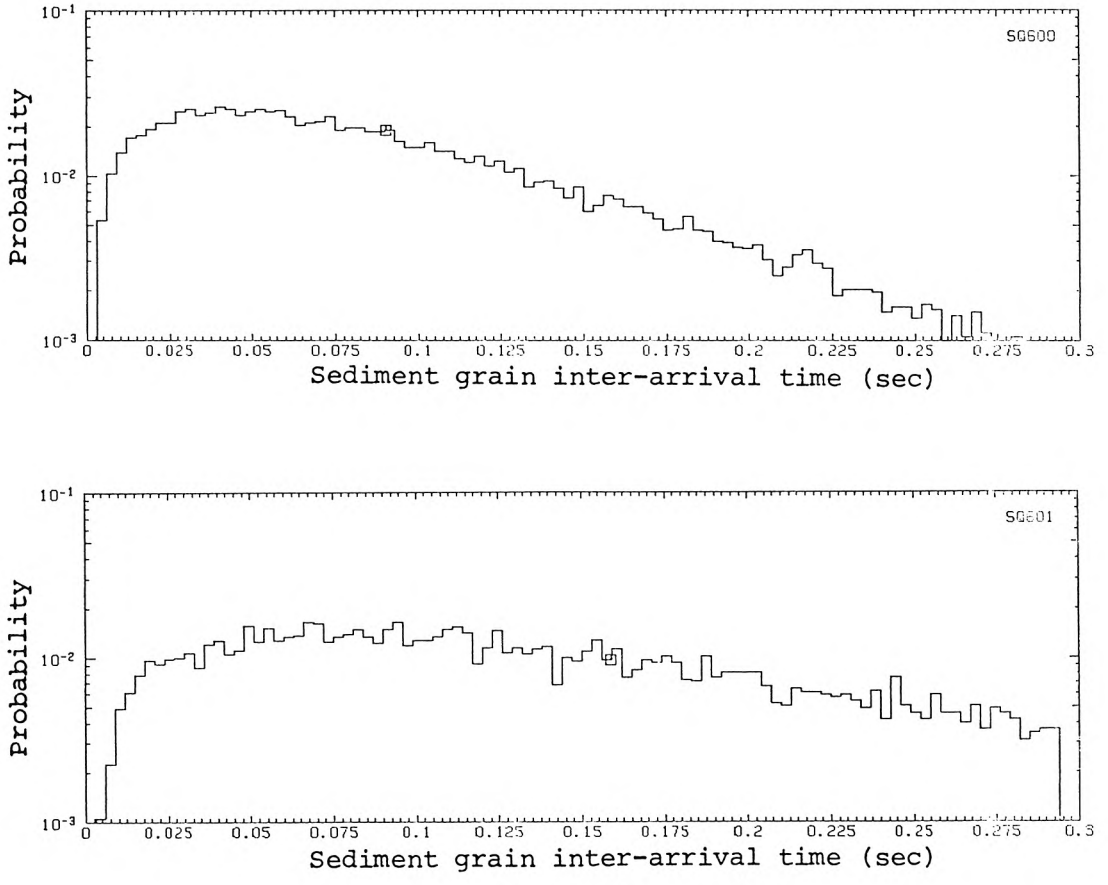

Figure 8.4.4.a Sediment grain inter-arrival time probability density functions, location 6.00

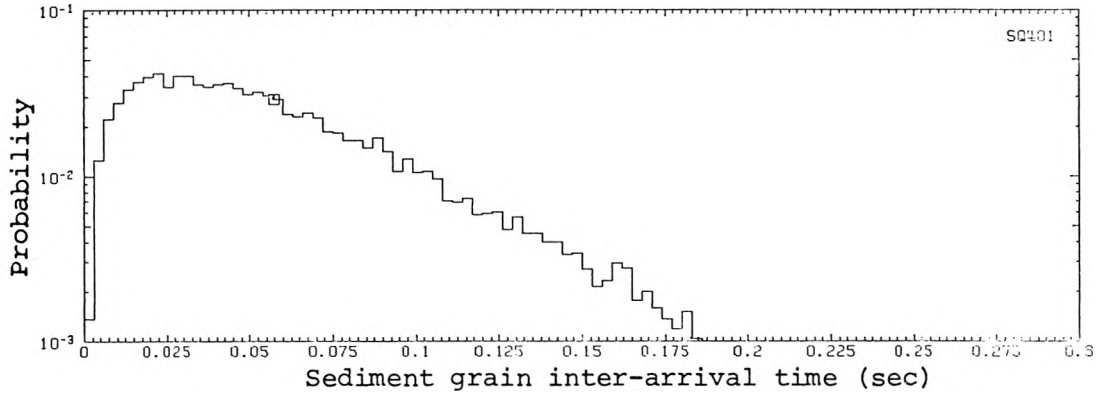

Figure 8.4.4.b Sediment grain inter-arrival time probability density function, location 4.00

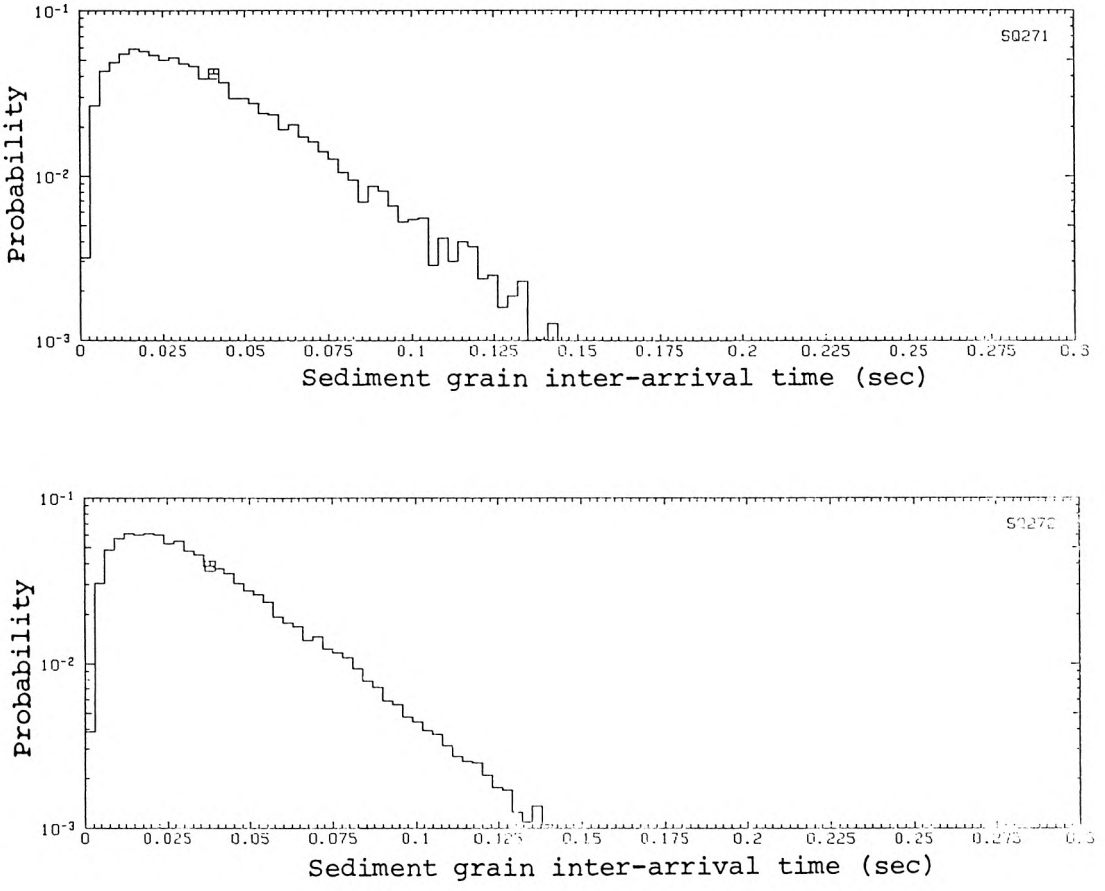

Figure 8.4.4.c Sediment grain inter-arrival time probability density functions, location 2.70

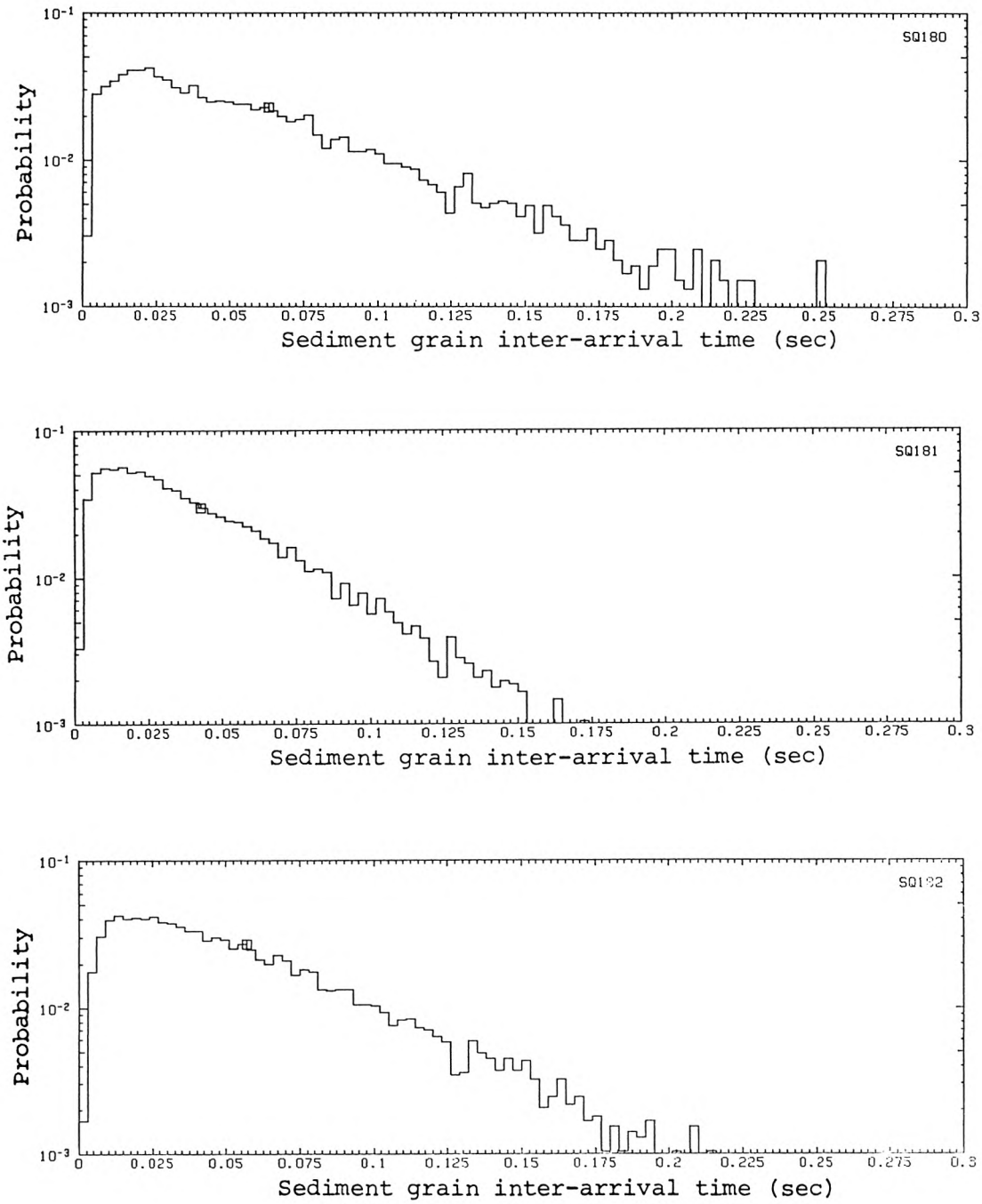

Figure 8.4.4.d Sediment grain inter-arrival time probability density functions, location 1.80

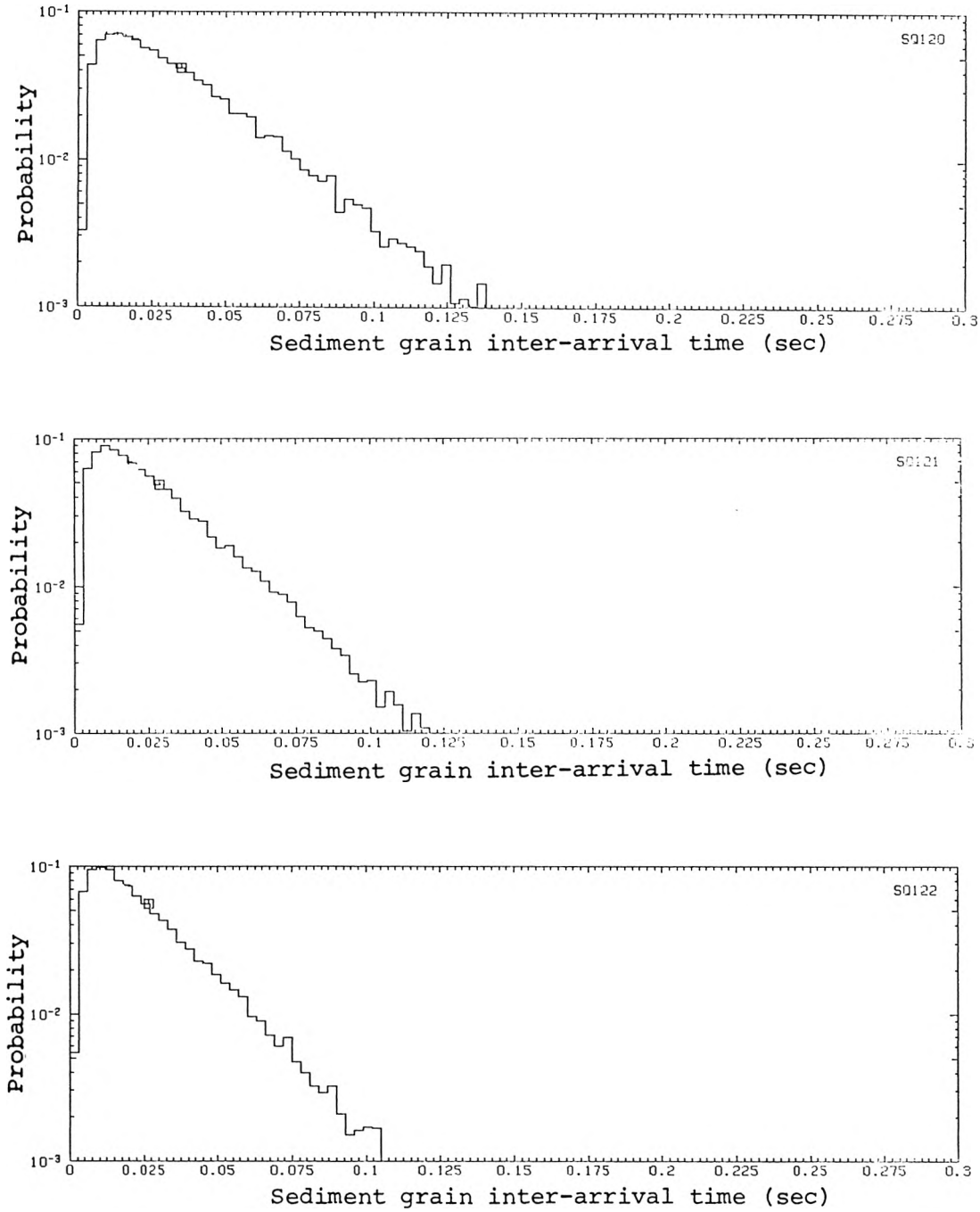

Figure 8.4.4.e Sediment grain inter-arrival time probability density functions, location 1.20

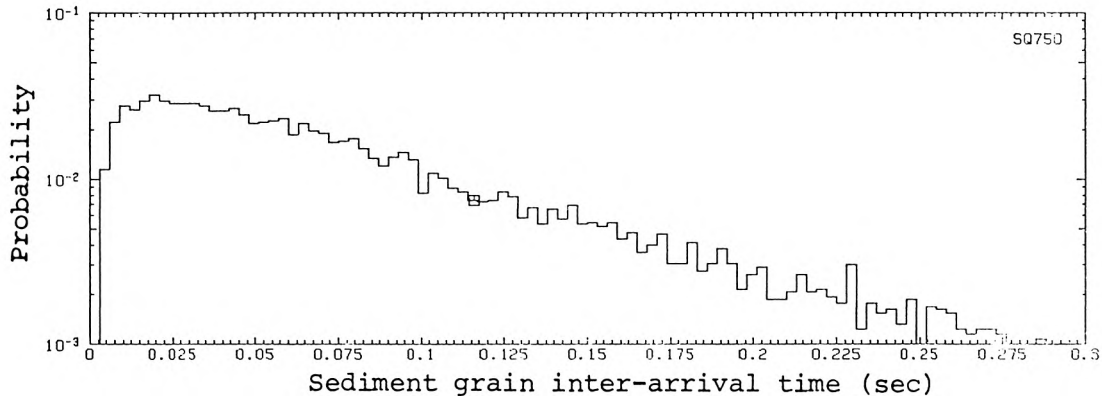

Figure 8.4.4.f Sediment grain inter-arrival time probability density function, location 0.75

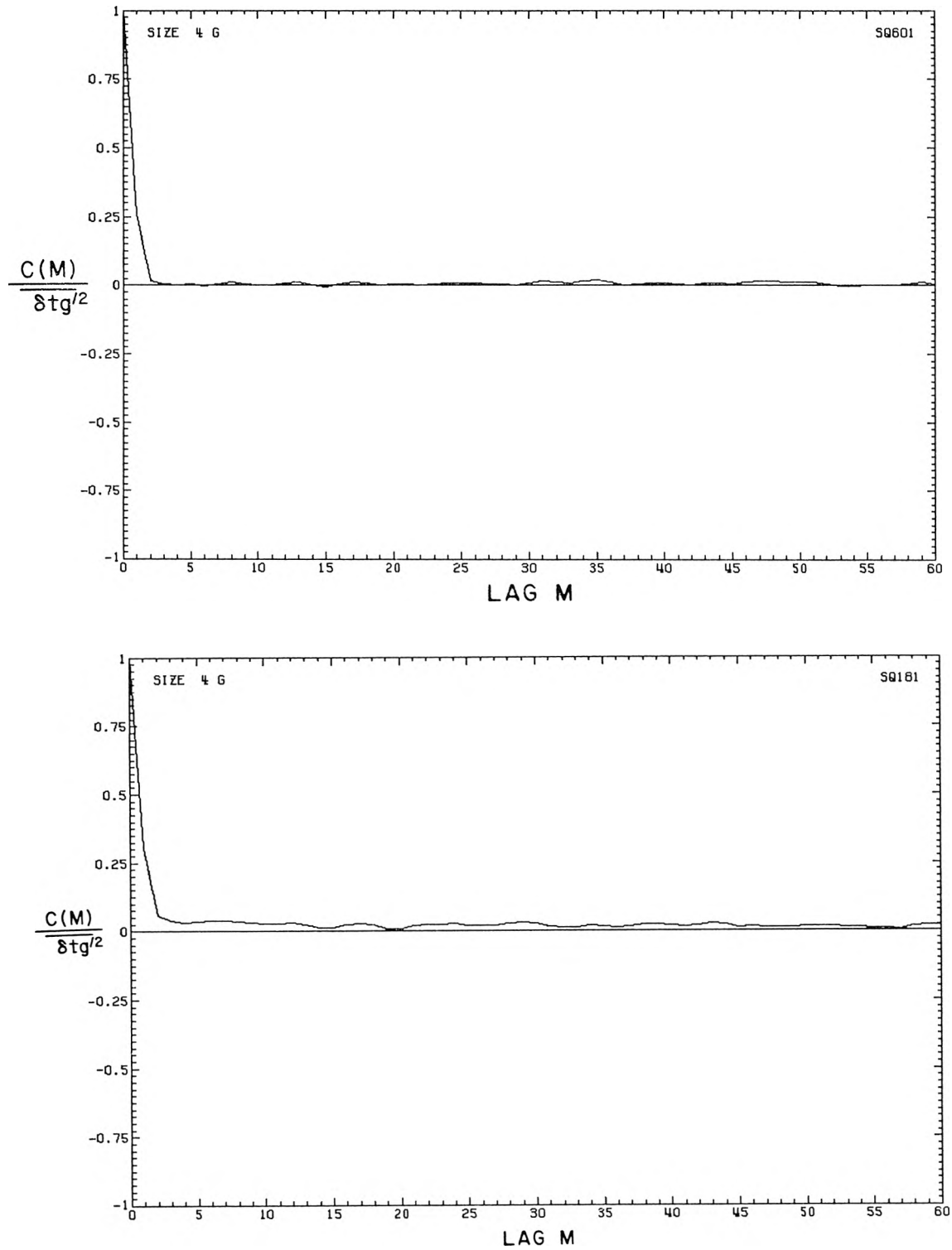

Figure 8.4.5 Sample simple lag correlation coefficients of sediment grain inter-arrival time fluctuations, locations 6.00 and 1.80

to be valid. Little or no correlation in the sediment grain inter-arrival times were observed. The passages of successive sediment grains through the measurement volume seem independent.

The normalized spectral estimate of the sediment grain inter-arrival time fluctuations and the relevant power spectral window function computed for one of the data records from location 6.00 are given in Figure 8.4.6. Theoretically, the power spectral estimate should reflect the contribution to the variance of the sediment grain inter-arrival times by the various time scales of the sediment movements. The power spectral window function should reflect the contributions to the mean sediment grain inter-arrival time. Again, however, the computed spectra are most likely dominated by computational errors. Physical interpretation of the spectra cannot be made with any degree of confidence.

No cross-correlations of fluid velocity and sediment grain velocity and inter-arrival time characteristics were computed with the data acquired in this study. Nor were any computations of the sediment grain slip velocity, defined by Equation 3.1.4, or any selective sampling of the fluid velocity data record based on chosen sediment transport characteristics performed. Such calculations require that the time between the measurement of the sediment grain velocity and the velocity of the associated fluid be small with respect to the turbulence time scale. The data records used in this study did not always have such time resolution. The time between the detection of a sediment grain and the closest fluid velocity realization was often larger than the turbulence time scale, estimated at approximately

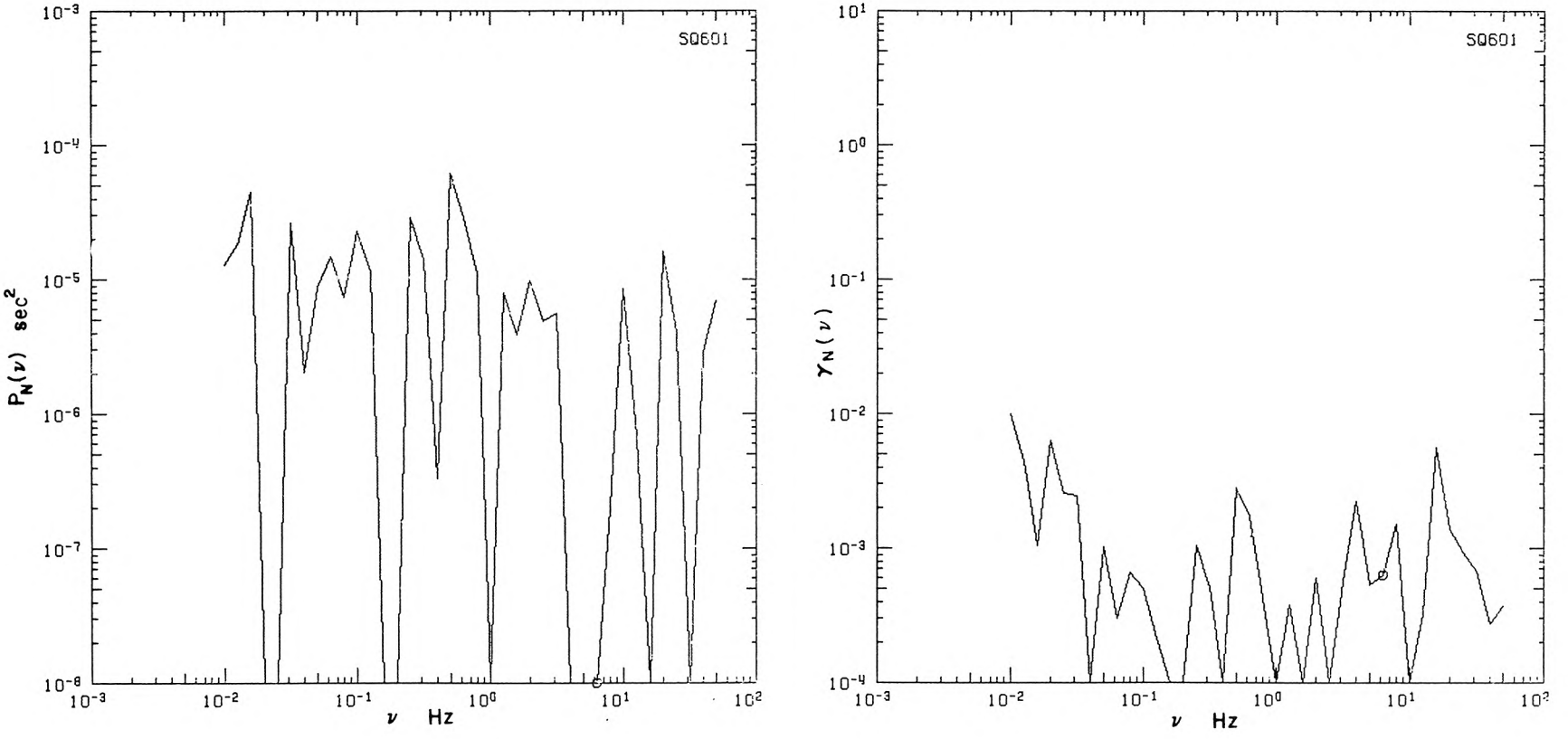

Figure 8.4.6 Sample sediment grain inter-arrival time fluctuation power spectral estimates and power spectral window functions, location 6.00

10 msec.

8.5 Summary

This chapter has presented the one-dimensional velocimetry data obtained in this study. Examples of the validated data records were given. The difficulties encountered in the computation of auto-correlations and power spectral estimates were discussed. The velocimeter was observed to be far from a simple grain counter. Further discussion of these results and suggestions for further work indicated by these results are given in the remaining chapters.

CHAPTER 9

DISCUSSION OF THE RESULTS

The results presented in Chapter 8 are discussed here. The applicability of the laser-Doppler technique for velocimetry to sediment-laden flows is assessed. The difficulties encountered in this study are reviewed. The implications of the data obtained are then examined for new insights into the mechanics of sediment suspension and entrainment. Specific suggestions for further research are given.

9.1 Discussion of the application of laser-Doppler velocimetry in sediment-laden flows

The advantages of the laser-Doppler velocimetry technique for use in sediment-laden flows were apparent prior to this study; certain disadvantages and uncertainties only became known during the research. This section details the discovered difficulties with the technique, evaluates their relative importance, and suggests improvements for subsequent applications of the technique to sediment-laden flows.

The first difficulty encountered in this study is the long length of record required for the investigation of fluid turbulence in sediment-laden flows. Such investigations require the acquisition and subsequent processing of a relatively large quantity of experimental data. This is due to the disparity between the time scales of the fine scale fluid turbulence and those of the sediment bed motions. To characterize accurately all of the time scales present, the flow velocity must be sampled at a relatively rapid rate, on the order of 100 Hz, for a relatively long observation period, at least greater than 10 minutes, at each measurement location. The quantity of data

required is, therefore, quite large with repect to that of previous investigations of sediment-laden flows or studies of turbulence in homogeneous fluid flows with fixed boundaries. For the small, preliminary experiment presented in this study over two million velocimetry events were recorded, even though the observation periods (5 to 20 minutes) were still too short to resolve fully the very slow transients in the sediment motion. The subsequent analysis of such an amount of data consumes both computer and human time.

The second difficulty encountered, also inherent in the investigation of fluid turbulence in sediment-laden flows, is gradual shifting of the sediment bed level, even in the nominally flat bed regime. Since the measurement location is fixed in space, the distance above the bed varies as the bed elevation changes, causing difficulties with the physical interpretation of the collected data. The understanding of the fine scale motions of a sediment-laden flow requires the appreciation of the larger scale features also.

The major difficulty encountered in this study is the possible conditional sampling of the flow velocity and is directly attributable to the laser-Doppler technique. The validated velocimetry events may be a conditionally selected subset of the recorded velocimetry events, which are, in turn, a conditionally selected subset of all possible velocimetry events. The resulting velocimetry data record is, possibly, biased in an unknown manner.

A velocimetry event is not validated if its Doppler burst signal does not remain regular in frequency during the time required to determine the Doppler burst frequency. Most probably, an irregular

Doppler burst signal is either the result of noise in the signal processing electronics or generated by multiple scattering particles passing simultaneously through or sufficiently near to the laser beam intersection volume. The primary source of electronic noise in apparatus employed in this study is the statistical quantum noise of the photodetector. While such noise may cause the loss of data, no biasing of the recorded data record will result. Biasing can, however, result from simultaneous scattering by multiple particles.

There is a particularly high occurrence of light scattering by multiple particles in the vicinity of the beam intersection volume in a sediment-laden fluid flow. The particle number density of the small fluid tracer particles is difficult to regulate and increases during the course of an experiment. The concentration of sediment grains is determined by the flow conditions; furthermore, a sediment grain need only graze the beam intersection volume to scatter sufficient light to mask that scattered by a particle passing directly through the volume. In this study, well over half of the recorded data events were not valid events. It is not possible to estimate the number of generated Doppler burst signals which were not recorded.

Simultaneous scattering by multiple particles is most likely to occur when the fluid flux is high and/or the sediment transport rate is high. In either case, the flux of scattering particles through the beam intersection region is relatively high. The velocimetry events generated in these instants are more likely to be invalid than those generated at other times. The validated velocimetry data record will tend to exclude the periods in which the sediment transport rate is

relatively high.

It is not possible to estimate accurately the relative importance of the two sources of invalid velocimetry events with the data obtained in this study. Further research in this direction is clearly required. The inherent noise in the photodetector was relatively high in the velocimeter employed in this study due to low incident light intensity and low light scattering efficiency resulting from the large beam intersection angle. Thus, the shot noise could be reduced by an increase in the laser light intensity. The detection of light scattered by sand grains passing near the beam intersection volume might be decreased by alterations to the receiving optical system to reduce the effective depth of field. Increased incident light intensity will allow the decrease of the solid collection angle. A smaller pinhole and other additional appertures between the collecting lens and the photodetector should be tried once again with the increased light scattered from more intense laser beams.

Given the possibility that the velocimetry data in sediment-laden flows may be conditionally sampled, the application of any bias correction procedure to the data does not seem warranted. Such correction procedures assume that the observed velocity is biased by the proportionately larger number of measurements generated by fluid tracer particles associated with fast-moving fluid parcels. In sediment-laden flows, the observed velocity may well be biased by the relative lack of those measurements. The corrected velocity may be more in error than the uncorrected velocity. Furthermore, as seen in Figures 8.2.11 and 8.2.12, the usual correction procedures have

relatively little impact on the observed velocimetry data. The application of a bias correction procedure to velocimetry data from a sediment-laden flow gives the impression of improved accuracy, without guarantee of any such improvement.

The velocimeter employed in this study is not an accurate sediment grain counter. As discussed in Section 8.4, the local mean sediment transport rate cannot be accurately estimated from the mean sediment grain inter-arrival time. Near the bed, the sediment transport rate estimated from the velocimeter measurements is one to three orders of magnitude lower than the transport rate as measured by suction sampling tube. Only a very small subset of the number of sediment grains which pass through the measurement volume during the period of data acquisition are counted by the velocimeter. The discrepancy between the estimated and the observed sediment transport rate may be attributed to two factors: the assumption that all of the recorded velocimetry events were generated by individual sediment grains and the rejection of Doppler burst signals which are highly irregular in frequency by the counter-processor. The first factor could account for a discrepancy of no more than a factor of two or three in the estimated and observed transport rates. The discrepancy is sufficiently large, see Figure 8.4.3, to imply that the data record is missing most of the sediment grains which actually passed through the measurement volume. Not all sediment grains which pass through the scattering volume are both detected by the counter-processor and reported to the mini-computer.

The development of the laser-Doppler technique for application to sediment-laden flows is still in the experimental phase. The simple system developed for this study may be greatly improved. The technique will never be without its particular disadvantages; however, no other approach currently holds as much promise for the measurement of the fine scale structure of sediment-laden flows.

9.2 Discussion of the mechanisms of sediment entrainment and suspension

Longitudinal velocity measurements alone are not sufficient to describe adequately even a two-dimensional fluid flow field. Measurements of the vertical motions are also necessary. Thus, the one-dimensional velocimetry results presented here can yield only limited insights into the mechanics of sediment suspension and entrainment. Nonetheless, the data do give some first glimpses into the time-varying nature of sediment-laden flows.

The observed longitudinal turbulence intensity, $\sqrt{\overline{u'^2}}$, does not differ significantly from measurements in clear water by previous investigators. In a clear water flow over a smooth boundary, Raichlen (1967) noted a steady increase in the relative longitudinal turbulence intensity, $\sqrt{\overline{u'^2}}/\overline{u}$, from a minimum of approximately 3.8% at y/d=0.8 to approximately 10% at y/d=0.16. Blinco and Partheniades (1971) report similiar values near the water surface, but a value of approximately 12% at y/d=0.14. The measurements obtained in this study, as illustrated in Figure 8.2.3, are seen to increase from values of nearly 6.4% at y/d=0.8 to values of approximately 12.6% at y/d=0.16. The data from these studies and the present study are drawn in Figure

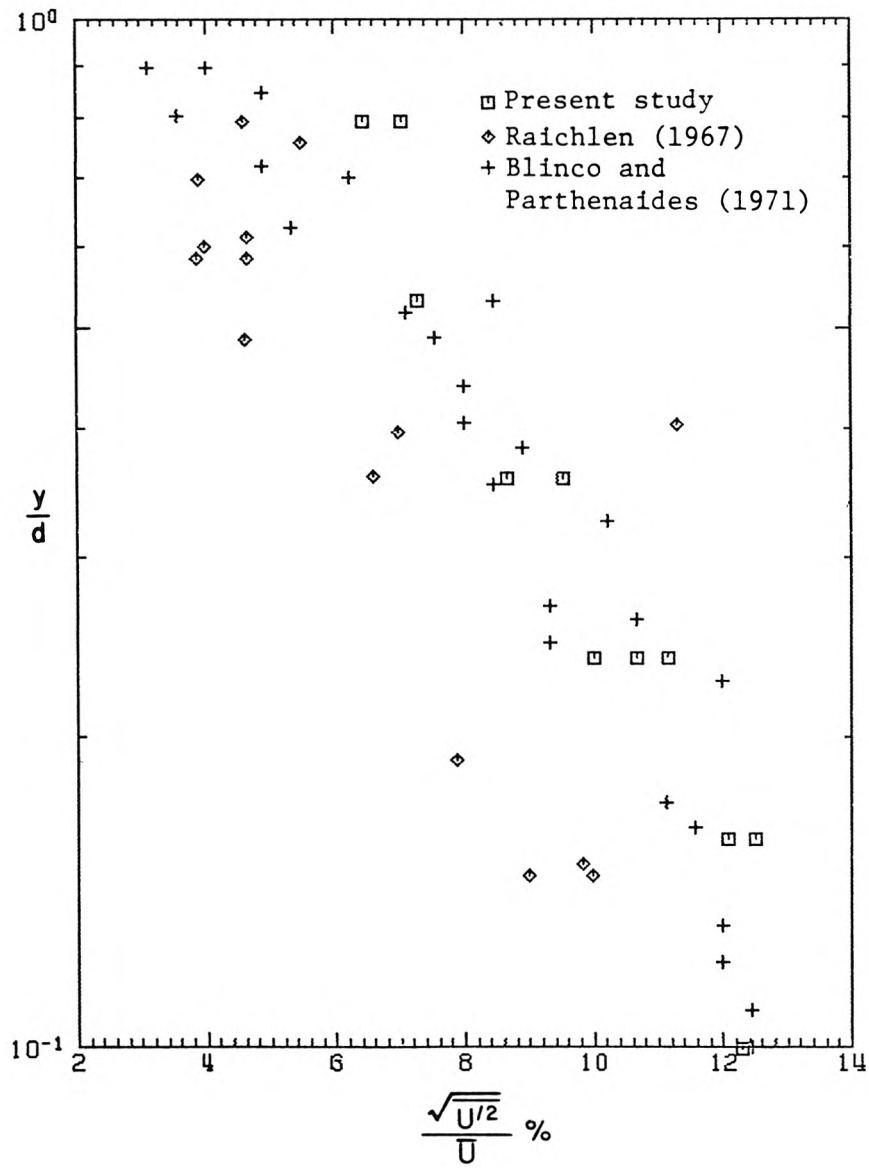

Figure 9.2.1 Comparison of longitudinal turbulence measurements

9.2.1. Since the fluid velocity fluctuations observed in this study are on the order of those observed in clear fluid flows, the presence of suspended sediment in the flow does not appreciably alter the longitudinal intensity of the fluid turbulence.

The longitudinal velocity of the sediment grains tends to be approximately 5 per cent less than that of the fluid in the lower half of the flow field. The variance of the sediment grain velocity is notably smaller than the variance of the fluid velocity. Near the water surface, the situation is reversed. The mean sediment grain velocity is greater than that of the fluid and the variance of the sediment grain velocity is significantly larger. To explain these observations, more experimental data are required. First, simultaneous vertical velocity measurements are essential. Second, data records should have sufficient time resolution or sampling frequency, to allow the cross-correlation or selected sampling of the velocities of the sediment grains and the closely surrounding fluid.

The sediment grain inter-arrival time data obtained in this study are not sufficiently reliable to yield much insight into the mechanics of sediment transport. Some of the recorded grain velocimetry events are caused by multiple grains passing simultaneously through the volume; hence, some fraction of the grain velocimetry events are not recorded. The grain inter-arrival data are only possibly valid in the upper portion of the flow (at locations 6.00 and 4.00). At these locations, as seen in Figure 8.4.3, the sediment transport rate as estimated from the mean sediment grain inter-arrival time is on the order of the mean sediment transport rate determined by suction sampling tube.

The sediment grain inter-arrival time data at these two upper locations do exhibit some interesting characteristics. The mean sediment grain inter-arrival time is approximately equal to the standard deviation. The probability density functions of the grain inter-arrival times are exponential in nature. The logarithm of the probability of a given grain inter-arrival time decays linearly with the grain inter-arrival time. Modeling the passage of successive sediment grains through the measurement volume as a Poisson process seems to be promising.

The ability to measure the motions of individual sediment grains forces thinking about the transport of sediment on the granular scale. Two-dimensional velocimetry measurements are required to begin to unravel the phenomena of sediment entrainment and suspension. The data of this study can only demonstrate the type of fluctuations which must be further investigated.

9.3 Suggestions for future work

This study is among the first attempts to apply the laser-Doppler velocimetry technique to two-phase flows. Furthermore, an attempt was made to obtain the time histories of the velocity measurements. The data reported here form one of very few sets of direct measurements of the small-scale characteristics of a fluid flow transporting relatively dense solid particles. Again, this work is only the preliminary portion of an ongoing research program.

The most pressing need in regard to the technique is an understanding of the causes of the invalid velocimetry events. Over

half of the recorded data events were not valid events. Both sediment grain and fluid velocimetry events were discarded. Invalid data events were present not only in the data records from locations near the sediment bed, where the sediment concentration is large, but also in data records from near the water surface. Following are four suggestions of further research to address this problem.

First, a more powerful laser should be used. Increasing the incident light intensity by increasing the laser power used should reduce any noise due to the photodetector and the first stage of the signal amplification electronics. Increased incident light intensity will also permit modifications to the receiving optics to reduce the optical depth of field. In other words, the detection of light scattered by particles passing through the laser beams outside of the beam intersection volume could be reduced. A smaller collection solid angle, additional and smaller apertures, and placing the axis of the receiving optical train at some angle to the transmitted laser beams should be tried. Unfortunately, such alterations must be done by trial and error.

Second, the band-pass filtered Doppler burst signal and the associated pedestal signal should be digitized directly and examined. The characteristics of the burst signal could then be quantitatively determined. The irregularity in the Doppler burst signal could be explicitly measured. Any correlation between pedestal amplitude and signal irregularity would be exposed. Simultaneous monitoring of the developed counter-processor would determine the relative number and characteristics of the incoming burst signals which are discarded by

the processor. Since the Doppler frequency is of the order of 500 KHz to ensure reasonable resolution of the burst signal, digitization at a rate of approximately 5 MHz would be desirable. Because of the acquisition rate and the quantity of the resulting data, disjoint portions of the incoming signal must be digitized at successive time intervals.

Third, an independent method of detecting the presence of sediment grains in the vicinity of the velocimetry measurement volume should be tried. Knowledge of the exact number of sediment grains scattering light at any given instant would allow an accurate determination of the local sediment transport rate. Independent measurements of both the velocimetry data and the local transport rate would determine if invalid velocimetry events are more often generated during instants of relatively high sediment transport. The nature of any biasing in the velocimetry data could be appreciated.

Lastly, the developed velocimeter should be applied to a less complex flow. Elimination of the movable sediment bed would allow some experimental control over the local sediment transport rate. The fluid could be seeded with sediment grains until the desired transport rate was achieved. The performance of the velocimeter at different local rates of sediment transport could be evaluated.

It is important to stress, however, that better understanding of the laser velocimetry technique applied to sediment-laden flows is primarily to allow the acquisition of better velocimetry data in such flows. Better velocimetry data, in turn, will allow better insights into the mechanics of sediment entrainment and suspension. Despite all

of the uncertainties with the technique as noted in this study, the implementation of a two-dimensional velocimeter for use in sediment-laden flows over movable sand beds is overwhelmingly recommended. Vertical velocity data are required to begin to understand the fundamental mechanics of sediment-laden flows. While the data acquired with a laser-Doppler velocimeter may be biased in an unknown manner, the observations can be made.

CHAPTER 10

SUMMARY

The basic laser-doppler velocimetry technique was adapted for use in sediment-laden flows. The developed instrumentation was employed to make one-dimensional, instantaneous measurements of both fluid and sediment grain velocity throughout the water column in such a flow. This work is the foundation of an ongoing program of experimental observations of the fine-scale, time-varying nature of sediment-laden flows.

This study has yielded information on three facets of the continuing effort. These aspects are: (1) the feasibility of laser-Doppler velocimetry in sediment-laden flows; (2) the inherent difficulties in direct experimental investigations of the mechanisms of sediment suspension and entrainment; and (3) the character of the interactions between the fluid turbulence and the motions of individual sediment grains.

10.1 Feasibility of laser-Doppler velocimetry in sediment-laden flows

Laser-Doppler velocimetry is particularly attractive for use in sediment-laden flows. No calibration is required and the flow field is not deformed in any way. The technique allows the measurement of the fluid velocity, the occurrence of individual sediment grains, and the velocity of those individual sediment grains. However, the resulting velocimetry data may be biased in some unknown manner; a large fraction of the measurements must be discarded due to the simultaneous light scattering by multiple sediment grains and fluid

particles. The resulting fluid velocity measurements may be biased in a manner different from the recognized bias inherent in the technique when applied to clear fluid flows. The sediment grain velocity data may also be biased. Also, the velocimeter is not a reliable particle counter, except possibly in the upper portions of the flow. The severity of these difficulties cannot be determined with the data obtained in this study. Even in light of these disadvantages, no other technique currently available allows such direct, instantaneous measurements.

10.2 Inherent difficulties in direct experimental investigations of the mechanisms of sediment suspension and entrainment

Since this study is among the first to measure directly the fine-scale motions of sediment-laden flows, it has pinpointed two difficulties inherent in such studies. First, the quantity of data required to describe adequately all of the processes present in the flow is quite large. The time scales of the flow range from the small-scale, relatively rapid fluctuations of the fluid turbulence to the long-scale, slowly varying changes in the sediment bed forms. Second, the subsequent physical interpretation of any data is complicated by the movements of the sediment bed. These problems are due to the complex nature of sediment-laden flows and are independent of the instrumentation used to observe the flow variables. Obtaining and interpreting measurements of the time-dependent characteristics of the interactions between the flowing fluid, the transported sediment and the accompanying motions of the sediment will always be difficult.

10.3 Interactions between fluid turbulence and the motions of individual sediment grains

Despite the various difficulties, the data obtained in this study do give insights into the mechanics of the suspension and entrainment of sediment. The values of $\sqrt{u'^2}$ determined for the sediment-laden flow observed in this study are on the order of those reported by previous investigators in clear fluid flows. The mean and standard deviation of the sediment grain velocity were observed to be less than those of the fluid velocity in the lower portion of the flow, but relatively greater near the water surface.

The data also demonstrates the shortcomings of the continuum approach to the mechanics of the suspension of sediment. A new conceptual model is required. The suspended load equation leads to an estimate of the vertical distribution of the mean concentration of suspended sediment for engineering purposes. It does not accurately reflect the mechanics of sediment suspension. The length, or time, scales of the fluid turbulence are much less than the length, or time, scales of the number of grains necessary to define the mean sediment concentration or its fluctuation. Computation of the term $\overline{v'c'}$ requires the correlation of two processes of widely disparate scale. Sediment suspension and entrainment should be explored on a granular scale.

In the upper portion of the flow, where the velocimeter apparently acts as a grain counter, the probability density functions of the recorded sediment grain inter-arrival times (the times between the detection of successive sediment grains) were observed to be

negative exponentials. The transport of sediment might be approached on a granular scale by modeling the sediment grain arrival as a Poisson process.

Direct observations of the turbulent structure of the fluid and the motions of the suspended sediment grains will contribute much to the knowledge of the small-scale, time-fluctuating characteristics of sediment-laden flows. Quantitative measurement may yield only qualitative insights into the complex phenomena of sediment suspension and entrainment. The instrumentation implemented in this study should be expanded to give two-dimensional velocimetry data and improved as a sediment grain counter.

REFERENCES

Bagnold, R. A., Experiments on a gravity free dispersion of large spheres in a Newtonian fluid under shear, Proceedings of the Royal Society of London, Series A, vol. 225, 1954, p. 49-70.

Blinco, P. H. and E. Partheniades, Turbulence characteristics in free surface flows over smooth and rough boundaries, Journal of Hydraulic Research, vol. 9, no. 1, 1971, p. 43-71.

Bohlen, W. F., Hot-wire anemometry study of turbulence in open-channel flows transporting neutrally buoyant particles, Report 69-1, Experimental Sedimentology Laboratory, Massachusetts Institute of Technology, Cambridge, Massachusetts, 1969.

Brooks, N. H., Laboratory studies of the mechanics of streams flowing over a movable bed of fine sand. Thesis presented to the California Institute of Technology, at Pasadena, California, in partial fulfillment of the requirements for the degree of Doctor of Philosophy, 1954.

Daily, J. W. and T. K. Chu, Rigid particle suspensions in turbulent shear flow: some concentration effects, Report Number 48, Hydrodynamics Laboratory, Massachusetts Institute of Technology, Cambridge, Massachusetts, 1961.

Daily, J. W. and R. L. Hardison, Rigid particle suspensions in turbulent shear flow: measurement of total-head, velocity and turbulence with impact tubes, Report Number 67, Hydrodynamics Laboratory, Massachusetts Institute of Technology, Cambridge, Massachusetts, 1964.

Daily, J. W. and P. Roberts, Rigid particle suspensions in turbulent shear flow: size effects with spherical particles, Report Number 69, Hydrodynamics Laboratory, Massachusetts Institute of Technology, Cambridge, Massachusetts, 1966.

Deeming, T. J., Fourier analysis with unequally-spaced data, Astrophysics and Space Science, vol. 36, 1975, p. 137-158.

Dimotakis, P. D., Single scattering particle laser-Doppler measurements of turbulence, AGARD Symposium on the Applications of Non-Intrusive Instrumentation in Fluid Flow Research, Saint-Louis, France, Paper Number 10, 1976.

Durst, F., A. Melling, and J. H. Whitelaw, Principles and Practice of Laser-Doppler Anemometry, Academic Press, New York, New York, 1976.

Durst, F., Studies of particle motion by laser-Doppler techniques, Proceedings of the Dynamic Flow Conference, I.M.S.T., Marseille,

France, September 11-14, and Johns Hopkins University, Baltimore, Maryland, September 18-21, 1978, p. 345-372.

Einstein, H. A. and N. Chein, Second approximation to the solution of the suspended load theory, Series 47, Issue 2, Institute of Engineering Research, University of California, Berkeley, California, January 31, 1952.

Einstein, H. A. and N. Chein, Effects of heavy sediment concentration near the bed on velocity and sediment distribution, MRD Series 8, University of California, Institute of Engineering Research and the United States Army Corps of Engineers, Omaha, Nebraska, August 1955.

Einstein, H. A. and H. Li, The viscous sublayer along a smooth boundary, Transactions, ASCE, vol. 123, paper 2992, 1958, p. 293-313.

Elata, C. and A. T. Ippen, The dynamics of open channel flow with suspensions of neutrally buoyant particles, Technical Report 49, Hydrodynamics Laboratory, Massachusetts Institute of Technology, Cambridge, Massachusetts, 1961.

Gartrell, G., Jr., A signal processor for a laser-Doppler velocimeter, Technical Memorandum 78-5, W. M. Keck Laboratory of Hydraulics and Water Resources, California Institute of Technology, Pasadena, California, 1978.

Gilbert, G. K., Transportation of debris by running water, United States Geological Survey, Professional Paper 86, 1914.

Hino, M., Turbulent flow with suspended particles, Journal of the Hydraulics Division, ASCE, vol. 89, HY 4, Proc. Paper 3579, July, 1963, p. 161-185.

Hunt, J., Private communication, 1980.

Ismail, H. A., Turbulent transfer mechanisms and suspended sediment in closed conduits, Transactions, ASCE, vol. 117, paper 2500, 1952, p. 409-454.

Jackson, R. G., Sedimentological and fluid dynamic implications of the turbulent bursting phenomenon in geophysical flows, Journal of Fluid Mechanics, vol. 77, part 3, 1976, p. 531-560.

Laufer, J., Recent measurement in a two-dimensional turbulent channel, Journal of Aeronautical Science, vol. 17, no. 5, May, 1950, p. 227-287.

Luque, R. F. and R. van Beek, Erosion and transport of bed-load sediment, International Association for Hydraulic Research, vol. 14, 1976, p. 127-144.

Mc Dougall, T. J., Bias correction for individual realization laser-Doppler anemometer measurements, Journal of Physics, Series E, Scientific Instruments, vol. 13, January, 1980, p. 53-60.

Mc Laughlin, D. K. and W. G. Tiederman, Biasing correction for individual realization of laser anemometer measurements in turbulent flows, Physics of Fluids, vol. 16, no. 12, December, 1973, p. 2082-2088.

Mc Quivey, R. S., Principles and measuring techniques of turbulence characteristics in open-channel flows, United States Geological Survey, Professional Paper 802A, 1973.

Müller, A., Turbulence measurements over a movable bed with sediment transport by laser-anemometry, Proceedings 15th Congress, International Association for Hydraulic Research, Istanbul, Turkey, September 3-7, 1973, p. 43-50.

Müller, A. and J. R. Glover, An LDA adapted to measure sediment-laden flows, Proceedings 17th Congress, International Association for Hydraulic Research, Baden-Baden, Germany, August 15-19, 1977, p. 647-650.

Nomicos, G., Effects of sediment load on the velocity field and friction factor of turbulent flow in an open channel, thesis presented to the California Institute of Technology, at Pasadena, California, in partial fulfillment of the requirements for the degree of Doctor of Philosophy, 1956.

O'Brien, M. P., Review of the theory of turbulent flow and its relation to sediment transportation, Transactions, American Geophysical Union, Washington, D. C., April 27-29, 1933, p. 487-491.

Offen, G. R. and S. L. Kline, A proposed model of the bursting process in turbulent boundary layers, Journal of Fluid Mechanics, vol. 70, part 2, 1975, p. 209-228.

Raichlen, F. R., Some turbulence measurements in water, Journal of the Engineering Mechanics Division, ASCE, vol. 93, EM 2, Proc. Paper 5195, 1967, p. 73-97.

Roberts, J. R. and M. Gaster, On the estimation of spectra from randomly sampled signals: a method of reducing variability, Proceedings of the Royal Society of London, Series A, vol. 371, 1980, p. 235-258.

Rouse, H., Modern conceptions of the mechanics of fluid turbulence, Transactions, ASCE, vol. 102, paper 1965, 1937, p. 463-543.

Shapiro, H.S. and R. A. Silverman, Alias-free sampling of random noise, Journal of the Society for Industrial and Applied Mathematics, vol. 8, no. 2, June, 1960, p. 225-248.

Sutherland, A. J., Proposed mechanism for sediment entrainment by turbulent flows, Journal of Geophysical Research, vol. 72, no. 24, 1966, p. 6183-6194.

Taylor, B. D., Temperature effects in alluvial streams, Report KH-R-27, W. M. Keck Laboratory of Hydraulics and Water Resources, California Institute of Technology, Pasadena, California, August, 1971.

Vanoni, V. A., Transportation of suspended sediment by water, Transactions, ASCE, vol. 111, Proc. Paper 2267, 1946, p. 67-133.

Vanoni, V. A. and N. H. Brooks, Laboratory studies of the roughness and suspended load of alluvial streams, Report E-68, Sedimentation Laboratory, California Institute of Technology, Pasadena, California, 1957.

von Karman, T., Turbulence and skin friction, Journal of Aeronautical Science, vol. 1, no. 1, January, 1934, p. 1-20.

van Ingen, C., A Processing system for laser-Doppler velocimetry in sediment-laden flows, Technical Memorandum 80-1, W. M. Keck Laboratory of Hydraulics and Water Resources, California Institute of Technology, Pasadena, California, 1980.

van Ingen, C., Guidelines for the acquisition and preliminary processing of laser-Doppler velocimetry data in sediment-laden flows, Technical Memorandum 81-1, W. M. Keck Laboratory of Hydraulics and Water Resources, California Institute of Technology, Pasadena, California, 1981.